Solar-Terrestrial Centre of Excellence

Annual Report 2023

Belgian Science Policy Office belspo

Royal Observatory of Belgium

RMI

BIRA-IASB

.be

STCE

Solar-**T**errestrial **C**entre of **E**xcellence

https://stce.be/

Ringlaan 3

B-1180 Brussels

Tel.: +32 2 373 0211

Fax: + 32 2 374 9822

Front page - *The Humain Radio Astronomy Station, located in Marche en Famenne, was founded in 1953 by the Royal Observatory of Belgium to house the very first Belgian radio telescopes dedicated to the observation of the Sun. On 9 and 10 September 2023, it opened for the first time its doors to the public. Despite the remote location and the ongoing heat wave, the event attracted hundreds of visitors. Credits: Christophe Marqué*

Table of Contents

A word from the STCE coordinator

Dear reader,

You see before you the annual report of the Solar-Terrestrial Centre of Excellence. It highlights some of the finest results that were achieved in 2023 through collaborations across teams, institutes and borders.

The STCE reached out to organizations and institutes that have a connection with space weather. The first step is raising awareness, the second step is providing info and education, the third step is offering services, tools and a help desk. The STCE has put considerable effort into showing the relevance of space weather for society. The Space Weather Education Center is the place where users can get what they need.

We expanded our services which form the ultimate bridge between the science community and the users. We guard the quality of these services by investing strongly in research in the different domains of solar-terrestrial sciences. Our solar research, ionospheric science, research of the Earth environment and collecting and analysing observational data are the keys to continuously improve and rethink our services.

We look to the future as well, and work hard on preparing new missions and initiate new projects that will guarantee the future of the collaborations fostered by the STCE.

Besides what is highlighted in this report, much other progress was achieved in 2023 in the form of fresh ideas, new results, new collaborations, and new methods. For many of these projects, the details can be found through our elaborate list of presentations and publications that are listed at the very end of this report. Please contact us if you would like more information on any of those.

For now, happy reading!

Ronald Van der Linden
General Coordinator of the Solar-Terrestrial Centre of Excellence
Director General of the Royal Observatory of Belgium

Structure of the STCE

The Solar-Terrestrial Centre of Excellence is a project of scientific collaboration that focuses on the Sun, through interplanetary space, up to the Earth and its atmosphere.

The solid base of the STCE is the expertise that exists in the 3 Federal Scientific Institutes of the Brussels Space Pole: the Royal Observatory of Belgium, the Royal Meteorological Institute and the Royal Belgian Institute for Space Aeronomy. The STCE supports fundamental solar, terrestrial and atmospheric physics research, is involved in earth-based observations and space missions, offers a broad variety of services (mainly linked to space weather and space climate) and operates a fully established space weather application centre. The scientists act at different levels within the frame of local, national and international collaborations of scientific and industrial partners.

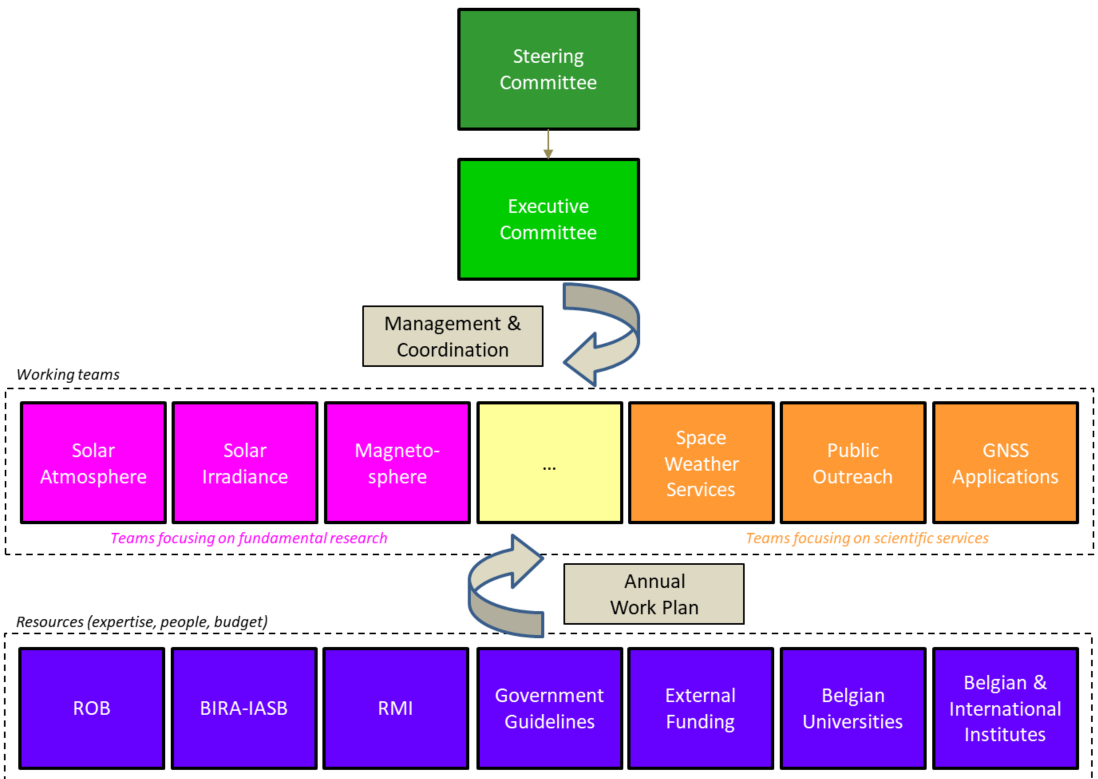

Figure 1: The STCE management structure

The STCE's strengths are based on sharing know-how, manpower, and infrastructure.

In order to optimise the coordination between the various working groups and institutions, as well as the available resources such as ICT, personnel and budget, a management structure for the STCE was put into place, consisting of a steering committee and an executive committee.

The ***steering committee*** takes all the final decisions on critical matters with regard to the STCE. It assures the integration of the STCE into the 3 institutions and the execution of the strategic plans. It is composed of:

- BELSPO General Director "Research and Space"

  Dr. Frank Monteny (BELSPO)

- Director General of each of the 3 institutions at the Space Pole

  Dr. Ronald Van der Linden (ROB)
  Dr. Daniel Gellens (RMI)
  Dr. Martine De Mazière (BIRA-IASB)

The ***executive committee*** assures the global coordination between the working groups and the correct use of the budgetary means for the various projects. It also identifies new opportunities and is the advisory body to the Steering Committee. It is composed of:

- STCE Coordinator

  Dr. Ronald Van der Linden

- Representatives of the research teams in the 3 institutes

  Dr. David Berghmans (ROB)
  Dr. Eric Pottiaux (ROB)
  Dr. Martine De Mazière (BIRA-IASB)
  Dr. Johan De Keyser (BIRA-IASB)
  Dr. Norma Crosby (BIRA-IASB)
  Dr. Daniel Gellens (RMI)
  Dr. Stanimir Stankov (RMI)
  Dr. Stijn Nevens (RMI)
  Dr. Roeland Van Malderen (RMI)

A promotional movie giving a flavor of the STCE's tasks, interactions and various research programmes can be found via the STCE website (in English, and subtitled in French and Dutch). A concise and more recent introduction to the STCE can be found on the STCE's YouTube channel (English).

A good portion of the Solar Influences Data analysis Center (SIDC) team of the Royal Observatory of Belgium during their Monthly Management Meeting (MMM) on 26 May 2023 (Credits: Sergei Shestov). During these near-monthly gatherings, held both on-site and online, topics such as well-being, science projects, people stuff, outreach events, and upcoming conferences are discussed. They usually start with a sandwich lunch.

Monitoring space weather: solar-terrestrial highlights in 2023

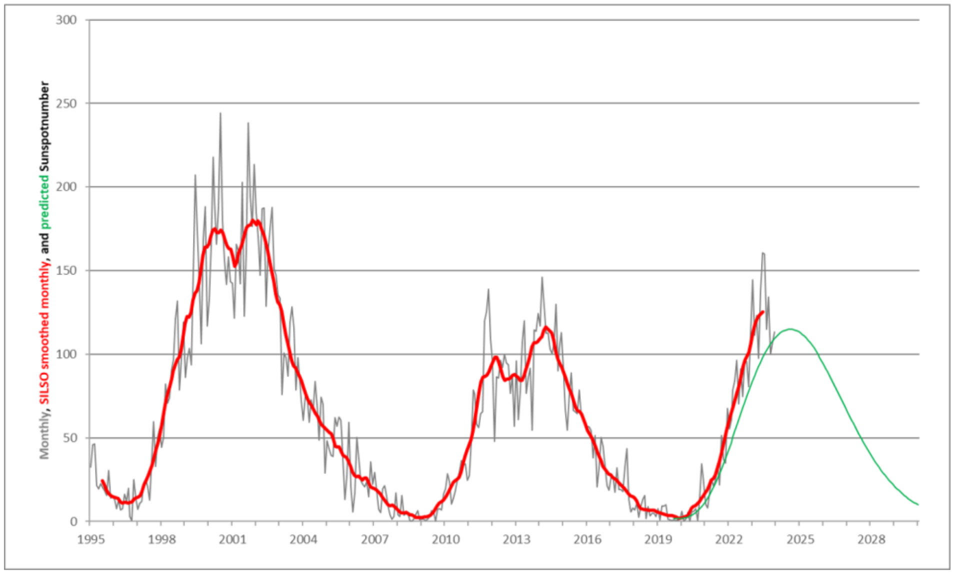

Figure 2: The evolution of the monthly and SILSO smoothed monthly S_N (1995-2023 ; [SILSO formula](#)). The monthly sunspot numbers in 2023 remained higher than the expected values (depicted in green), with the predicted maximum advanced and occurring in August 2024.

The official annual sunspot number (SN) for 2023, as determined by the WDC-SILSO (World Data Centre - Sunspot Index and Long-term Solar Observations), was 125.5. This is a significant increase compared to 2022 (83.2). The highest monthly sunspot numbers were recorded during June and July (resp. 160.5 and 160.0), and the smoothed monthly sunspot number reached a maximum of 125.3 in June, which is already higher than the maximum of the previous solar cycle SC24 (116.4). A second cycle maximum is expected in 2024, with a smoothed monthly sunspot number of around 140 (SILSO forecasts). SC25 maximum would then be somewhat higher and occur somewhat earlier than the original prediction of 115+/-10 in July 2025 +/- 8 months by the SC25 prediction panel. The evolution of SC25 for various space weather (SWx) parameters can be followed on the STCE's SC25 Tracking page.

The highest daily sunspot number was observed on 22 June (240), but also January , July and September had days when the sunspot number was at or above 200. Daily highs of 225 or more had not been observed since the Halloween groups in October 2003. The observed (and flare-corrected) 10.7cm radio flux (Penticton) reached its highest daily value for the entire year already on 15 January (231.8 sfu, with 1 sfu = 10^{-22} W m^{-2} Hz^{-1}), up from 179.9 sfu recorded on 18 May the previous year. The adjusted monthly radio flux reached 176.6 sfu in January and 183.3 sfu in July, well above the 143.8 sfu recorded in December 2022.

Several sunspot groups were reported visible with the protected naked eye (eclipse glasses) in January, February, May, June and July. They belonged to the largest groups observed in 2023, reaching maximum sunspot areas of about 3 to 6 times the total surface area of the Earth. NOAA 3354 was the largest group of 2023, and the second largest so far in SC25. Mid-July, 2 sunspot groups (NOAA 3363 and 3372) were visible with the naked eye at the same time.

The Sun produced 13 X-class ("eXtreme") flares in 2023, bringing the total for SC25 to 22. The X-class flares in 2023 all had different source regions, except NOAA 3386 which managed to produce 2: an X1 on 5 August, and another X1 on 7 August. The strongest flares of 2023 and as such also of SC25 (so far) were

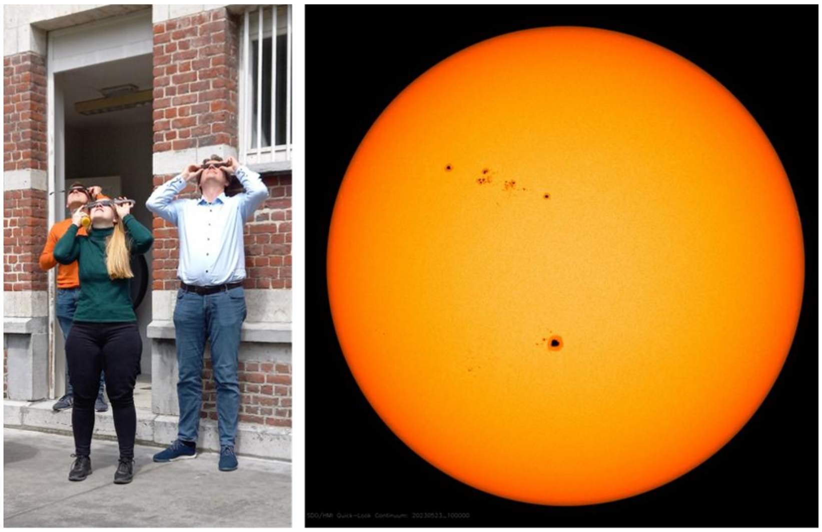

*Figure 3: NOAA 3310 was a small but compact sunspot group having a sunspot area about 3 times the total surface area of the Earth. Nonetheless, participants from the SWIC (STCE's Space Weather Introductory Course) were able to see the "tiny dot" using eclipse glasses on 23 and 24 May, as shown in the picture above. They did comment that it was on the limit, which is no surprize in view of its size and the fact that different observers have a different eye resolution. (Credits solar image: **SDO/HMI**).*

all produced in December: NOAA 3514 was the source of an X2.8 flare that peaked on 14 December, and an impressive X5.0 flare originated from NOAA 3536 on New Year's Eve.

The X2.8 flare was also associated with a strong radio burst, in particular at frequencies below 1GHz and lasting more than an hour. Intensities around 900.000 sfu were reached at 410 and 610 MHz, and 600.000 sfu at 245 MHz. The "strong x-ray flare + strong radio burst" tandem caused severe high frequency communication (HF Com) problems in aviation. SWPC, the American space weather forecast centre, mentioned that *"… multiple pilots and ground stations reported communication disruptions, with the impact felt across the country [USA]."* Two hours of strong radio interference were also reported from other sunlit parts of the world (Phys.org, Earth.com). Over South-America, all HF Com for aviation virtually disappeared and was re-established only very gradually (Tamitha Skov).

The radio burst was also very strong at GNSS frequencies (Global Navigation Satellite Systems, such as GPS or Galileo), but didn't last as long: about 40 minutes with a peak intensity of 99.000 sfu, the strongest of the year at these frequencies. Usually, the intensity at these frequencies during solar cycle maximum

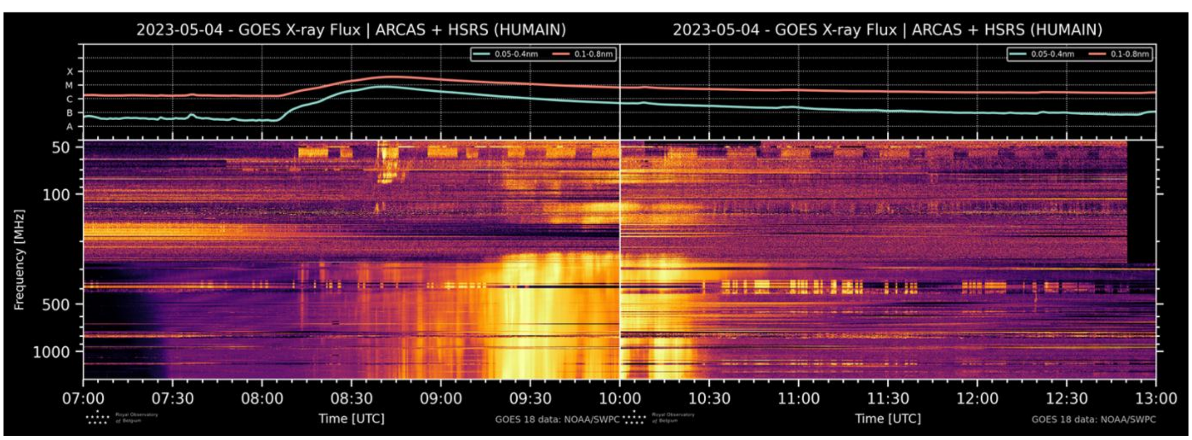

*Figure 4: Radio telescopes of the **Humain Radioastronomy Station** recorded the M3.9 eruption of 4 May in frequencies between 45 and 1495 MHz. Scanning continuously the intensity at these frequencies, disturbances can be discerned which are in this case associated with a CME-driven shock (Type II) and electrons trapped in closed magnetic field lines in the post-flare coronal loops (Type IV) - See the STCE's **SWx classification page** for more examples and info on Type II, Type IV and other radio bursts. The top portion of the graph shows the evolution of the x-ray flux as measured by **GOES**.*

is only around 120 sfu, and there are typically only a handful of such strong bursts during an entire solar cycle! The second strongest burst at GNSS frequencies occurred on 4 May around 08:44 UTC and was accordingly registered by the Humain Radioastronomy station. Produced by NOAA 3296, this long-duration M3.9 flare had an associated radio burst at 1415 MHz of 26.000 sfu.

In 2023, the GOES recorded 352 M-class ("medium") flares, up from the 185 in 2022. We have to go back to 2002 to find comparable numbers. No less than 98 active regions contributed with at least 1 M-class flare, but 20% of the M-class flares were produced by just 4 regions: NOAA 3311 (25), NOAA 3213 (16), NOAA 3372 (13) and NOAA 3380 (15). At this stage of the solar cycle, the number of strong (M5+) flares is a bit higher than during SC24 (resp. 75 vs 64), but well below the numbers from SC21-23 (106 or higher).

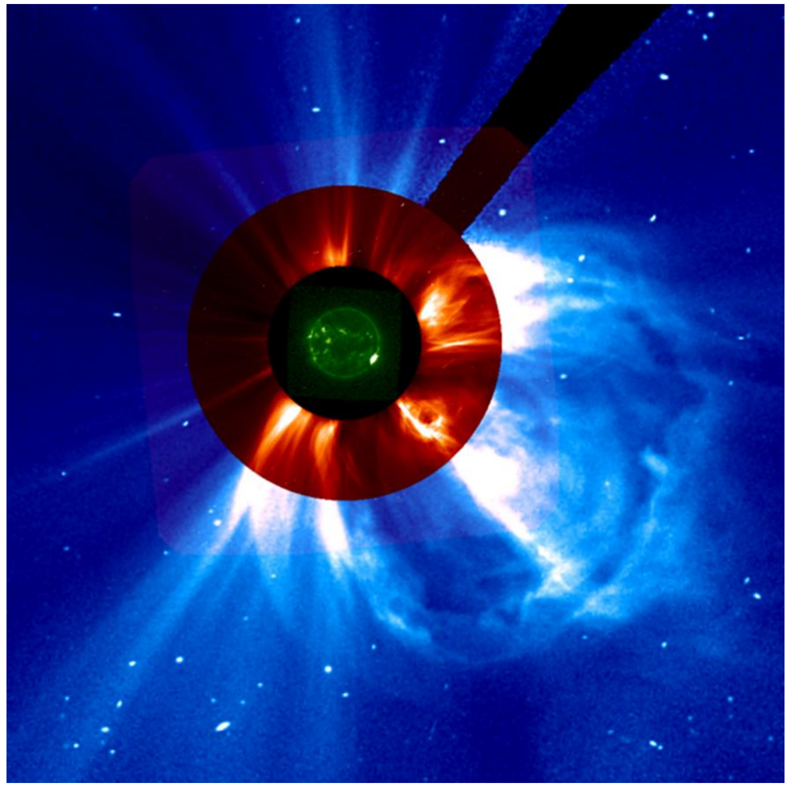

Figure 5: The impressive CME associated with the M5 flare produced by NOAA 3363 on 17-18 July. The EUV image was taken by GOES/SUVI 094 (green) and is overlaid by coronagraphic imagery from SOHO/LASCO C2 (red) and C3 (blue). The images were taken on 18 July at 00:48 UTC. The dots in the coronagraphic images are not all stars, but some are impacts from the high-energetic particles (protons) on the camera's pixels. The associated moderate proton event was the strongest of 2023.

During the year, several -mostly minor- proton events were recorded. A proton event occurs when the greater than 10 MeV proton flux exceeds the threshold of 10 pfu. The particle detector on board GOES recorded 10 minor and 2 moderate proton events in 2023. The strongest proton event (620 pfu) was associated with an M5.7 flare produced by NOAA 3363 near the southwest solar limb on 18 July. The second moderate proton event was associated with an M4 flare by NOAA 3376 and reached 154 pfu on 29 July. No Ground Level Enhancements (GLE) were recorded by ground-based neutron monitors throughout the year.

Several stunning filament eruptions were observed throughout the year. Solar filaments are clouds of charged particles ("plasma") above the solar surface squeezed between magnetic regions of opposite polarity. Being cooler and denser than the plasma underneath and their surroundings, they appear as dark lines when seen on the solar disk and as bright blobs when seen near the solar limb (then they are called "prominences"). Particularly eye-catching filament eruptions were the ones from 20 January, 12 June, 19 July, and 16 September. There were also earth-directed coronal mass ejections (CME) associated with filament eruptions that subsequently resulted in strong geomagnetic storms (K_p = 7). This was in particular the case for the eruptions on 24-25 February, 2-3 November, and 27-28 November.

The daily CME rate increased further to 6 by the middle of 2023. Often, these CMEs had an earth-directed component disturbing the Earth's magnetic field. A filament eruption in the northeast solar quadrant on 20 March was associated with a long-duration C4 flare and a partial halo CME. The latter would result in the first of two severe geomagnetic storms (K_p = 8) on 23-24 March. The second severe geomagnetic storm took place on 23-24 April. It was the result of an earth-directed full halo CME that was associated with the eruption of a filament anchored in the foot point of decaying active region NOAA 3283, source of the resulting long-duration M1 flare. The Dst index reached -213 nT, a value not seen since the St-Patrick's Day storm of 17 March 2015.

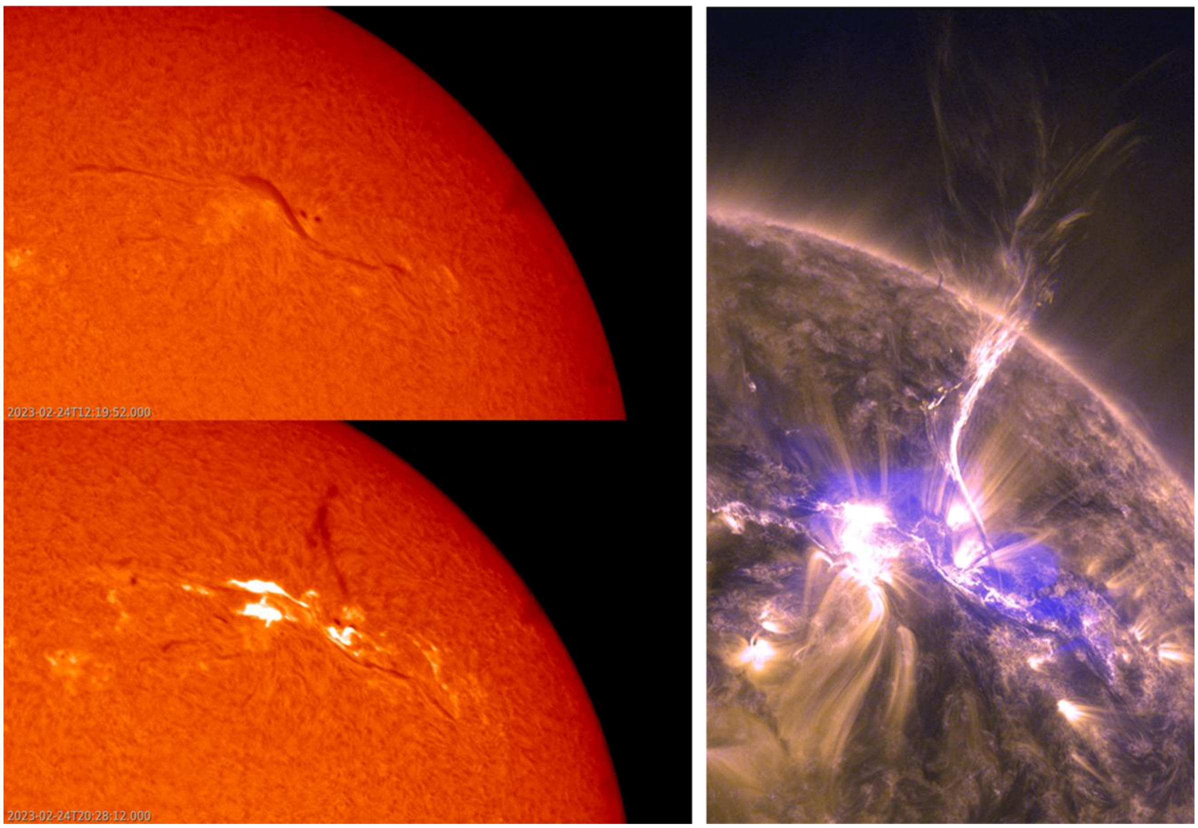

*Figure 6: Sunspot group NOAA 3229 was already decaying when it produced an M3.7 flare associated with an impressive filament eruption on **24 February**. The images on the left show the filament prior and during the eruption in H-alpha (absorption line in the red portion of the solar spectrum). The image on the right combines AIA171 (yellowish) with AIA131 imagery, the latter allowing a better contrast between the "cold" (dark purple) and "hot" (sky blue) areas of the eruption. The eruption was associated with a minor **proton event** observed by GOES, **STEREO-A** and Solar Orbiter (Grimani et al. **2024**).*

Space weather wise, the two severe geomagnetic storms as well as the three strong ones (26-27 February, 5 November and 1 December) had important impacts in several technological and service domains. The powerful storm in late February forced SpaceX to delay a Starlink launch from Florida with more than 4 hours (Space.com). The same storm also temporarily disrupted operations of several Canadian oil rigs as the geomagnetically induced currents (GICs) interfered with the directional electronics in the rigging tool to such an extent that the readings were unreliable (Facebook link).

On 24 March, Rocket Lab's early morning launch from New Zealand got delayed by 90 minutes because of the unexpectedly powerful geomagnetic storm (Space.com). The strong March and April geomagnetic storms increased atmospheric drag considerably which resulted in the premature re-entry of the trunk of

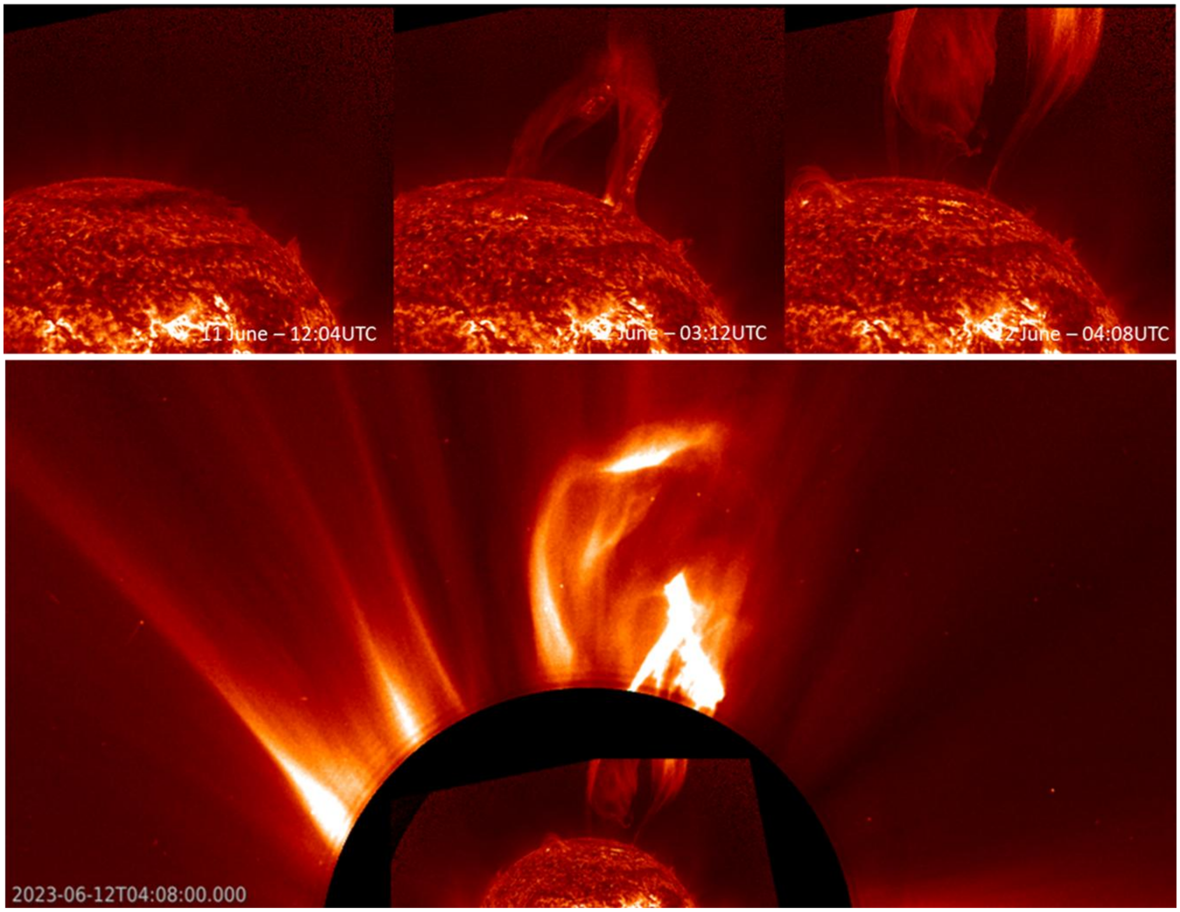

Figure 7: Polar crown filaments (PCF) are located at the highest latitudes, separating the predominant polar field of the previous solar cycle and the dispersed field of the current cycle, which is drifting poleward from the trailing polarities of sunspot groups at lower latitudes. The "old" polar magnetic field is currently still strong enough to keep the newly arriving opposite polarity field at bay, and where the two encounter each other, a solid filament can form. This also means that small changes in these magnetic fields may result in instabilities in and the subsequent eruption of (a portion of) the filament. The PCF eruption near the Sun's north pole early on 12 June is shown here with contrast-enhanced GOES/SUVI 304 images. Eruptions such as these indicate that the polar field has not completely reversed yet, and that solar cycle maximum is still to come. The lower image combines SUVI 304 (EUV) imagery with LASCO/C2 coronagraphic imagery (white light) showing the associated departing CME.

SpaceX Dragon capsule "Endurance" on 27-28 April. This capsule had returned an astronaut crew from the International Space Station (ISS) on 12 March, during which the capsule was jettisoned (a standard procedure). Normally, these capsules can stay for years in orbit around the Earth, but in this case and very likely due to the increased atmospheric drag, the piece of space junk burned already up in the Earth's atmosphere after only 6 weeks (Spaceweather.com).

During the severe geomagnetic storm of 23-24 April, aurora were photographed as far south as Texas and Arizona in the USA, and Spain in Europe (spaceweather.com). The weather was not always collaborating, but aurorae were also observed from Belgium on 26-27 February and especially on 5 November. Several advisories for civil aviation were issued by PECASUS. During geomagnetic storms, this concerned mostly disturbances in High Frequency communications (HF Com; 3-30 MHz) and with GNSS applications (Global Navigation Satellite Systems, such as e.g. GPS and Galileo). During the February and November storms, several pilots flying over Canada reported navigational problems when approaching the runway (landing).

High-speed streams from coronal holes (CHs) regularly disturbed the earth environment, but they were less prominent and had a smaller SWx impact than in previous years. High speed wind streams (HSS) related to these CHs drove the maximum solar wind speeds near Earth occasionally to values between upward of 600 km/s, with the highest values recorded around 27 February (830 km/s). The passage of these HSS generated elevated levels of energetic (energies of more than 2 MeV) electrons in the Earth's outer radiation belt, as measured by the GOES satellites. Daily electron fluences (24 hours accumulated values) showed a declining trend, reaching at most moderate levels.

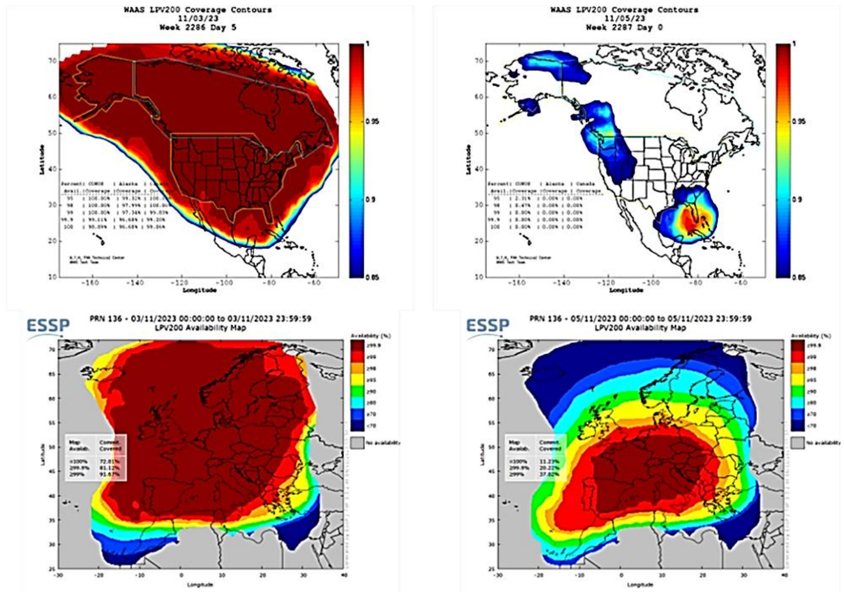

Figure 8: During the strong geomagnetic storm of 5 November 2023, certain satellite-based applications for aviation in USA (WAAS; upper row) and Europe (EGNOS; lower row) and were affected as shown in the availability maps underneath for an undisturbed day (left) and on 5 November (right). A red colour in this case means good coverage and availability, something that was severely compromised during the geomagnetic storm.

Public outreach meets Science

Open doors at the Humain radioastronomy station

The Humain radioastronomy station was founded in 1953, when the Observatory purchased a small piece of land, near the city of Humain, after a year-long search by R. Coutrez and E. Pourbaix for a favourable place to host the first two radio telescopes operated in Belgium. Seventy years later, and for the first time in its history, the station was open to the public in the frame of the European Heritage days, organised in Wallonia on 9 and 10 September 2023. The event was supported by the STCE, and made possible by many volunteers from the Royal Observatory (ROB) and the Aeronomy Institute (BIRA-IASB), with logistic support from the Meteorological Institute (RMI).

Figure 9: The public visiting the Humain station and its science exhibition (Credits: Le Binh San Pham)

Personnel from ROB and BIRA-IASB presented the scientific activities taking place on the site of the station: solar radio astronomy, optical astronomy, radio and optical observations of meteors, and radio observations of whistler waves in the plasmasphere.

Figure 10: The inflatable planetarium set up by the Planetarium team in Humain. (Credits: Le Binh San Pham)

Special activities were set up for the public. For example, there were real-time observations of the Sun with SolEx (short for Solar Explorer), a small but powerful spectroheliograph with which the Sun can be observed in different wavelengths. The instrument officially made its first optical solar observations in Humain! There was also a small inflatable planetarium, several fun activities for children, and an exhibition on the history of the station and its main instrument, the decommissioned solar interferometer.

Despite challenging weather conditions (the event took place during the late heat wave of September 2023), and the remoteness of the Humain radioastronomy station, nearly 630 visitors came on-site from nearby cities, the whole of Belgium, but also from France and The Netherlands.

The event received considerable attention from local and national authorities, as well as from local and national media outlets. The organisers were busy giving interviews throughout almost the entire weekend! As such, these Open Doors could certainly be considered as very successful!

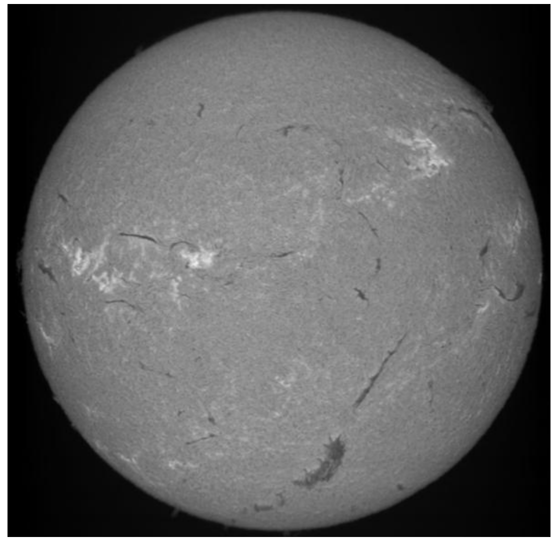

Figure 11: The first optical observation of the Sun in Humain with SolEx, (Credits: Sabrina Bechet)

The Space Weather Education Center

Organisations have a keen interest in space weather courses tailored to their needs and to the presence or absence of knowledge of their employees. From different sides, the STCE received requests for information on space weather and its impact on their activities. To meet their requirements, the STCE Space Weather Education Center (SWEC) has expanded in 2023 its course offer both in number and in content.

The German Federal Agency for Cartography and Geodesy (BKG) reached out to us for a course on space weather and how space weather could potentially impact their operations. A tailored course and a working meeting were the result. The STCE experts in Global Navigation Satellite Systems (GNSS) and ionospheric science together with the teaching team of the STCE set up a scientific and educational three-day programme.

This was the start for more dedicated courses and collaborations, this time with NATO partners and the Belgian Defence. NATO established a working group on space weather and how space weather impacts military operations. In 2022 already, the STCE presented its Space Weather Education Center at the NATO meeting in Rome. Nations are aware that space

Figure 12: The dedicated SWIC for the BKG.

weather needs to be followed up, but they don't have the knowledge or capability to do this. The STCE combines both: an education centre and a service centre. The military sends staff to the Space Weather Introductory Course (SWIC) during which they get introduced to space weather, data, products and services.

Figure 13: The E-SWAN school during the ESWW2023 in Toulouse.

The next step is to set up more advanced courses for even more specific needs. In collaboration with the STCE GNSS and ionospheric expert group, the STCE programmed the course "Space Weather impacts on ionospheric wave propagations - focus on GNSS and HF Com" (High Frequency communication). Our Belgian Defence is highly interested too because HF radio communication has again proven to be essential. If SATCOM (Satellite Communication) is not available, the military could use the classical way of communicating with HF radio waves. But this knowledge is literally retired. To revive this sort of communication, Belgian Defence and the STCE collaborate strongly. One pathway is by transferring scientific insight in this matter.

A similar story holds true for aviation. Eurocontrol is a pan-European, civil-military organisation dedicated to supporting European aviation. Space weather impacts aviation because the sector relies strongly on GNSS and HF radio communication and because crew, passengers and onboard electronics are vulnerable to solar particles. Eurocontrol is aware of this and organised a space weather exercise at the end of 2023. The STCE reached out and developed an online introductory course for aviation that went live later.

SWEC also supported the E-SWAN school at the European Space Weather Week in Toulouse and offered a full on-site course to 50 students prior to the ESWW.

Some statistics: from its start in 2017 until end 2023, SWEC offered 23 Space Weather Introductory Courses and kicked-off two courses on ionospheric wave propagation. SWEC welcomed 183 participants.

International Meteor Conference 2023

The 42nd International Meteor Conference (IMC) 2023 was held at the Euro Space Center in Redu, Belgium. It was organised by BIRA-IASB with financial support of the STCE. The conference was a testament to the dynamic and ever-expanding world of meteor science, and was very successful with 86 on-site and 43 virtual attendees, fostering a global community of meteor enthusiasts and researchers. IMC is also a hybrid conference gathering professionals and amateurs, the latter having a great deal of importance for meteor observations.

The meeting covered a wide range of topics related to meteoroid streams, modelling, meteor-related software and hardware, visual meteor observations, video meteor work, and the use of meteor spectroscopy and seismology to understand meteor physics and dynamics.

A specific session was organised on the topic of predicted meteorite impacts, with a particular focus on the successful recovery and study of the Saint-Pierre-le-Viger Meteorite in France at the beginning of 2023. This remarkable achievement underlined the collaborative spirit of the meteor community, highlighting the synergy between asteroid hunters, meteor camera operators, software developers, meteorite experts, and amateurs searching on the field.

Figure 14: Official picture of the participants to the IMC 2023 at the Euro Space Center in Redu (Credits : IMO).

A one-day radio meteor workshop was organised prior to the event, exploring advancements in radio meteor detection algorithms, radar observations, and the status and perspectives of various meteor detection networks, with an emphasis on how the BRAMS (Belgian Radio Meteor Stations) network can benefit from these discussions and what are its strongest points. There were 20 attendees participating to this workshop on-site and about 10 online.

The IMC 2023 was a huge success both in terms of participation and scientific return, but also in terms of atmosphere and social gathering, which is an extremely important aspect of this meeting that binds participants together for many years. The Euro Space Center was a fantastic host providing a number of facilities such as a very modern and comfortable auditorium for the talks, many rooms for the coffee breaks, meals and social gathering, bedrooms for most of the participants, organising a VIP event for those willing to participate in the space activities, and bringing a constant good spirit to the event.

Figure 15: Participants of the IMC 2023 in the modern auditorium of the Euro Space Center (Credits: IMO).

An excursion was organised to the caves of Han and to the radioastronomical site of Humain where people could receive a short introduction about the solar, meteor and plasmaspheric observations carried out there.

Note: all the pictures come from the Flickr account of the IMO (International Meteor Organization). They can be used freely. The website of the event is https://imc2023.imo.net/

Training of the French polar crew: theory and operation of neutron monitors

For the past three years, the STCE team at Dourbes is hosting regular courses of the French Polar Institute (Institut Polaire Français Paul-Émile Victor, IPEV) antarctic crew on theory and operation of Super Neutron Monitors. The two members of the IPEV crew are part of the voluntary personnel for civil services (Volontaire Service Civique, VSC) and spend 12 months at the antarctic stations at Kergeulen and Terre-Adélie. The formation consists of theoretical courses on Solar physics and space-weather, theory of neutron monitors and hands-on practice on instrument operation and maintenance. The training course was organised and delivered by the STCE team in collaboration with the Paris Observatory. The objective is to provide the knowledge and the practical skills of the VSC personnel necessary to ensure continuous operation of the instrument. The neutron monitors at Kergeulen and Terre-Adélie (being the nearest to the south magnetic pole) are important instruments for solar cosmic rays spectral calculations. This collaboration and our contribution were acknowledged during the evaluation of Project 227 by IPEV in their evaluation report.

Figure 16: The instructor, Dr. D. Sapundjiev (left), with the trainees from the French crew at the cosmic ray lab in Dourbes.

Experienced space weather forecasters Jasmina Magdalenic (second from right) and Judith de Patoul (head of the SIDC SWx forecaster team; fourth from right) teaching tips and tricks of SWx forecasting to some eager, freshly arrived members of the team.

Fundamental research

EUI on board Solar Orbiter discovers jets that could drive the solar wind

The solar wind is a steady breeze blowing from the Sun into interplanetary space at speeds of hundreds of km/s. The fastest gusts of solar wind can drive geomagnetic storms and come from special locations in the solar atmosphere called coronal holes. These are areas where the Sun's magnetic field stretches out in space instead of looping back onto itself. The Extreme Ultraviolet Imager (EUI), part of the Solar Orbiter mission and operated by the Royal Observatory of Belgium, has given a close-up view of these coronal holes like never before. On 30 March 2022, one of its telescopes, the HRIEUV (High Resolution Imager in the EUV), snapped images every 3 seconds during 30 minutes with pixels corresponding to roughly 120 km on the Sun (see Figure 17 below). The Sun is the only star whose atmosphere we can observe in such detail, but it is likely that what we learn about the Sun is relevant for the other stars as well.

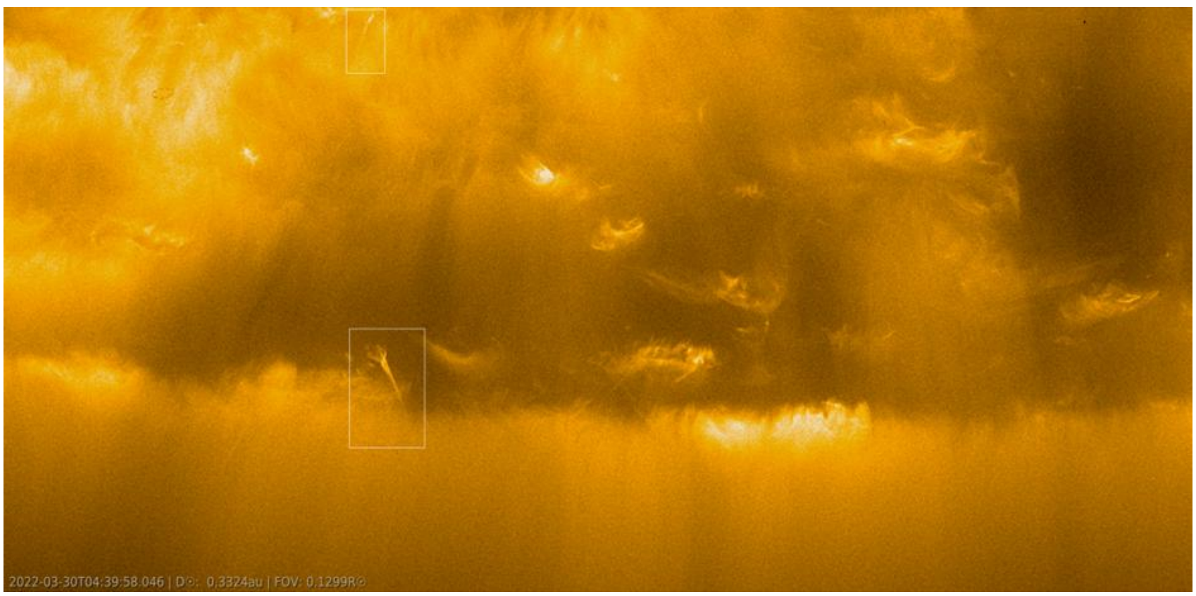

Figure 17: The south pole of the solar corona as imaged by EUI on board Solar Orbiter. The darker area corresponds to a coronal hole where the magnetic field does not return to the Sun and from where the fast solar wind is emanating. We also see large jet-like eruptions (white boxes), caused by magnetic activity on the Sun's surface. These eruptions create streams of solar material along magnetic field lines.

Large jet-like eruptions are frequently seen in the solar corona. They are understood as events in which a small local magnetic loop reconnects with the ambient 'open' magnetic field line. In the process, an eruptive flow is created along the open magnetic field line and potentially contributes to the solar wind. But it's not just the big events that catch our attention. The Solar Orbiter mission has unveiled something new: miniature jets, lasting only 20 to 100 seconds, and spanning just a few hundred kilometers wide. Despite their small size and brief lifespan, these jets propel solar material at astonishing speeds, up to hundred kilometers *per second*.

Finding these tiny jets wasn't easy. Given the small dimensions and short timescales, the smallest events are not resolved, not even with the state-of-the-art HRIEUV performance. Also, as these events are close to the instrument noise level, it is very hard to detect them by software. The data were therefore scanned manually, and careful visual checking revealed 120 jets.

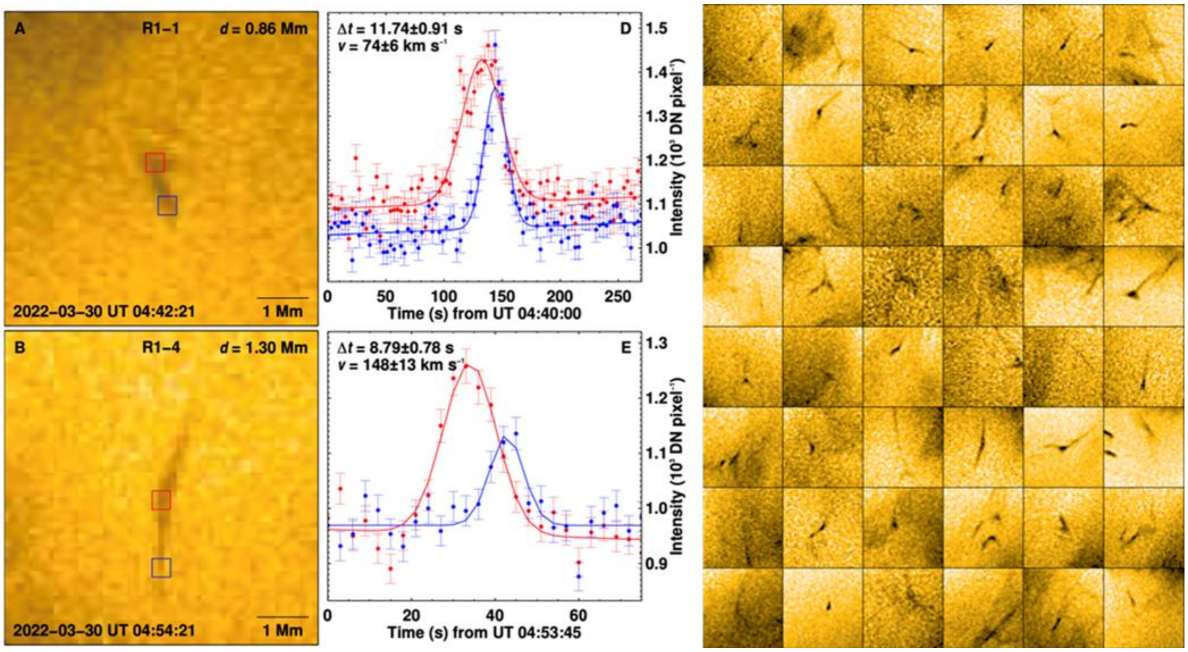

Figure 18: Some examples of the newly discovered miniature jets. The images on the left and right have an inverted color table such that the bright jets are seen as dark features. As these small jets are close to the spatial resolution of the instrument and barely stand out above the noise, it is hard to see the individual motion. Therefore, a special technique was employed for the graphs in the middle panel: The red and blue curves are the light curves of the respective squares on the left. One can see that the foot points (red squares) brighten systematically earlier than the jet tops (blue squares).

Based on these 120 jets, an analysis was performed on the morphology (Y-shaped jets, linear jets), the origin (so-called plume and inter-plume regions), and the mass and energy flux. It was estimated that these jets have an energy content of 10^{17} J (10^{24} erg), which is 10^{12} times smaller than the larger flares, therefore, these jets have been baptised “picoflare jets”. Further, conservative, estimates revealed that the picoflare jets can account for at least 20% of the solar wind mass flux and energy flux of the solar wind from coronal holes. This estimate is considered a lower limit as there is little doubt that smaller, yet more frequent, unresolved events are hiding in the data.

During the timeframe these observations were conducted, the solar corona exhibited what's known as a “solar minimum configuration.” This phase is marked by the presence of large coronal holes at each pole of the Sun, forming an overarching dipole structure in the solar magnetic field. As we edge closer to solar maximum, this orderly dipole structure breaks down into numerous smaller dipoles known as active regions, and with coronal holes appearing anywhere on the solar surface.

Looking ahead to the later years of the Solar Orbiter mission, around 2030, we anticipate the return of solar minimum conditions, characterised by coronal holes reappearing at the poles. However, by that time, plans are in place to tilt the satellite's orbit out of the ecliptic plane by more than 30°. This adjustment opens up exciting possibilities. It will enable us to revisit these observations and study the picoflare jets from a different vantage point: a more top-down perspective rather than the current sideways view. By changing our angle of observation, we can gain fresh insights into the behavior of these miniature solar phenomena, enriching our understanding of the Sun's dynamic processes.

This research was published in Science (Chitta et al. 2023), and advertised in a press release by ESA and by the STCE.

Travelling ionospheric disturbances caused by the Turkey earthquake

The ionosphere is mostly driven by the Sun, and most ionospheric disturbances can be traced back to solar and heliospheric sources, such as solar flares and CMEs. However, it has been known for a long time that the ionosphere can also be affected from the bottom side, by disturbances travelling up from the lower atmosphere or the lithosphere. These kinds of disturbances tend to be smaller in amplitude and shorter in wavelength than those produced by solar phenomena. Nevertheless, they can have significant effects in technologies such as HF radio and high-precision GNSS applications. As such, in recent years, the ionospheric disturbances from the bottom side have seen a lot of renewed research interest. Due to their generally short periods, bottom side disturbances are more difficult to detect and characterise. In order to complement the observations of the Dourbes ionosonde, which in its nominal configuration observes only with a five-minutes time-resolution, a continuous Doppler sounder system has recently been installed in Belgium. By observing the Doppler variations in a continuous wave, this instrument can observe much faster variations in the ionosphere.

Figure 19: Transmission antenna in Dourbes, continuously transmitting at 4.59 MHz.

On 13 February 2023, there was a major earthquake in Turkey. In fact, there were two almost equally powerful shocks at 01:17 UT with magnitude 7.8 and one at 10:24 UT with magnitude 7.7. Earthquakes of this magnitude are known to be able to cause disturbances in the ionosphere, via atmospheric waves travelling up from the ground. The plot below shows the Doppler shifts detected over Belgium between 10:30 and 11:30 UT (due to the low ionization level during the night, effects from the first shock were not clearly observed).

Two different types of disturbances can be seen. First, there is a sharp disruption at 10:43 UT. This happened about eight minutes after the seismological station in Dourbes detected the arrival of the Rayleigh surface wave. This delay of about eight minutes is typically seen in such events, and corresponds to the time it takes for a disturbance to travel from the ground to the ionosphere. Starting at 10:46 UT, a longer period of disturbances is seen. These are related to the infrasound propagating horizontally from the epicentre. Following the earthquake, a joint effort by various European ionospheric observatories was undertaken to analyse the ionospheric disturbances resulting from it, using not only the Doppler sounder data but also ionosondes and other instruments.

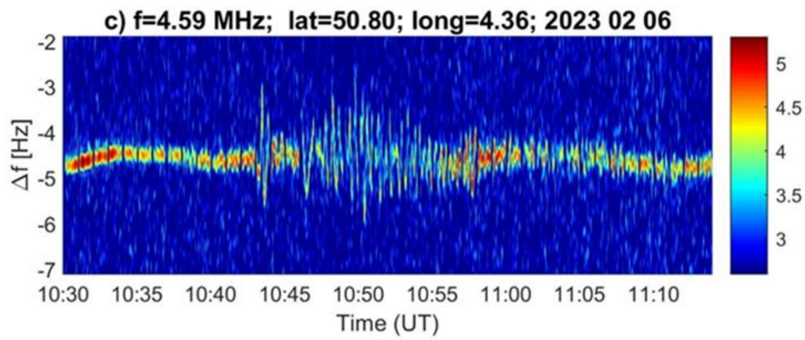

Figure 20: Doppler shift measured over Belgium after the Turkey earthquake of 13 February 2023.

Effects of Solar Energetic Particle (SEP) events on the radiation belts

The Energetic Particle Telescope (EPT) is a charged-particle spectrometer that allows us to measure the fluxes of energetic electrons, protons and alpha particles trapped in the Van Allen radiation belts and

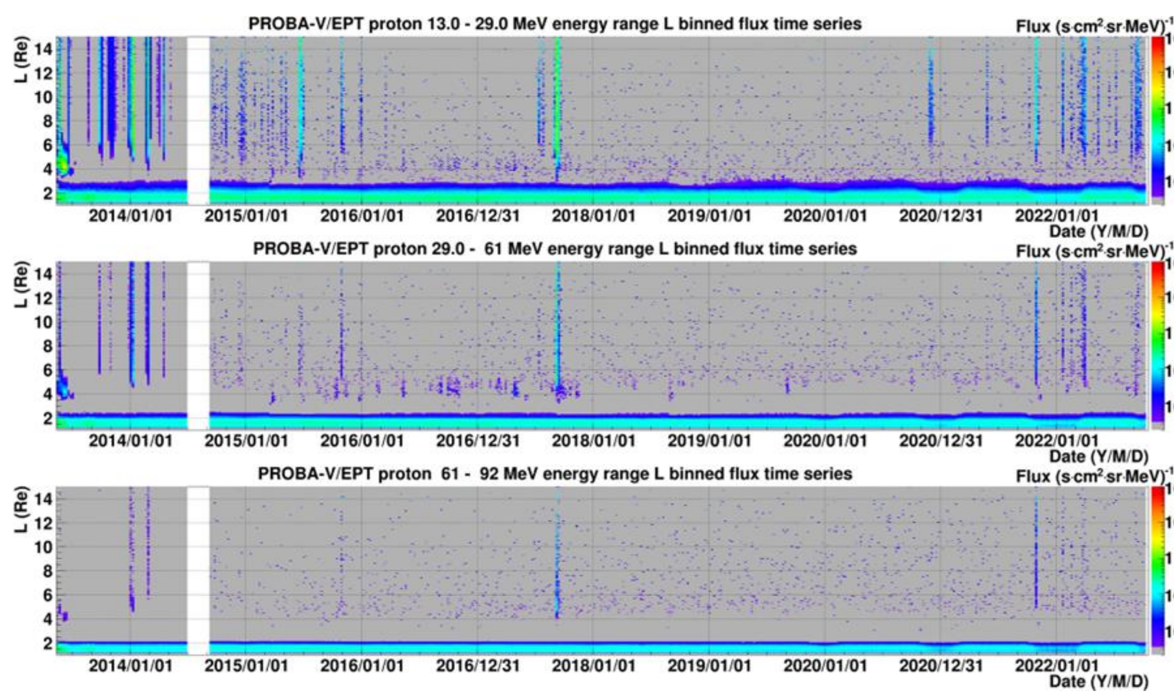

Figure 21: Proton flux (color scale) observed by EPT in Channel 2 (13-29 MeV, upper panel), Channel 3 (29-61 MeV, middle panel) and Channel 4 (61-92 MeV) (bottom panel) as a function of L and time from 7 May 2013 up to October 2022. The parameter L describes the set of magnetic field lines that cross the Earth's magnetic equator at L earth radii.

especially those injected in the magnetosphere during solar events. The EPT is accommodated on board the PROBA-V satellite launched on 7 May 2013 on a Low Earth Orbit (LEO), 820 km altitude, and 98.7° inclination. More than 10 years of data are now available and provide many new results.

As illustrated in Figure 21, strong Solar Energetic Particle (SEP) events, like in January 2014, June 2015 and September 2017, injected energetic protons at high latitudes and at high values for the McIlwain parameter L (i.e. at high radial distances (in earth radii) in the equatorial plane). Moreover, big geomagnetic storms, including those following SEP a few days after, can cause losses of protons at the outer border of the proton belt which are continuously trapped at L<2, due to magnetic field perturbations.

The analysis of the proton flux variations observed by the EPT at energies > 9.5 MeV from the launch of the PROBA-V satellite on 7 May 2013 up to October 2022 showed also an anti-correlation between the proton fluxes and the solar activity. From Figure 22 showing the map of proton flux ratio of 2019/2014 between 92 and 126 MeV, it can be observed that the fluxes are higher at solar minimum (2019) than at solar maximum (2014) at low L corresponding to the northern border (see red colour) of the South Atlantic Anomaly (SAA), the coloured region in Figure 22 where the measured fluxes are observed to be very high at low altitude. On the contrary, in the southern part of the SAA, along L=1.7-2, the flux has decreased in 2019 by a factor 1.5-2 (see dark blue region). This observed solar cycle modulation of the inner belt is mainly due to losses by increased atmospheric interactions during solar maximum.

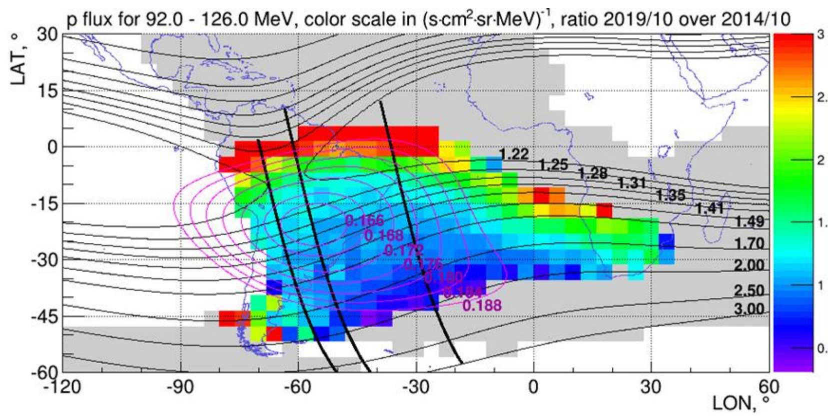

Figure 22: Geographical maps of the ratio of 2019 data divided by 2014 data for the monthly averaged proton flux in Channel 5. The bold black lines are parts of trajectories showing how EPT crosses the SAA during night passes from south to north. The grey areas are those where the fluxes are below minimum, i.e. 10^{-2} s^{-1} cm^{-2} sr^{-1} MeV^{-1}, and the white areas are those where no data fulfill the selection criteria: night side data with boresight orientation 90°±10°. Iso-L lines and Iso-B lines are shown by black and pink lines respectively. (from Pierrard et al. 2023)

A double peak in the proton belt is also observed during long period of measurements for the EPT channel of 9.5-13 MeV only. The narrow gap between the two peaks in the inner belt is located around L=2. This corresponds to a splitting of the proton belt, separating the SAA into two different parts, North and South. The high-resolution measurements of PROBA-V/EPT allow the observation of small-scale structures that brings new elements to the understanding of the different source and loss mechanisms acting on the proton and electron radiation belts at low altitude.

Auroral research from Skibotn, Sweden

Optical auroral spectra obtained at the Skibotn Observatory

In October 2023, a spectrograph ASIS (Auroral Spectrograph In Skibotn) has been permanently installed by BIRA-IASB at the Skibotn Observatory in Norway, in collaboration with University of Tromsø and IPAG (Institut de Planétologie et Astrophysique de Grenoble, France). The goal is to routinely monitor the auroral spectrum during the entire winter period. Currently, only the TREx (Transition Region Explorer) spectrographs located in Canada can provide similar type of data.

The instrument uses a 60 mm diameter guiding lens with a field-of-view of about 4° pointing field-aligned (approximately 11° from the vertical). Light is collected using a reflective collimator to create an output beam into a 600 μm optical fiber and inject it into the entrance slit of a spectrograph. The spectrograph has an adjustable slit and a turret with 3 gratings with 300, 600 and 1800 lines/mm. The dispersed light is imaged on a 16-bit CCD camera with 1024 x 256 pixels, and cooled down to -70°C using a Peltier.

Figure 23: Pictures of the ASIS spectrograph. (left) The guiding lens pointing field-aligned and looking through the acrylic dome at the Skibotn observatory. Also visible are the fiber collimator and the optical fiber. (right) the SR303i spectrograph and the iDUS CCD camera from Andor.

Auroral spectra between about 400 and 700 nm have been continuously recorded during the entire 2023-2024 winter with a time resolution of 30 seconds, using the 300 lines/mm grating and a slit of 100 nm width providing a wavelength resolution of approximately 0.3 nm.

An example of uncalibrated spectrum obtained on 5 November 2023 with ASIS during a strong geomagnetic storm is provided in Figure 24. The top panel shows the horizontal component of the magnetic field recorded in Tromsø (about 60 km from the Skibotn observatory) which displays a strong sudden drop below -1000 nT followed by a recovery phase around 17-18h UT. The spectrum recorded at 17h31m30s is shown in the middle panel and is dominated by very intense emission lines from the atomic oxygen at 577.7 nm (green line), at 630.0 and 636.6 nm (red line doublet), and an intense band from N_2^+

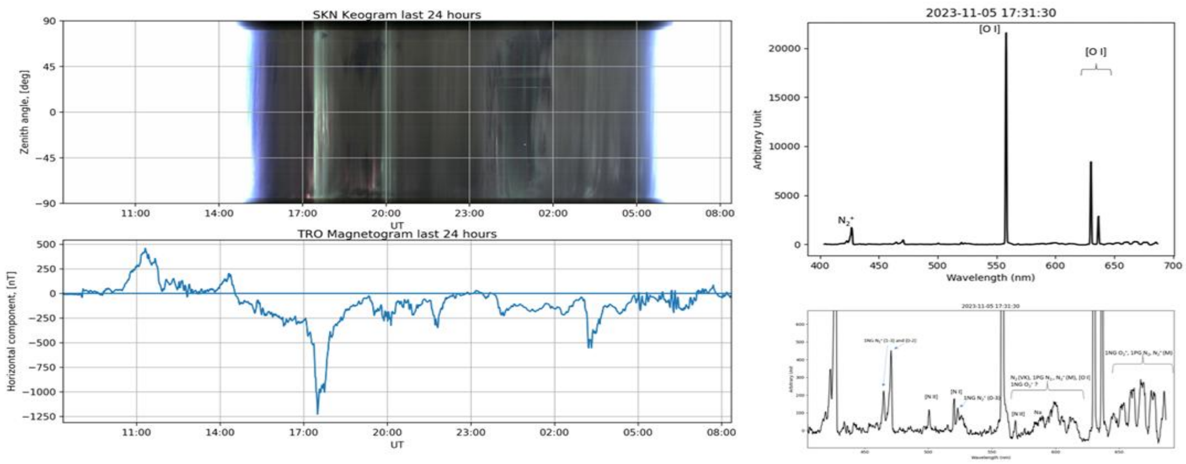

Figure 24: Data from 2023-11-05. (left) Magnetogram at Tromsø (upper right) Raw spectrum at 17h31m30s (lower right) Zoom in intensity of the same spectrum.

at 427.8 nm (blue line). A zoom in intensity is provided in the bottom panel showing a large number of additional emission bands, mostly from N_2 and N_2^+. These emissions occur at much lower altitude indicating the presence of very energetic electrons precipitating from the magnetosphere.

A calibration in flux is currently under way with the help of the Belgian Radiometric Calibration Laboratory (B.RCLab) and will allow the computation of line ratios or a comparison with synthetic spectra generated using kinetic electron transport codes. Both approaches will provide an estimate of the precipitating fluxes for electrons but also possibly for protons.

In 2024, a database of these low resolution auroral spectra will become accessible to the community. These data will nicely complement those obtained with the upcoming EISCAT_3D radar located a few kilometers from the observatory and data from other optical instruments located at the Skibotn observatory itself. We will also consider extending the wavelength range to 800 nm (hence covering interesting lines such as e.g. the 777.4 nm line from atomic oxygen) and using the 1800 lines/mm grating during specific campaigns to obtain higher resolution spectra.

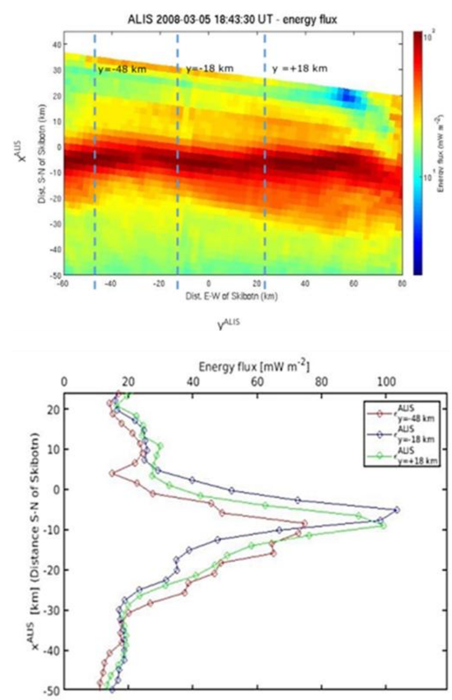

Figure 25: (top) The 2D flux of energy precipitating into the auroral ionosphere reconstructed from ALIS observations performed at Skibotn (Sweden) of an electrostatic auroral arc, on 5 March 2008. (bottom) 1D slices extracted from the 2D map at three different longitudes eastward from Skibotn (from Echim et al. 2023).

Magnetosphere - Ionosphere coupling studies

The STCE participates in the development of new capacities to better understand the coupling between the magnetosphere and the auroral ionosphere and to quantify the effects due to the solar wind driving. Part of this effort is represented by modelling activities devoted to the magnetospheric generator of quiet stable discrete arcs.

Optical observations of aurora provide information about the local electromagnetic and plasma conditions in the ionosphere, where the impact of energetic electrons produces auroral light emissions. The electrons gain energy through acceleration by static or dynamic electric fields formed along their path, extending, along magnetic field lines, from the magnetospheric source down to the upper ionized atmospheric layers where they collide with atoms (e.g., Oxygen and/or Nitrogen) which emit light at various wavelengths. We use a magnetosphere-ionosphere coupling model developed originally to estimate the intensity of auroral emissions for various magnetospheric configurations, to solve the inverse problem this time. Indeed, we use the optical observations of steady electrostatic auroral arcs to identify the conditions in the magnetospheric source, at high altitudes, in other words to characterise the physical properties of aurora's "roots".

We first created a database where we included a family of models for the magnetospheric generator and the auroral arc it produces. Then we developed a mathematical algorithm which searches in the database which model fits best the optical observations from ground. Thus, we obtain an estimation of the magnetospheric plasma properties at the origin of the quiet discrete arc. We recently applied this approach on observations of a quiet electrostatic arc performed by the Scandinavian ALIS network, in Skibotn (Sweden). The data were processed such that we were able to extract the flux of energy precipitating from the magnetosphere into the auroral ionosphere, as shown in Figure 25. We apply our mathematical algorithm for three different azimuthal locations along this arc and reconstruct the structure of the magnetospheric structure at the origin of the arc, as shown in Figure 26.

We find that the auroral arc is likely produced by a plasma interface formed at the contact between plasma sheet-like plasma and trough plasma at roughly 4 earth radii altitude (approx. 25.000 kilometer) above the arc. This interface bears properties typical for a tangential kinetic equilibrium between two plasmas with different properties; it sustains a V-shaped electrostatic potential that drives the auroral current system, with field-

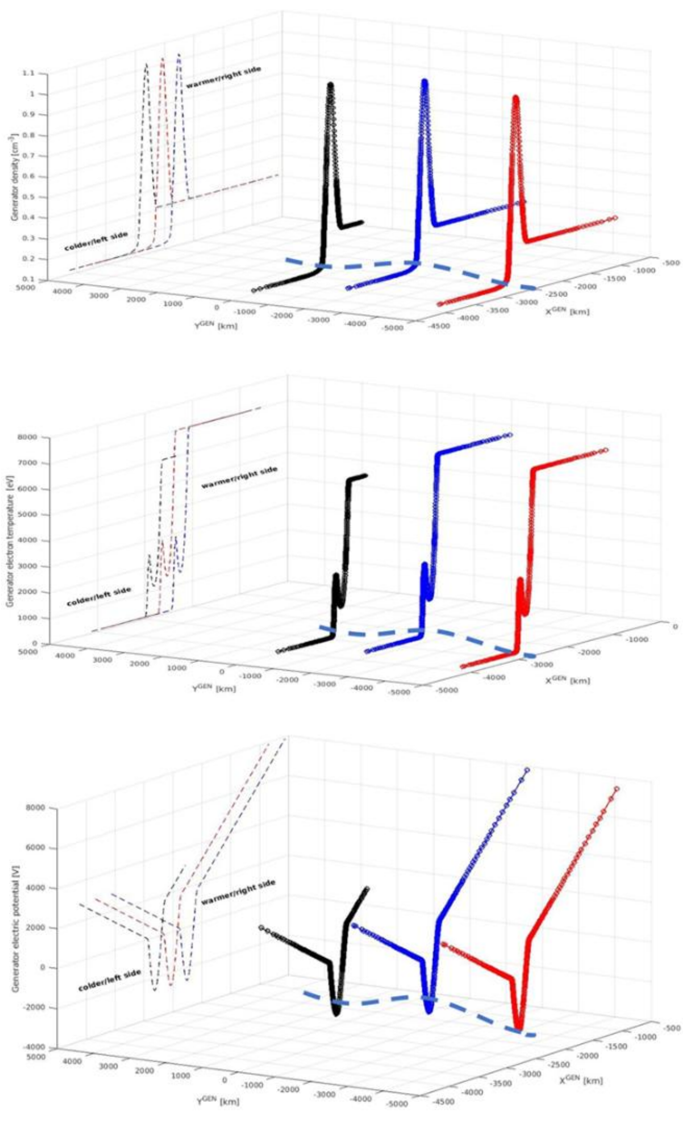

Figure 26: Description of the magnetospheric plasma properties at the origin of the quiet electrostatic arc observed by ALIS on 5 March 2008 at 18:43:30 UT. The panel shows the magnetospheric plasma density, the magnetospheric electron temperature; the magnetospheric electrostatic potential. The dashed blue line suggests the position of the interface's centre interpolated from the positions of the centres of the three 1D cuts (from Echim et al. 2023)

aligned currents closing through the topside ionosphere. It is precisely this current system which allows the formation of a parallel potential difference that accelerates electrons downward into the auroral ionosphere and contributes to a relative increase of the arc's brightness in the azimuthal direction. The geometry of the arc may be linked to a local spatial deformation (over roughly 500 km) of the magnetospheric plasma generator interface (Echim et al. 2023).

Deep learning helps scientists in classifying sunspot groups

Solar activity has long been measured by the number of dark spots, called sunspots, appearing on the Sun's surface and visible from the Earth. Sunspots appear in groups as a manifestation of solar magnetic activity. The intense magnetic fields embedded within sunspots inhibit convection, cooling the corresponding surface regions. Corresponding areas on the solar surface where temperature has been reduced as compared to their surroundings appear as dark spots when viewed in the visible continuum spectrum, also known as White Light (WL). This enhanced magnetic field is the driving force behind the solar variability that influences the space environment of the Earth on a day-to-day basis. Its evolution may lead to magnetic reconnection and subsequent energy release, causing solar flares, or coronal mass ejections when material is ejected. The morphology of sunspots is correlated with solar flare occurrence and has therefore received a lot of attention since the end of the 19th century.

The McIntosh classification scheme describes the WL structure of sunspot groups. This scheme has three components: the first component ‘Z’ describes the longitudinal extent of the sunspot group, component ‘p’ provides information on the size and symmetry of the gray area around a sunspot called ‘penumbra’, and component ‘c’ gives information on the distribution or compactness of spots within a group. This scheme supports several flare forecasting methods based on historical records of flares occurring in each McIntosh class. Attributing a McIntosh class to a sunspot group is thus fundamental for space weather operations. Traditionally such attribution is done manually, a time-consuming task prone to errors.

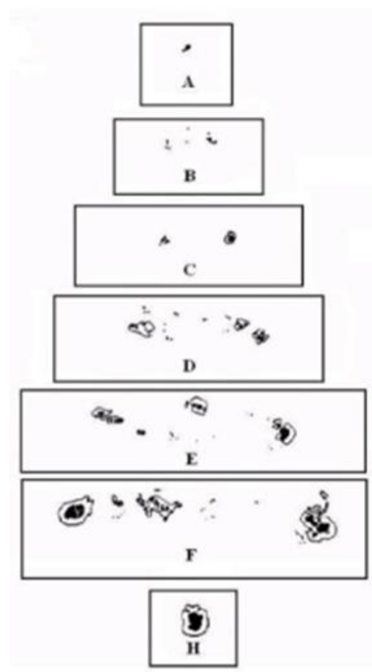

Figure 27: Representation of the Z component in the McIntosh scheme, describing the longitudinal extend of sunspot groups, and the process of development (class A to F) and decay (class H) of a sunspot group.

The USET ground-based station located at the Royal Observatory of Belgium provides since 2002 WL images of the Sun. In the BRAIN DeepSun project, we employed such WL observations recorded from 2002 till 2019 to build “SunSCC”, a fully automated system addressing three essential tasks: the segmentation of sunspots from their background, their clustering into sunspot groups, and finally their classification according to the McIntosh scheme. The SunSCC pipeline is depicted in Figure 28. It takes as input 2048x2048 USET WL images and returns as output segmentation masks of individual sunspots as well as sunspot groups and their McIntosh classification, to which a reliability factor is attributed.

The first block in SunSCC deploys a convolutional neural network (CNN) with a 'U-shape'. These so-called U-net architecture have proved efficient in segmenting images in various fields such as medical imaging and natural images analysis. Their weights or parameters are estimated during a training phase, which requires a first assessment of segmentation masks. The latter are typically provided by a traditional, unsupervised, segmentation method involving a thresholding on the WL intensity image. Having a unique threshold is however not optimal, as the level of illumination may differ locally e.g. due to the presence of clouds or atmospheric seeing. Our solution was to train the CNN using three different segmentation masks corresponding to different thresholds. The trained CNN is then able to segment small and large sunspots more accurately than traditional methods.

The second block receives as input the segmentation map from the first block and aggregates the detected individual spots into sunspot groups. We developed a tailored clustering method based on the mean-shift algorithm. It exploits local gradients of a density function to find modes, corresponding to clusters of spots. We employed anisotropic kernels to estimate this density function, to account for the fact that sunspots groups are more elongated in longitude than in latitude. We matched sunspot groups bounding boxes from the USET sunspot group catalog with bounding boxes found by the mean-shift algorithm and obtained that 80% of USET sunspot groups were correctly recovered by our clustering method.

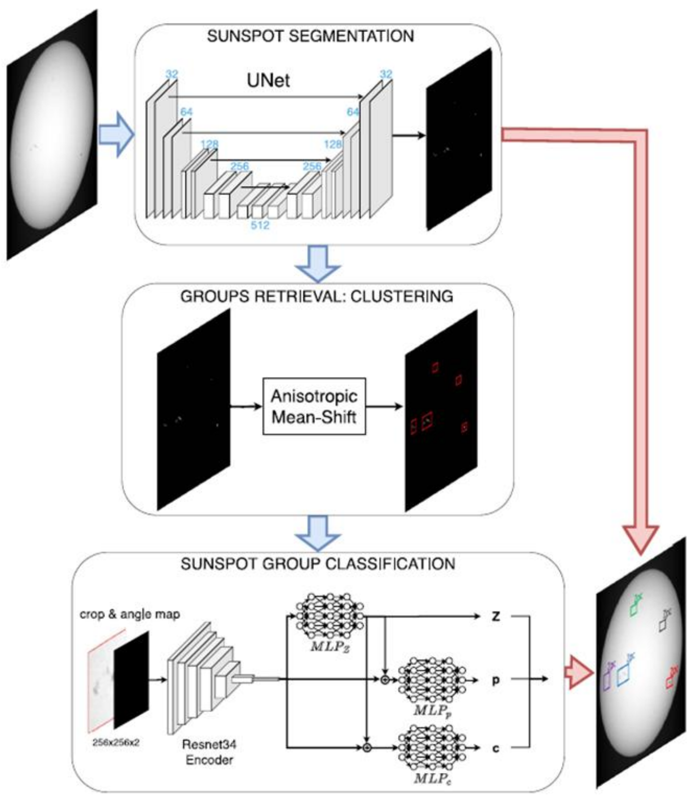

Figure 28: SunSCC pipeline for sunspot segmentation, clustering, and classification. Full-disc images with a resolution of 2048×2048 are provided as input. For segmentation, the U-net network comprises 5 levels and 4 down-sampling steps in the encoding part, and reversely 5 levels and 4 up-sampling steps in the decoding part. The detected sunspots are aggregated into sunspot groups by a modified mean-shift algorithm. Each identified group is provided along with an angular distance map to a classification network composed of a Resnet34 image encoder and three MLPs with 4 hidden layers and Rectified Linear Unit (ReLU) activation function. Each MLP is specialised in the classification of one component in the McIntosh system.

An identified sunspot group is provided to the third block, together with its angular distance map, for classification task. This third block is composed of an image encoder followed by three Multi-Layer Perceptrons (MLP), one for each component of the McIntosh scheme. More precisely, our classifier relies on a convolutional backbone with 34 layers called ResNet34 to encode the visual information associated to the sunspot group to be classified. Output of the ResNet34 is given as input to three MLPs. To mimic the dependency of the p- and c-components on the Z-component, the MLPs are organised hierarchically so that the output of MLP_Z is concatenated with the output of ResNet34 and given as input to MLP_p and MLP_c.

To obtain a measure of confidence in the chosen class, we adopt the precepts of ensemble learning. Multiple instances of the classification network are initialized with different seeds and trained independently, to produce multiple classifiers. For each sunspot group, we obtain a pool of predictions, which are then combined into one single output via a majority vote. Inconsistencies across the ensemble of classifiers are a valuable clue to identify misclassification by the majority vote: We observed that correct ensemble prediction have low discrepancies amongst the votes, while incorrect ensemble predictions have their votes more distributed among the classes. This CNN-based classifier shows comparable performance to methods using continuum as well magnetogram images recorded by instruments onboard space mission. We plan to have the SunSCC pipeline running at ROB and producing daily sunspot masks, grouping, and classification. This will constitute an aid to space weather operators and allow quality control on the USET sunspot group catalog.

This research was published in Journal of Geophysical Research: Space Physics (Sayez et al. 2023).

STCE seminar on "Point spread function corrections in solar physics" by Stefan Hofmeister. The wide-field image shows many on-site attendees, but the seminar could also be followed online. Throughout the year, there are a few dozen of -mostly hybrid- seminars and presentations organised by several institutes such as the STCE, KUL (CmPA), SCOSTEP, ISWI,… (Set-up: Petra Vanlommel)

Instrumentation and experiments

Delivery of the spacecraft platform for the PROBA-3 mission

PROBA-3 is a technology demonstration mission of ESA. It will be launched in September 2024 and will demonstrate techniques and technologies of precise formation flying. The PROBA-3 platform will consist of two spacecraft that will fly in a precise formation. The bigger spacecraft (coronagraph spacecraft) hosts the optical telescope, and the smaller spacecraft (occulter spacecraft) carries the circular occulting disk. During extended periods of time (up to 6 hours), the occulter spacecraft will cover the bright solar disk, thus allowing the dimmer corona to be seen, similarly to observations of a total solar eclipse. Together, the two spacecraft form a giant coronagraph (i.e. an instrument to observe the corona by occulting the solar disk) called ASPIICS, which stands for the Association of Spacecraft for Polarimetric and Imaging Investigation of the Corona of the Sun.

The two spacecraft must keep the precise position and orientation ("fly in formation") with respect to each other and to the Sun. The distance between the two spacecraft during coronal observations will be around 144 meters, and the precision of their alignment will be around a few millimeters. This will allow blocking the bright light of the solar disk to observe the corona in eclipse-like conditions, i.e. close to the solar limb and with very low straylight. The ASPIICS observations will provide data that are crucial to solving several outstanding problems in solar physics, namely the origin of the solar wind and the physics of coronal mass ejections. ROB hosts the Principal Investigator (PI) of ASPIICS who leads the international science team, makes sure that the coronagraph is manufactured in agreement with the scientific requirements, and prepares the data exploitation.

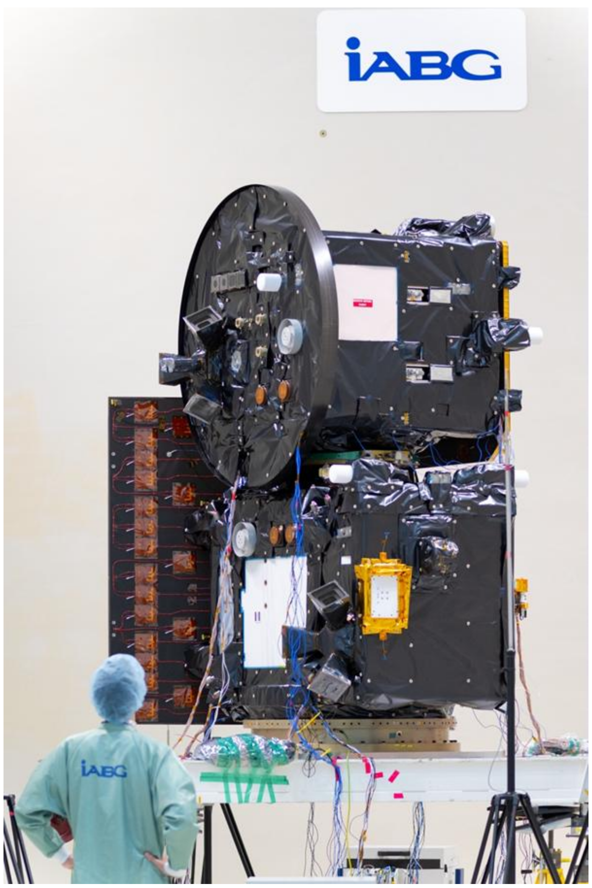

Figure 29: The two PROBA-3 spacecraft in stack before thermal vacuum testing at IABG (Germany) in July 2023. The occulter spacecraft is on the top, featuring a circular occulting disk. The coronagraph spacecraft is at the bottom, with solar panels extending to the left. The spacecraft will be launched in this stack configuration in September 2024. (Credits: ESA - S. Corvaja)

Significant progress was reached by the engineering teams assembling the PROBA-3 spacecraft platform in 2023. The spacecraft delivery event was held on 9 March at the premises of Redwire Space in Kruibeke, Belgium. This event marked the successful completion of the integration of the two spacecraft, which was led by Redwire Space. The assembled spacecraft were presented to the representatives of funding agencies of Belgium and Spain (two countries contributing the most to the PROBA-3 spacecraft platform), industry (Redwire Space, Sener

Aerospace), as well as ESA and the scientists. The ASPIICS PI gave a presentation about the upcoming ASPIICS science to the funding agencies, science and engineering teams.

In July - August, the two spacecraft underwent thermal vacuum testing at IABG (Germany). This type of testing is always made to simulate the space environment, in which the spacecraft will operate. Thermal vacuum testing demonstrated that the two spacecraft are able to withstand successfully the harsh conditions of the space flight. After that, the final testing of the two spacecraft continued at Redwire Space in Kruibeke.

Figure 30: Members of the Science Working Team of PROBA-3 inspecting the occulter spacecraft. The coronagraph spacecraft can be seen in the background behind the curtain. (Credits: ESA - J. Versluys)

On 27 November, the members of the international Science Working Team of PROBA-3 paid a visit to the spacecraft in the clean room in Kruibeke. The ASPIICS PI gave a presentation about the PROBA-3 mission to the science and engineering teams.

Publication of Earth radiation balance dataset (2018 to 2023)

The RMI's "remote sensing from space" team has published a new dataset from the GERB instrument. These observations are important for Earth's radiation balance.

Since 2004, the RMI's "remote sensing from space" team has participated in the operation of the Geostationary Earth Radiation Budget (GERB) instrument, in a consortium led by the Rutherford Appleton Laboratory (RAL; UK). The fourth such instrument is on board of EUMETSAT's Meteosat Second Generation 4 satellite. EUMETSAT is the European organisation for the operation of meteorological satellites, which also provides images of atmospheric conditions for the RMI's team of forecasters.

Continuous measurements of the Earth's radiation balance are important for studying climate, as it is one of the ways to understand climate warming. The radiation balance consists of incoming solar radiation on one side, and reflected solar radiation and thermal radiation on the other. Reflected solar radiation contains visible light, and thermal radiation contains infrared light. In both parts, there is an influence of atmospheric conditions, in the form of aerosols and clouds.

GERB is a broadband radiometer specialising in the measurement of total (shortwave and longwave) radiation and is the only such instrument in geostationary orbit: at about 35.800 km altitude, the satellite remains at a fixed longitude over the Earth, allowing it to make continuous observations over the European and African continents. In contrast, satellites in low orbit can observe the entire Earth, but never stay over the same region.

The GERB instrument provides data in the form of images, containing solar and thermal radiation measured at the top of the atmosphere, and with a pixel size of about 50 km at the equator.

Data reception from GERB is provided by Rutherford Appleton Laboratory; then the data are transmitted to the RMI in a format that is not directly usable for scientific research. The RMI team is then responsible for creating "level 2" data, by using additional information from another instrument on the satellite and from specialised models. The resulting products also have a much higher spatial resolution, with pixels the size of 9 km at the equator.

A total of four GERB instruments have been launched, active from 2004 to 2007 (GERB-2), from 2007 to 2013 (GERB-1), from 2013 to 2018 (GERB-3), and from 2018 to 2023 (GERB-4), respectively. Currently, GERB-3 (at 0° longitude) and GERB-1 (over the Indian Ocean) provide data. GERB-4 sits on a still-active satellite and could be reactivated in the future.

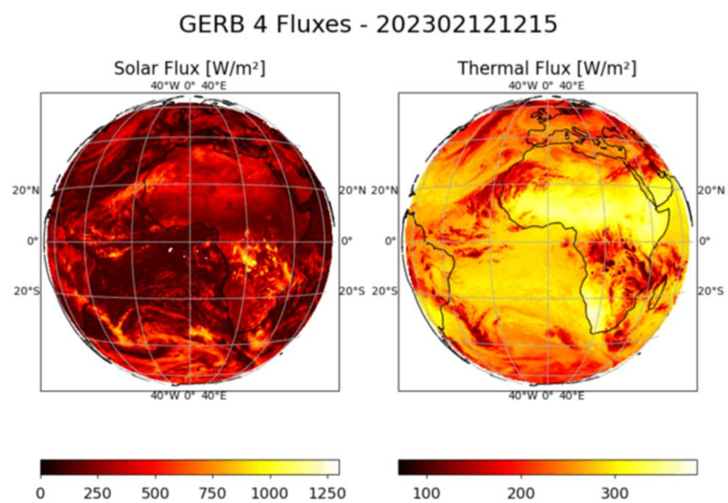

Figure 31: Data from the GERB instrument, fluxes of reflected solar radiation on the left and of emitted thermal radiation on the right). Data from EUMETSAT - RAL - RMIB. For an animation showing a whole day, see: ***https://gerb.oma.be/public/pdebuyl/G4_20230212_FD.gif***

Data from the GERB-4 instrument were recently released to the scientific community under the name "GERB 4 V100 level 2 dataset", which contains short- and longwave radiation and fluxes at the top of the atmosphere. Data from GERB-3 and GERB-1 will also be used in the future, to make the best use of the instruments' lifetime.

Radiometric characterisation and calibration of INSPIRE-SAT 7 sensors

BIRA-IASB has a long-standing involvement in space experiments and many contributions were provided for the design of electronics or opto-mechanic devices and pre-flight characterisations. The D42 section of BIRA-IASB is dedicated to solar irradiance measurements and radiometry. A continuous collaboration with the LATMOS (Laboratoire Atmosphères, Milieux, Observations Spatiales; France) took place since the 80's for Solar Spectral Irradiance (SSI) from space using space qualified instrumentation. For example, the spectroradiometer SOLSPEC (for SOLar SPECtrum) contributed to the dissemination of reference solar spectra above the atmosphere (a key input for climate research), measured during six short- and long-duration space missions (Meftah et al. 2018).

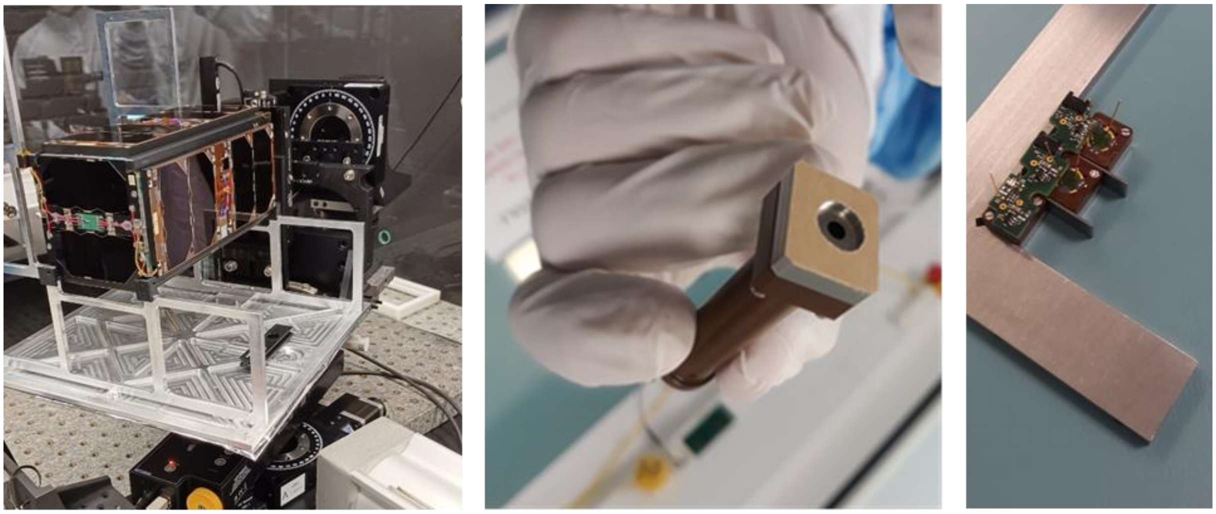

Figure 32: Integration of INSPIRE-SAT 7 on its dedicated motorized mount at B.RCLab and view of miniaturized sensors.

Now, the LATMOS is active in New Space for faster development of payloads, namely for nanosatellites within the INSPIRE (International Satellite Program In Research and Education) program, dedicated to Earth Radiation Budget (ERB) measurements. Within this SOLSPEC heritage, the D42 was involved in 2023 in the radiometric characterisation and calibration of some Flight model (FM) and Spare flight model (SM) sensors of the 2-unit INSPIRE-SAT 7 satellite. Mainly those dedicated to UV and VIS solar irradiance. BIRA-IASB provided the D42 in-house laboratories and facilities equipped for radiometric pre-flight characterisations in the B.RCLab (Belgian Radiometric Characterization Laboratory). The LATMOS sensors tested in Belgium were designed for wavelength integrated SSI measurements in the UV (around 220 nm) and the visible part of the solar spectrum. Respectively: UV (based on gallium oxide) and TSI sensors. For a full pre-flight characterisation, it was required to:

- measure the linearity, angular and relative spectral responses,
- perform the absolute calibration to convert the electronic signal in irradiance (W/m²)
- perform a thermal characterisation of dark current and sensor responsivity

With the support of PRODEX and STCE funding, the facilities were optimised to integrate the sensors (or the whole satellite for the FM campaign) on the benches and to adjust the performances (dedicated light sources, adjustment of their intensity). For example, a full characterisation of UV sensors required the use of a spectrometer working under vacuum to explore the spectral response for wavelengths shorter than 200 nm. For the angular responses, rotating stages were used to control the depointing in front of light sources. For the thermal characterisation, a small thermal vacuum chamber was used to explore the temperature range [-20, +40] °C. For the absolute calibration, secondary standards of spectral irradiance (calibrated quartz-halogen and deuterium lamps) were used. Two campaigns were organised, mainly in 2023 to characterise the UV and TSI sensors: FM integrated on all sides of the satellite and several individual spare models.

Thanks to these radiometric campaigns applied to INSPIRE-SAT 7 (now in orbit), it is currently possible to convert electronic signals collected in space from UV and visible sensors into scientific meaningful quantities using measurement equations that apply fine corrections depending on the solar pointing, the thermal environment and the spectral sensitivity of the sensors.

The SIDC team-building day had a lot of fun group and individual activities and experiments. Even preparing your lunch required a serious amount of dedication! (Credits: Luciano Rodriguez and Sergei Shestov)

Applications, modeling and services

Space weather operations and anniversaries

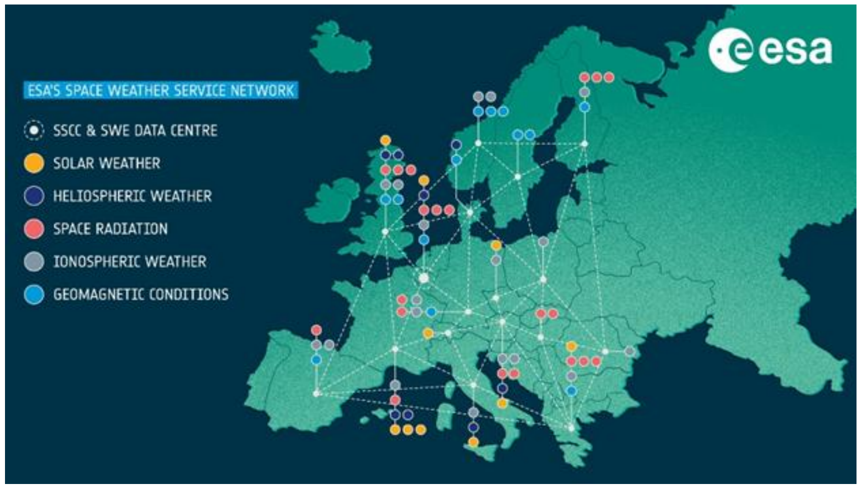

Figure 33: The ESA Space Weather Service Network with the SSCC at the centre.

The year 2023 impels us to look back at the achievements of the ROB Space Weather Operations Team. For many years, the ROB has invested in our aim to become an operational space weather centre. Two of the main projects through which we accomplish this and reach a large number of users, are via the ESA Space Weather Network and the PECASUS consortium. In April 2023, the SSA Space weather Coordination Centre (SSCC) of the ESA Space Weather Network celebrated 10 years since its official inauguration, while November 2023 marked officially 5 years since the Council of ICAO, the International Civil Aviation Organisation, selected "PECASUS" as one of the World Centres for space weather services.

2013-2023: SSCC - the focal point of a growing network

The SSCC is located at the ROB and runs in coordination with our partners at BIRA-IASB. It was originally set up in the context of the Space Situational Awareness (SSA) programme in 2013. As such, it was the first European Space Weather Helpdesk, with operators available to answer questions about the ESA SWE (space weather) Service Network or space weather conditions in general. Since 2020, the ESA SSA programme was replaced by ESA's Space Safety Programme, which aims at mitigating and preventing the impact of hazards from space, protecting our planet, activities and infrastructures. At this time, ROB also took over the leadership of the SSCC at the Space Pole from BIRA-IASB and through these transitions the SSCC has continued to be the focal point of the ESA Space Weather Network user support, providing coordination and the day-to-day monitoring of the continuity and quality of the service.

Figure 34: SSCC room in 2023

The SSCC has led multiple user engagement activities in the network over the last 10 years, with several highlights including the provisioning of dedicated tailored bulletins to high priority users, facilitated by ROB's expert forecaster team. The SSCC has provided bulletins to ESA spacecraft operators such as for GAIA, Venus Express, Mars Express, and BepiColombo, as well as bulletins for spacecraft operators outside ESA and users in other sectors such as Aviation, GNSS and Power System Operations.

Since 2013 the SSCC has coordinated more than 25 releases of the ESA Space Weather Portal (https://swe.ssa.esa.int): the central location for space weather data and products in Europe. The ESA Space Weather Portal now provides access to more than 300 products submitted by more than 50 expert groups. During this period, the number of users registered for the ESA Space Weather Portal has increased from 80 users in April 2013 to over 3600 users in April 2023, highlighting the important work done by the team in raising the awareness of the network.

Additionally, the Solar Expert Service Centre (ESC) in the ESA Space Weather Network, also led by ROB, continues to develop the functionalities, capabilities and expertise in the domain of Solar Weather that are needed within the ESA SWE Network.

2018-2023: PECASUS - the creation of a 24/7 operational system to support civil aviation

PECASUS is the Pan-European Consortium for Aviation Space Weather User Services (https://pecasus.eu/), which was selected to be one of the 3 world centres to provide operational space weather services to the International Civil Aviation Organization (ICAO) in 2018. This service has been continuously provided since it became operational in November 2019.

The countries that make up the PECASUS consortium are Finland (Lead), Belgium (advisory generation hub), UK (internal backup), Poland, Germany, Netherlands, Italy, Austria, and Cyprus.

Since 2019, the STCE has been acting operationally as the central data repository for PECASUS, including continuous monitoring and advisory production hub. Our team of operators is available on-call 24/7, ready to respond and issue warning messages for aviation, based on a set of thresholds pre-defined by ICAO. To achieve prompt and efficient response to any space weather event, the space weather operation team created detailed operator procedures and interfaces allowing the operator to quickly and easily assess the data and create space weather advisories as soon as possible.

As the primary data centre and monitoring hub within the PECASUS consortium, the STCE has designed specific data infrastructure to support regular data inflow from all the data-providing partners, post-processing, and to display the data on internal interactive operational monitoring dashboards.

Additionally, the STCE serves as the Solar Expert Group as well as the Radiation Expert Group, and is also a data provider for models of GNSS impacts.

Since 2020 an additional fourth world centre was added by ICAO, and the task of providing a space weather services for the aviation sector is now divided between the four centres in a rotational system with two weeks of On Duty Center (ODC) periods, followed by Primary Backup Center (PBC), Secondary Backup Center (SBC) and a Maintenance and Observations Center (MOC).

Trajectory and speed reconstruction of meteoroids using BRAMS data

The BRAMS (Belgian RAdio Meteor Stations) network is a project that utilizes forward scatter of radio waves to detect and study meteoroids. This network consists of a dedicated transmitter beacon located in the South-West of Belgium and 50 radio receivers spread across Belgium and neighbouring countries. The transmitter emits a continuous wave radio signal at 49,97 MHz, which is detected by the receiving stations.

The method for the reconstruction of the trajectory of a meteoroid relies on the specular reflection of radio waves off the meteor ionization trail. The specular reflection point is the location along the meteoroid's path where the total distance travelled by the radio wave (from transmitter to meteor and then to receiver) is minimal. To reconstruct a meteoroid's trajectory, the coordinates of one specular point and the three velocity components are needed, leading to six unknowns. Using geometrical considerations and time delays between meteor echoes at different receiving stations, a set of non-linear equations is formed and solved to estimate these unknowns.

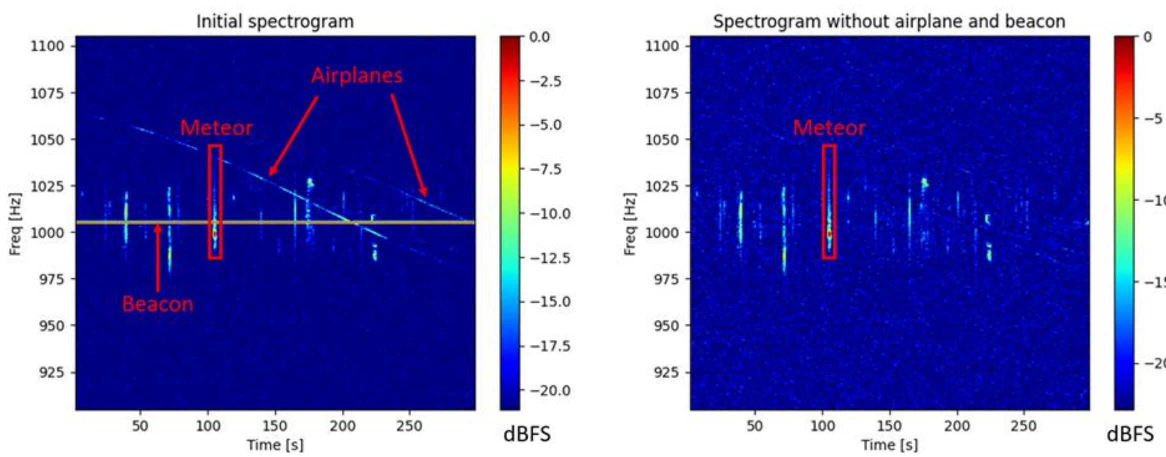

Figure 35: Example of a BRAMS spectrogram before and after airplane and beacon removal. In the two panels, the power is color-coded in dB FS (Decibels relative to Full Scale) and the same meteor echo is highlighted in the red rectangle.

The time delays are a critical part of the measurement. The determination has been improved by the so-called "pre-t_0 technique". This is a method that is used in backscatter radar systems, but that we have adapted for forward scatter systems such as BRAMS. It involves analysing the phase of the meteor echo to extract information about the meteoroid's speed. The phase variation is extracted from the signal and the slope of the distance-time curve obtained from this phase data provides the meteoroid's speed.

One of the nuisances in the analysis of radio reflections off meteor trails is the presence of reflections created by airplanes. Reflection of the BRAMS beacon signal on the metallic structure of airplanes is problematic for the systematic study of meteor echoes. Such airplane reflections can create "wave beating" phenomena when combined with the meteor reflections, perturbing the determination of specular timings. It also destroys useful phase information, necessary for the computation of the pre-t_0 speeds. We have developed a method to automatically filter airplane signals. The main criteria are the duration of the signal (much longer than meteors) as well as its spectral extension (much narrower than meteors). An example of a radio echo spectrogram before and after this process is shown in Figure 35.

To validate the methods, the reconstructed trajectories were compared with optical data from the CAMS (Cameras for Allsky Meteor Surveillance) network in Benelux. The pre-t_0 phase technique significantly improves the accuracy of the trajectory reconstructions. Six out of eight test cases show discrepancies of less than 5% in velocity and less than 2° in inclination compared to CAMS data.

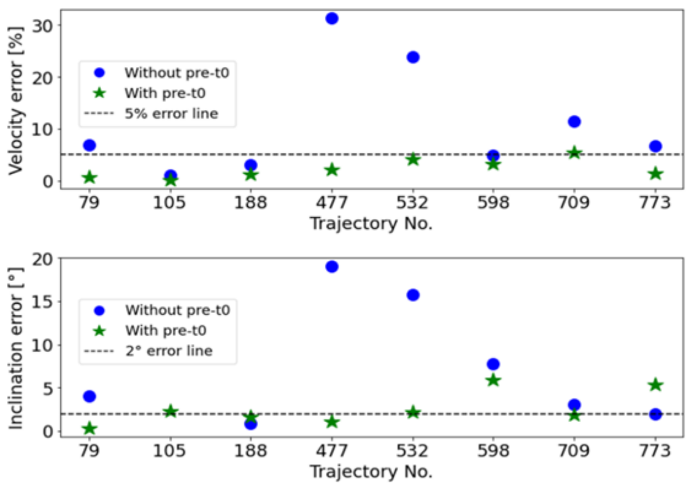

Figure 36: Velocity and inclination errors without interferometry obtained without and with pre-t_0 phase information. The trajectory numbers correspond to the 8 selected CAMS trajectories.

Knowing the meteoroid trajectories and speeds is essential for most applications using BRAMS data. The novel pre-t_0 method allows us to fully exploit the capabilities of BRAMS for applications such as the determination of meteoroid fluxes or sounding of the upper atmosphere (e.g. wind speed measurements). This will also allow us to obtain accurate orbits for faint and small meteors which are not detected by optical systems.

Predicting radiation belts dynamics using neural networks with PROBA-V/EPT data

PROBA-V/EPT electron flux data have been used for the first time to train a deep learning data-driven model with the purpose of investigating the Earth's radiation belts dynamics. The Long-Short Term Memory Neural Network was employed to predict the electron fluxes between 1 and 8 earth radii (R_E) along a Low Earth Orbit. Different groups of inputs involving solar wind and geomagnetic data were tested, based on previous knowledge of their impact onto the high energy radiation fluxes. Two EPT energy

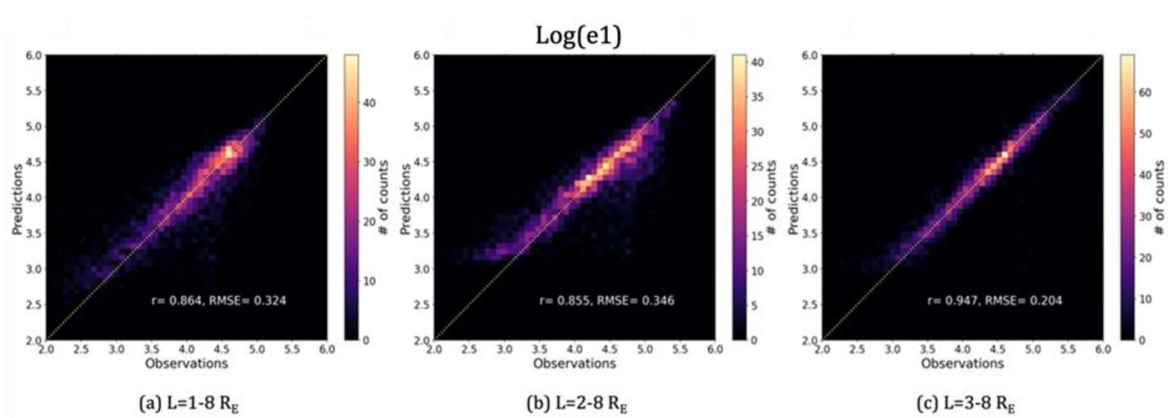

Figure 37: Correlation between hourly Log(e1) observed and predicted fluxes in #/(cm^2 s sr MeV) for a look-back of 48 hours and 1 hour forecast at different L ranges. The group of inputs include L, MLT, Latitude satellite coordinates, SYM-H index and Log(e1).

channels feed the learning procedure for nonrelativistic (e1 = 0.5-0.6 MeV) and relativistic (e5 = 1.0-2.4 MeV) energy electron fluxes. When comparing different L-shell ranges as in Figure 37, deviations from the main diagonal concentrate around the strongest distribution $10^{3.5}$ to 10^{5} electron fluxes units, whereas for the L=2-8 R_E, the extreme lowest count tail seems to deviate more, showing the limitations of the model to simulate the dropouts and the higher flux increments.

The metrics of a simulation considering 48 hours look-back and 12 hours ahead were reported for each hour of the simultaneous forecast. The performance is slightly poorer than one-step forecasts, but they are still very good, in particular for the first steps, and very promising for further investigations. Here, the RMSE remain smaller for the fluxes of higher energy than for those of lower energy.

In summary, a good performance of the model employing different time resolutions from hours to days was demonstrated with a correlation of more than 0.9 between the predicted and out-of-sample fluxes. Further work is in progress to completely tune the present model to predict the electron flux of the radiation belts at LEO with high accuracy and higher resolutions down to steps of some minutes.

A risk indicator tool for deep dielectric spacecraft charging at geostationary orbits

Satellite charging is one of the major risks for satellite failure in orbit due to exposure to high energy electrons (>100 keV). Satellite charging can lead to an electrostatic discharge (ESD) resulting in component damage, phantom commands, and loss of service and in exceptional cases total satellite loss. A tool has been developed by the BIRA-IASB Space Weather Group for evaluating the risk for deep dielectric charging at geostationary orbit (GEO). Nowcasts and forecasts are made by combining the Space ENVironment Information System (SPENVIS) DICTAT charging tool with resp. near real-time GOES electron flux measurements and with daily predicted high energy electron spectra produced by the Sheffield NARMAX (Nonlinear AutoRegresssive Moving Average eXogenous model; Boynton et al. 2015) model at GEO.

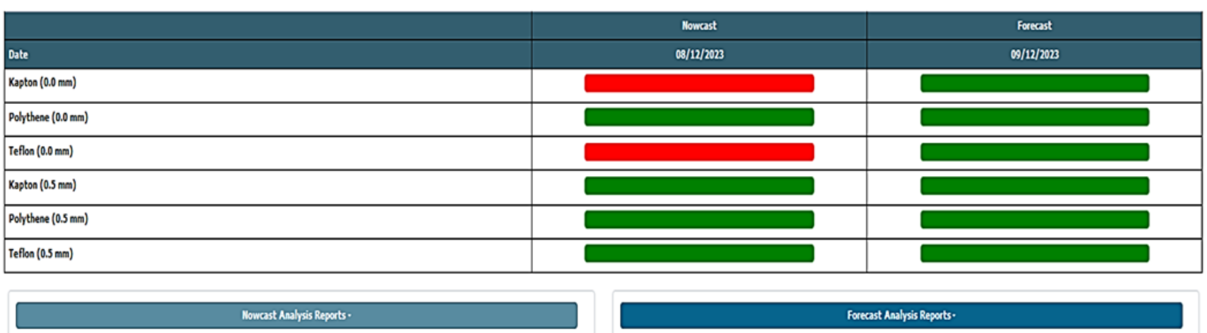

Figure 38: Example of an internal charging risk nowcast and forecast for a set of shielded (0.5 mm Kapton, Polythene, Teflon) and unshielded (0.0 mm) dielectrics. Green indicates no risk and red stands for high risk. The nowcast (8 December 2023) and forecast (9 December 2023) charging risk analysis reports including mitigation steps in case of a high risk for ESD, are also provided.

Daily automated simulations are performed through the Virtual Space Weather Modelling System (VSWMC) hosted at KU Leuven. The charging risks are computed for a set of simplified satellite configurations at GEO considering electronic devices of various dielectric materials outside (unshielded) and inside (shielded) the satellite. Besides a quick overview table of the latest nowcast and forecast risk indicators, a timeline of the risk indicator evolution for a period of 7 days leading up to the selected day can also be shown. For each derived risk indicator, the detailed DICTAT analysis report can be downloaded as well. The tool is available on the ESA Space Weather Portal (https://swe.ssa.esa.int/), as part of the demonstration products provided by the Space Radiation Expert Service Centre (R-ESC ; https://swe.ssa.esa.int/space-radiation) coordinated by the BIRA-IASB Space Weather Group.

Radiation analysis service to support space mission design

Proper assessment of potential adverse effects is a vital part of the engineering process leading to the production of a spaceborne instrument. Besides thermal, stress and vibration tests, evaluating the space radiation impact on its various components allows space engineers to anticipate problems that could disrupt the operation and possibly reduce the expected lifetime of the instrument.

Within the frame of ESA's EnVision space mission design, a radiation analysis was performed with the aid of ESA's Space ENVironment Information System (SPENVIS, https://www.spenvis.oma.be), developed at BIRA-IASB. The analysis includes the specification of the energetic particle environment that the EnVision spacecraft is expected to encounter on its way to Venus, and a first estimate of the resulting short-term and long-term radiation effects on the VenSpec-H instrument which was designed by the BIRA-IASB engineering department. After quickly leaving the Earth's magnetosphere, the spacecraft will be fully exposed to a constant flux of galactic cosmic rays and sporadic bursts of solar energetic particles originating from solar eruptions like flares and coronal mass ejections. Without the shielding by Earth's magnetosphere, these high energy particles (tens of MeV up to several GeV) may easily penetrate through the skin of the spacecraft and damage the inside electronic devices if not sufficiently radiation hardened.

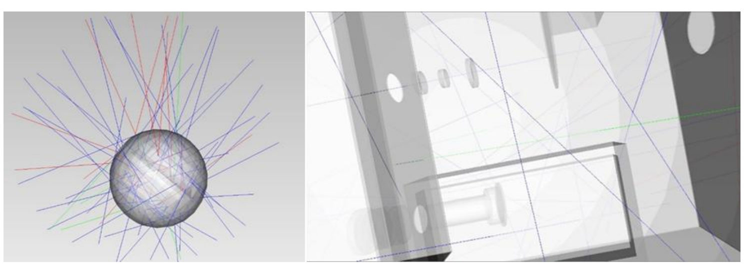

Figure 39: Geant4 simulation of the interaction of solar energetic protons (blue tracks) with the VenSpec-H instrument. The red and green tracks represent secondary electrons and neutrons respectively. Left: A hollow aluminium sphere was placed around the instrument to model the spacecraft shielding. Right: Geant4 simulation of the interaction with the various components inside the VenSpec-H instrument. The generated secondary radiation could cause further damage to the instrument.

To estimate the ionizing and non-ionizing radiation dose (i.e. the cumulated deposited energy over time), Monte Carlo simulations were performed with the SPENVIS Geant4 Radiation Analysis for Space (GRAS) tool considering simplified geometric models of the instrument and its electronics box. For a set of characteristic micro-devices, the single event upset rate (sudden transient disruption due to ionizing radiation causing memory errors) was calculated.

Having a better understanding of the potential radiation environment and expected effects, helps engineers in selecting the appropriate electronic parts for their instrument that can tolerate the amount and intensity of high energy particle radiation. The radiation analysis is a service offered by the BIRA-IASB Space Weather Group in support of space mission design.

Improvement of radiative transfer and retrieval tools

Implementation of 4D LUTs in ASIMUT

The ASIMUT code is a radiative transfer and retrieval tool developed at the Royal Belgian Institute for Space Aeronomy (BIRA-IASB). In order to speed up the radiative transfer computations, ASIMUT has the option to use pre-calculated absorption cross-section lookup tables (LUTs) instead of the computationally expensive line-by-line approach. The existing implementation uses 3D lookup tables, the absorption cross-sections are tabulated in function of three variables: pressure, temperature and wavelength. Under certain atmospheric conditions, however, self-broadening of spectral lines can become important, e.g. for water vapour. In those cases, the cross-sections also depend on the volume mixing ratio of the molecule. The 3D LUT approach is not sufficient in this case, hence the need for 4D LUTS, where the absorption cross-sections depend on pressure, temperature, wavelength and volume mixing ratio. During retrievals, cross-sections are similarly computed from the LUTS by means of interpolation, now with one additional dimension. We have now successfully implemented 4D LUTS as an option in ASIMUT. The implementation was validated through comparison with reference results obtained using the line-by-line method. The use of 4D LUTs does come at a small computational cost compared to 3D LUTs, which depends on the exact interpolation method used. Several interpolation options are available, which can be set for each independent variable.

Optimisation of ASIMUT for IASI methane retrieval

The IASI instrument (Infrared Atmospheric Sounding Interferometer) provides an excellent dataset for long-term methane observations and trend studies, given its large spatial, spectral and temporal coverage and its low radiometric noise levels.

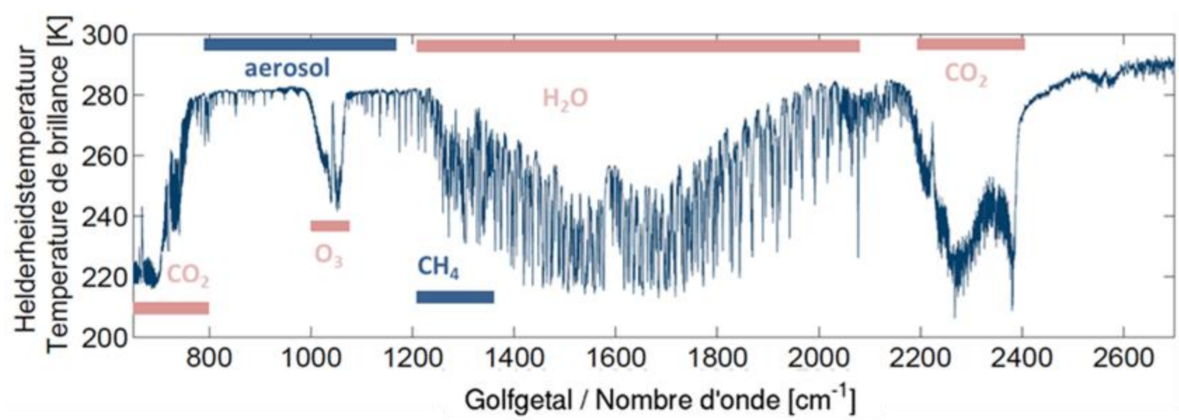

Figure 40: Example IASI spectrum in the thermal infrared, with regions of line signatures corresponding to different molecules and aerosols indicated. Vertical axis: Brightness temperature ; Horizontal axis: Wavenumber.

The high spectral resolution and large number of vertical pressure levels required for accurate methane retrieval makes analyzing the entire IASI dataset a very CPU intensive and costly task. ASIMUT offers a very flexible and accurate radiative transfer model, but it was not originally developed for the processing of such large datasets. Even with the LUT approach it is still prohibitively expensive to use for methane retrieval from IASI radiances. In an effort to reduce the computation time, we first used profiling software to locate the computational bottlenecks in the code. Focusing on the most CPU intensive subroutines/functions, we managed to reduce the computation time by around 40%, without resorting to numerical approximation techniques. While this gain is significant and beneficial for other applications of ASIMUT as well, it is still insufficient to make IASI methane retrieval feasible.

Water vapour in the troposphere from GNSS measurements

Due to climate change, intensive storms and severe precipitation will continue to happen, causing destructive flooding. In July 2021, a series of storms with prolonged rain episodes took place in Europe. Several countries were affected by severe floods following that rainfall, causing many deaths and material damage. Thus, a good understanding and forecasting of such events are of uttermost importance. This study highlights the interest of multi-GNSS tomography for the 3D modelling of the neutral atmosphere refractivity, which is related to the water vapour content. The tropospheric parameters have been retrieved for the July 2021 flood in Germany from two tomographic solutions with different constraining options using either GPS-only or multi-GNSS estimates (i.e., GPS-GLONASS-GALILEO solutions: GNSS(GRE)).

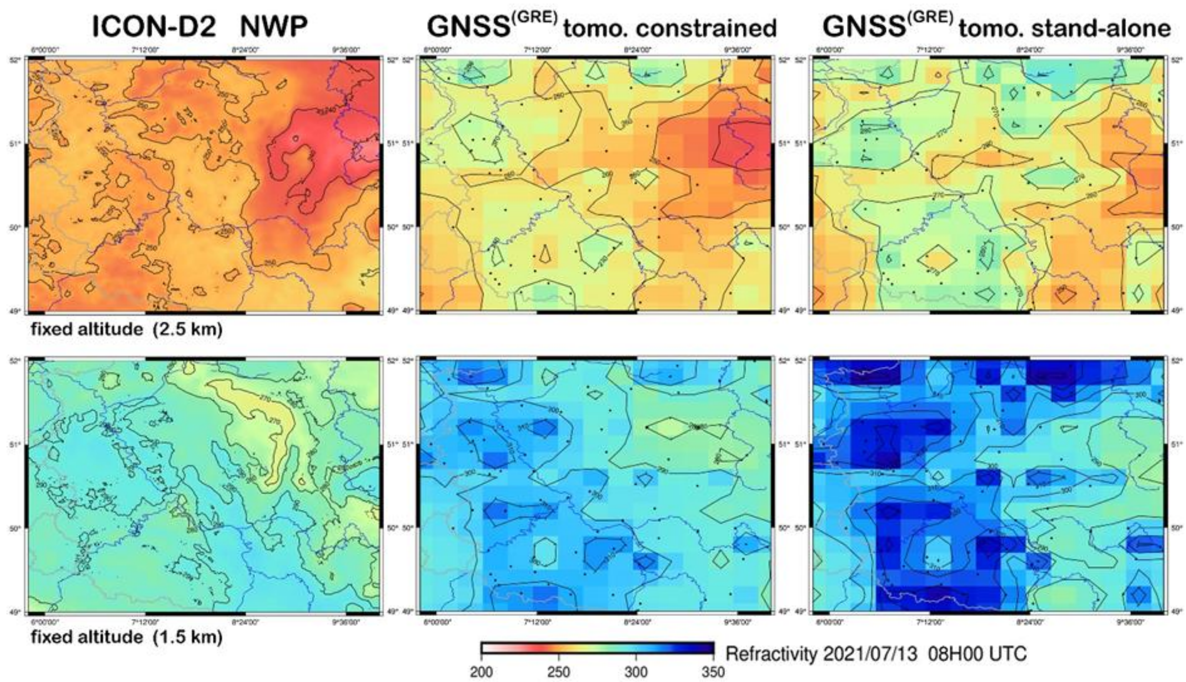

Figure 41: Comparison of ICON (left), GNSS(GRE) tomography constrained (middle) and GNSS(GRE) tomography stand-alone (right) for 13 July (08:00 UTC), height 2.5 km (top) and 1.5 km (bottom).

Our investigations show that the stand-alone solution (especially the multi-GNSS) is producing more patterns of refractivity and is temporally more stable (see Figure 41). GNSS tomography is producing wetter conditions than the reference (ICON-2 numerical weather model). Precursor information of the initiation of deep convection is observed in the ground-based GNSS technique.

Conference dinner at the European Space Weather Week in Toulouse, France (ESWW2023). Members of the SIDC are sharing the table with Kari Österberg, Chief Operating Officer of PECASUS at the Finnish Meteorological Institute (FMI).

Publications

This overview of publications consists of three lists: the peer-reviewed articles, the presentations and posters at conferences, and the public outreach talks and publications for the general public. It does not include non-refereed articles, press releases, the daily, weekly and monthly bulletins that are part of our public services,… These data are available at the STCE website or upon request.

Authors belonging to the STCE have been highlighted in the list of peer-reviewed articles.

Peer reviewed articles

1. Antolin, P.; Dolliou, A.; Auchère, F.; … ; **Parenti, S.; Berghmans, D.**; … ; **Gissot, S.**; … ; **Kraaikamp, E.**; … ; **Rodriguez, L.**; … ; **Stegen, K.**; … ; **Verbeeck, C.**; … ; **Zhukov, A.N.**; … and 26 co-authors
Extreme-ultraviolet fine structure and variability associated with coronal rain revealed by Solar Orbiter/EUI HRIEUV and SPICE
Astronomy & Astrophysics, 676, A112, 2023, DOI: 10.1051/0004-6361/202346016

2. Auchère, F.; **Berghmans, D.**; Dumesnil, C.; … ; **Kraaikamp, E.**; … ; **Stegen, K.; Verbeeck, C.**; … ; **Gissot, S.**; … ; **Mierla, M.; Nicula, B.**; … ; **Zhukov, A.N.** and 31 co-authors
Beyond the disk: EUV coronagraphic observations of the Extreme Ultraviolet Imager on board Solar Orbiter
Astronomy & Astrophysics, 674, A127, 2023, DOI: 10.1051/0004-6361/202346039

3. Baker, D.; Démoulin, P.; Yardley, S.L.; … ; **Berghmans, D.; Zhukov, A.N.; Rodriguez, L.; Verbeeck, C.** and 21 co-authors
Observational Evidence of S-Web Source of the Slow Solar Wind
The Astrophysical Journal, 950, 65, 2023, DOI: 10.3847/1538-4357/acc653

4. **Balis, J.; Lamy, H.; Anciaux, M**.; Jehin, E.
Reconstructing meteoroid trajectories using forward scatter radio observations from the BRAMS network
Radio Science, 58, e2023RS007697, 2023, DOI: 10.1029/2023RS007697

5. Barczynski, K.; Harra, L.; Schwanitz, C.; … ; **Berghmans, D.**; … ; **Kraaikamp, E.**; … ; **Rodriguez, L.**; … ; **Verbeeck, C.; Zhukov, A.N.** and 11 co-authors
Slow solar wind sources: High-resolution observations with a quadrature view
Astronomy & Astrophysics, 673, A74, 2023, DOI: 10.1051/0004-6361/202345983

6. Berger, T.E.; **Dominique, M.**; Lucas, G.; Pilinski, M.; Ray, V.; Sewell, R.; Sutton, E.K.; Thayer, J.P.; Thiemann, E.
The Thermosphere is a Drag: the 2022 Starlink Incident and the Threat of Geomagnetic Storms to Low Earth Orbit Space Operations
Space Weather, 21, 3, e2022SW003330, 2023, DOI: 10.1029/2022SW003330

7. **Berghmans, D.**; Antolin, P.; Aucjère, F.; … ; **Gissot, S.**; … ; **Kraaikamp, E.**; … ; **Mierla, M.; Parenti, S.**; … ; **Rodriguez, L.**; … ; **Stegen, K.**; … ; **Verbeeck, C.**; … ; **Zhukov, A.N.** and 27 co-authors
First Perihelion of EUI on the Solar Orbiter mission
Astronomy & Astrophysics, 675, A110, 2023, DOI: 10.1051/0004-6361/202245586

8. **Bhattacharya, S.; Lefèvre, L.**; Hayakawa, H.; Jansen, M.; **Clette, F.**
Scale Transfer in 1849 : Heinrich Schwabe to Rudolf Wolf
Solar Physics, 298, A12, 2023, DOI: 10.1007/s11207-022-02103-4

9. **Botek, E.; Pierrard, V.; Winant, A.**
Prediction of radiation belts electron fluxes at a Low Earth Orbit using neural networks with PROBA-V/EPT data
Space Weather, 21, 7, e2023SW003466, 2023, DOI: https://doi.org/10.1029/2023SW003466

10. Brunet, A.; Dahmen, N.; Katsavrias, C.; … ; **Pierrard, V.; Botek, E.; Darrouzet, F.**; … and 7 co-authors
Improving the electron radiation belt nowcast and forecast using the SafeSpace data assimilation modelling pipeline
Space Weather, 21, 8, e2022SW003377, 2023, DOI: 10.1029/2022SW003377

11. Bučík, L.; Mason, G.M.; Nitta, N.V.; Krupar, V.; **Rodriguez, L.**; Ho, G.C.; Hart, S.T.; Dayeh, M.A.; Rodríguez-Pacheco, J.; Gómez-Herrero, R.; Wimmer-Schweingruber, R.F.
Recurrent 3He-rich solar energetic particle injections observed by Solar Orbiter at ~0.5 au
Astronomy & Astrophysics, 673, L5, 2023, DOI: 10.1051/0004-6361/202345875

12. Cheng, X.; Priest, E.R.; Li, H.T.; … ; **Berghmans, D.**; … ; **Zhukov, A.N.**; … ; **Rodriguez, L.**; **Verbeeck, C.**; … and 17 co-authors
Ultra-high-resolution Observations of Persistent Null-point Reconnection in the Solar Corona
Nature Communications, 14, 2107, 2023, https://doi.org/10.1038/s41467-023-37888-w

13. Chitta, L.P.; **Zhukov, A.N.; Berghmans, D.**; … ; **Kraaikamp, E.**; … ; **Rodriguez, L.**; … ; **Verbeeck, C.**; … and 14 co-authors
Picoflare jets power the solar wind emerging from a coronal hole on the Sun
Science, 381, 6660, 867-872, 2023, DOI: 10.1126/science.ade5801

14. Chitta, L.P.; Solanki, S.K.; del Toro Iniesta, J.C.; … ; **Berghmans, D.; Verbeeck, C.; Zhukov, A.N.**; … and 16 co-authors
Fleeting Small-scale Surface Magnetic Fields Build the Quiet-Sun Corona
The Astrophysical Journal Letters, 956, L1, 2023, DOI: 10.3847/2041-8213/acf136

15. **Cisneros-González, M.E.; Bolsée, D.; Pereira, N.; Van Laeken, L.; Jacobs, L.; Vandaele, A.C.; Karatekin, Ö.**; Lauzin, C.**; Robert, S.**
Facility for the radiometric characterization of space-based visible-near infrared detectors
Journal of Astronomical Telescopes, Instruments, and Systems, 9, 3, A036001, 2023, DOI: 10.1117/1.JATIS.9.3.036001

16. **Clette, F.; Lefèvre, L.**; Chatzistergos, T.; Hayakawa, H.; Carrasco, V.M.; … and 16 co-authors
Re-calibration of the Sunspot Number: Status Report
Solar Physics, 298, 44, 2023, DOI: 10.1007/s11207-023-02136-3

17. Dabrowski, B.; Mikuła, K.; Flisek, P.; … ; **Magdalenić, J.**; … and 17 co-authors
Interferometric imaging of the type IIIb and U radio bursts observed with LOFAR on 22 August 2017
Astronomy & Astrophysics, 669, A52, 2023, DOI : 10.1051/0004-6361/202142905

18. Davies, E.E.; **Scolini, C.**; Winslow, R.M.; Jordan, A.P.; Möstl, C.
The Effect of Magnetic Field Line Topology on ICME-related GCR Modulation
The Astrophysical Journal, 959, 133, 2023, DOI: 10.3847/1538-4357/ad046a

19. **Dewitte, S.; Abdul Nazar, A.; Zhang, Y.**; Smeesters, L.
A Multispectral Camera Suite for the Observation of Earth's Outgoing Radiative Energy
Remote Sensing, 15, 5487, 2023, DOI: 10.3390/rs15235487

20. Dolliou, A.; Parenti, S.; Auchère, F.; … ; **Berghmans, D.**; … ; **Kraaikamp, E.**; **Stegen, K.**; **Verbeeck, C.**; **Gissot, S.**; … ; **Mierla, M.**; … ; **Zhukov, A.N.** and co-authors
Temperature of quiet Sun small scale brightenings observed by EUI on board Solar Orbiter: Evidence for a cooler component
Astronomy & Astrophysics, 671, A64, 2023, DOI: 10.1051/0004-6361/202244914

21. **Echim, M.**; Voiculescu, M.; Munteanu, C.; Teodorescu, E.; Voitcu, G.; Negrea, C.; Condurache-Bota, S.; Bujor Dănilă, E.
On the phenomenology of magnetosheath jets with insight from theory, modelling, numerical simulations and observations by Cluster spacecraft
Frontiers in Astronomy and Space Science, Sec. Space Physics, 10, 2023, DOI: 10.3389/fspas.2023.1094282

22. **Echim, M.; Lamy, H.**; Simon-Wedlund, C.; **De Keyser, J.; Cessateur, G.**
Probing the magnetospheric generator of quiet electrostatic auroral arcs from ground based optical observations and magnetosphere-ionosphere coupling modelling
Geophysical Research Letters, 50, 24, e2023GL103689, 2023, DOI: 10.1029/2023GL103689

23. Elisa, R.; Barthelemy, M.; **Cessateur, G.**; Woelfflé, A.; **Lamy, H**.; Bouriat, S.; Gullikstad Johnsen, M.; Brändström, U.; Biree, L.
Reconstruction of electron precipitation spectra at the top of the upper atmosphere using 427.8 nm auroral images
Journal of Space Weather and Space Climate, 13, 30, 2023, DOI: 10.1051/swsc/2023028

24. Goldstein, J.; Usanova, M.; Toledo-Redondo, S.; **Pierrard, V.**; … and 15 co-authors
Geospace Core Plasma Supply and Refilling (CPSR): Science and Observations for the Next Decade
Decadal Survey website, 55, 3, 2023, DOI: 10.3847/25c2cfeb.d02a145a

25. Grimani, C.; Andretta, V.; Antonucci, E.; … ; **Gissot, S.**; … and 25 co-authors
Particle monitoring capability of the Solar Orbiter Metis coronagraph through the increasing phase of solar cycle 25
Astronomy & Astrophysics, 677, A45, 2023, DOI: 10.1051/0004-6361/202346679

26. Harra, L.K.; Mandrini, C.H.; Brooks, D.H.; … ; **Berghmans, D.**; … ; **Kraaikamp, E.**; … ; **Rodriguez, L.**; … ; **Verbeeck, C.**; **Zhukov, A.N.**; and 16 co-authors
The source of unusual coronal upflows with photospheric abundance in a solar active region
Astronomy & Astrophysics, 675, A20, 2023, DOI: 10.1051/0004-6361/202245747

27. Hayakawa, H.; Suyama, T.; **Clette, F.; Bhattacharya, S.; Lefèvre, L.**; Ohnishi, K.
Katsue Misawa's sunspot observations in 1921-1934: a primary reference for the Wolfer-Brunner transition
Monthly Notices of The Royal Astronomical Society, 532, 4, 4289-4303, 2023, DOI: 10.1093/mnras/stad2791

28. Hayakawa, H.; Cliver, E.W.; **Clette, F.**; … and 19 co-authors
The Extreme Space Weather Event of 1872 February: Sunspots, Magnetic Disturbance, and Auroral Displays
The Astrophysical Journal, 959, 23, 2023, DOI: 10.3847/1538-4357/acc6cc

29. Hayakawa, H.; **Bechet, S.; Clette, F.**; Hudson, H.S.; Maehara, H.; Namekata, K.; Notsu, Y.
Magnitude Estimates for the Carrington Flare in 1859 September: As Seen from the Original Records
The Astrophysical Journal, 954, L3, 2023, DOI: 10.3847/2041-8213/acd853

30. Janvier, M.; Mzerguat, S.; Young, P.R.; … ; **Berghmans, D.**; **Verbeeck, C.**; … ; **Rodríguez, L.**; … ; **Kraaikamp, E.**; … and co-authors
A multiple spacecraft detection of the 2 April 2022 M-class flare and filament eruption during the first close Solar Orbiter perihelion
Astronomy & Astrophysics, 677, A130, 2023, DOI: 10.1051/0004-6361/202346321

31. **Jebaraj, I.C.; Magdalenic, J.**; Krasnoselskikh, V.; Krupar, V.; Poedts, S.
Structured type III radio bursts observed in interplanetary space
Astronomy & Astrophysics, 670, A20, 2023, DOI: 10.1051/0004-6361/202243494

32. **Jebaraj, I.C.**; Kouloumvakos, A.; Dresing, N.; … ; **Magdalenic, J.**; … and 11 co-authors
Multiple injections of energetic electrons associated with the flare and CME event on 9 October 2021
Astronomy & Astrophysics, 675, A27, 2023, DOI: 10.1051/0004-6361/202245716

33. **Jebaraj, I.C.**; Krasnoselskikh, V.; Pulupa, M.; **Magdalenic, J.**; Bale, S.D.
Fundamental-Harmonic Pairs of Interplanetary Type III Radio Bursts
The Astrophysical Journal Letters, 955, L20, 2023, DOI: 10.3847/2041-8213/acf857

34. Kawo, A.; **Schaeybroeck, B.; Van Malderen, R.; Pottiaux, E.**
Precipitable water vapor in regional climate models over Ethiopia: model evaluation and climate projections
Climate Dynamics, 61, 5287-5307, 2023, DOI : 10.1007/s00382-023-06855-y

35. Khazanov, G.V.; **Pierrard, V.**; Ma, Q.; **Botek, E.**
The Role of Plasmasphere in the Formation of Electron Heat Fluxes
Journal of Geophysical Research: Space Physics, 128, 11, e2023JA032013, 2023, DOI: 10.1029/2023JA032013

36. Girgis, K.M.; Hada, T.; Yoshikawa, A.; Matsukiyo, S.; **Pierrard, V.**; Samwel, S.W.
Geomagnetic Storm Effects on the LEO Proton Flux during Solar Energetic Particle Events
Space weather, 21, 12, e2023SW003664, 2023, DOI: 10.1029/2023SW003664

37. Li, Z.F.; Cheng, X.; Ding, M.D.; … ; **Berghmans, D.**; … ; **Verbeeck, C.**; … ; **Zhukov, A.**; … ; **Rodriguez, L.** and 12 co-authors
Evidence for External Reconnection Between an Erupting Mini-filament and Ambient Loops Observed by Solar Orbiter/EUI
Astronomy & Astrophysics, 673, A83, 2023, DOI: 10.1051/0004-6361/202245814

38. **Lim, D.**; Van Doorsselaere, T.; **Berghmans, D.**; Morton, R. J.; Pant, V.; Mandal, S.
The Role of High-frequency Transverse Oscillations in Coronal Heating
The Astrophysical Journal Letters, 952, L15, 2023, DOI: 10.3847/2041-8213/ace423

39. Long, D.M.; Chitta, L.P. ; Baker, D.; Hannah, I.G.; Ngampoopun, N.; **Berghmans, D.; Zhukov, A.N.**; Teriaca, L.
Multistage Reconnection Powering a Solar Coronal Jet
The Astrophysical Journal, 944, 19, 2023, DOI: 10.3847/1538-4357/acb0c9

40. Long, D.M.; Green, L.M.; Pecora, F.; … ; **Mierla, M.**; … ; **Berghmans, D.**; **Zhukov, A.N.**; … and 8 co-authors
The Eruption of a Magnetic Flux Rope Observed by Solar Orbiter and Parker Solar Probe
The Astrophysical Journal, 955, 152, 2023, DOI: 10.3847/1538-4357/acefd5

41. Mandal, S.; Peter, H.; Chitta, L.P.; … ; **Berghmans, D.**; … ; **Zhukov, A.N.**; … ; **Verbeeck, C.**; **Kraaikamp, E.**; **Rodriguez, L.**; … ; and 15 co-authors
Signatures of dynamic fibrils at the coronal base: Observations from Solar Orbiter/EUI
Astronomy & Astrophysics, 670, L3, 2023, DOI: 10.1051/0004-6361/202245431

42. Mandal, S.; Peter, H.; Chitta, L.P.; … ; **Berghmans, D.**; … ; **Zhukov, A.N.**; … ; **Verbeeck, C.; Kraaikamp, E.; Rodriguez, L.**; … and 12 co-authors
Evolution of dynamic fibrils from the cooler chromosphere to the hotter corona
Astronomy & Astrophysics, 678, L5, 2023, DOI: 10.1051/0004-6361/202347343

43. **Mierla, M.**; Cremades, H.; Andretta, V.; … ; **Zhukov, A.N.**; … ; **Talpeanu, D.-C.; Rodriguez, L.; Janssens, J.; Nicula, B.**; … ; **Berghmans, D.**; … ; **D'Huys, E.; Dolla, L.; Gissot, S.**; … ; **Kraaikamp, E.**; … ; **Mampaey, B.**; … ; **Stegen, K.**; … ; **Verbeeck, C.**; … and 18 co-authors
Three Eruptions Observed by Remote Sensing Instruments Onboard Solar Orbiter
Solar Physics, 298, 42, 2023, DOI: 10.1007/s11207-023-02137-2

44. Munteanu C., Kovacs P., **Echim M.**
An Integrated Nonlinear Analysis (INA) Software for Space Plasma Turbulence
Earth and Space Science, 10, 3, e2022EA002692, 2023, DOI: 10.1029/2022EA002692

45. Nelson, C.J.; Auchère, F.; Aznar Cuadrado, R.; … ; **Verbeeck, C.; Zhukov, A.N.; Berghmans, D.** and 10 co-authors
Extreme-ultraviolet brightenings in the quiet Sun: Signatures in spectral and imaging data from the Interface Region Imaging Spectrograph
Astronomy & Astrophysics, 676, A64, 2023, DOI: 10.1051/0004-6361/202346144

46. Niembro, T.; Seaton, D.B.; Hess, P.; **Berghmans, D.**; Andretta, V.; Reeves, K. K.; Riley, P.; Stevens, M.L.; Landini, F.; Sasso, C.; **Verbeeck, C.**; Susino, R.; Uslenghi, M.
A prominence eruption from the Sun to the Parker Solar Probe with multi-spacecraft observations
Frontiers in Astronomy and Space Sciences, 10, 1191294, 2023, DOI: 10.3389/fspas.2023.1191294

47. **Niemela, A.**; Wijsen, N.; Aran, A.; **Rodriguez, L.; Magdalenic, J.**; Poedts, S.
Advancing interplanetary magnetohydrodynamic models through solar energetic particle modelling. Insights from the 2013 March 15 SEP event
Astronomy & Astrophysics, 679, A93, 2023, DOI: 10.1051/0004-6361/202347116

48. Nölke, J.D.; Solanki, S.K.; Hirzberger, J.; … ; **Berghmans, D.; Kraaikamp, E.; Rodriguez, L.; Verbeeck, C.; Zhukov, A.N.**; … and 63 co-authors
Coronal voids and their magnetic nature
Astronomy & Astrophysics, 678, A196, 2023, DOI: 10.1051/0004-6361/202346040

49. Palmerio, E.; **Maharana, A.**; Lynch, B.J.; Scolini, C.; Good, S.W.; Pomoell, J.; Isavnin, A.; Kilpua, E.K.J.
Modeling a Coronal Mass Ejection from an Extended Filament Channel. II. Interplanetary Propagation to 1 au
The Astrophysical Journal, 958, 91, 2023, DOI: 10.3847/1538-4357/ad0229

50. Panesar, N.K.; Hansteen, V.H.; Tiwari, S.K.T.; Cheung, M.C.M.; **Berghmans, D.**; Mueller, D.
Solar Orbiter and SDO Observations, and Bifrost MHD Simulations of Small-scale Solar Coronal Jets
The Astrophysical Journal, 943, 24, 2023, DOI: 10.3847/1538-4357/aca1c1

51. Paul, K.S.; Haralambous, H; Oikonomou, C.; Sing, A.K.; Gulyaeva, T.L.; Pancheko, V.A.; Altadill, D.; Buresova, D.; Mielich, J.; **Verhulst, T.G.W.**
Mid-latitude spread F over an extended European area
Journal of Atmospheric and Solar-Terrestrial Physics, 248, 106093, 2023, DOI: 10.1016/j.jastp.2023.106093

52. Petrova, E.; Magyar, N.; Van Doorsselaere, T.; **Berghmans, D.**
High frequency oscillations with significant energy in Solar Orbiter/EUI observations
The Astrophysical Journal, 946, 36, 2023, DOI: 10.3847/1538-4357/acb26a

53. **Pierrard, V.**; Benck, S.; **Botek, E.**; Borisov, S.; **Winant, A.**
Proton flux variations during Solar Energetic Particle Events, minimum and maximum solar activity and splitting of the proton belt in the South Atlantic Anomaly
Journal of Geophysical Research: Space Physics, 128, 5, e2022JA031202, 2023, DOI: 10.1029/2022JA031202

54. **Pierrard, V.**; Péters de Bonhome, M.; Halekas, J.; Audoor, C.; Whittlesey, P.; Livi, R.
Exospheric Solar Wind Model Based on Regularized Kappa Distributions for the Electrons Constrained by Parker Solar Probe Observations
Plasma, 6, 518-540, 2023, DOI: 10.3390/plasma6030036

55. **Poraicu, C.; Müller, J.-F.; Stavrakou, T.; Fonteyn, D.; Tack, F.**; Deutsch, F.; **Laffineur, Q.; Van Malderen, R.**; Veldeman, N.
Cross-evaluating WRF-Chem v4.1.2, TROPOMI, APEX, and in situ NO_2 measurements over Antwerp, Belgium
Geoscientific Model Development, 16, 2, 479-508, 2023, DOI: 10.5194/gmd-16-479-2023

56. Ripoll, J.-F.; **Pierrard, V.**; Cunningham, G.S.; Chu, X.; Sorathia, K.A.; Hartley, D.P.; Thaller, S.A.; Merkin, V.G.; Delzanno, G.L.; De Pascuale, S.; Ukhorskiy, A.Y.
Modeling of the cold electron plasma density for radiation belt physics
Frontiers in Astronomy and Space Sciences, 10:1096595, 2023, DOI : 10.3389/fspas.2023.1096595

57. **Rodriguez, L.**; Warmuth, A.; Andretta, V.; **Mierla, M.**; **Zhukov, A.N.**; **Shukhobodskaia, D.**; **Niemela, A.**; **Maharana, A.**; … ; **D’Huys, E.**; … ; **Berghmans, D.**; … ; **Dominique, M.**; **Gissot, S.**; … ; **Katsiyannis, A.C.**; **Kraaikamp, E.**; … ; **Magdalenic, J.**; … ; **Nicula, B.**; … ; **Stegen, K.**; … ; **Verbeeck, F.**; and 18 co-authors

The eruption of 22 April 2021 as observed by Solar Orbiter: continuous magnetic reconnection and heating after the impulsive phase
Solar Physics, 298, 1, 2023, DOI: 10.1007/s11207-022-02090-6

58. Sayez, N.; De Vleeschouwer, C.; **Delouille, V.; Bechet, S.; Lefèvre, L.**
SunSCC: segmenting, grouping and classifying sunspots from ground-based observations using deep learning
Journal of Geophysical Research: Space Physics, 128, 12, e2023JA031548, 2023, DOI: 10.1029/2023JA031548

59. Schwanitz, C.; Harra, L.; Mandrini, C.H.; … ; **Berghmans, D.**; … ; **Kraaikamp, E.**; … ; **Rodriguez, L.**; … ; **Verbeeck, C.; Zhukov, A.N.** and 13 co-authors
Small-scale EUV features as the drivers of coronal upflows in the quiet Sun
Astronomy & Astrophysics, 674, A219, 2023, DOI: 10.1051/0004-6361/202346036

60. Seaton, D.B.; **Berghmans, D.**; Bloomfield, D.S.; De Groof, A.; **D'Huys, E.; Nicula, B.**; Rachmeler, L.A.; West, M.J.
The SWAP Filter: A Simple Azimuthally Varying Radial Filter for Wide-Field EUV Solar Images
Solar Physics, 298, 92, 2023, DOI: 10.1007/s11207-023-02183-w

61. Shaifullah, G.M.; **Magdalenic, J.**; Tiburzi, C.; **Jebaraj, I.; Samara, E.**; Zucca, P.
Validation of heliospheric modeling algorithms through pulsar observations II: Simulations with EUHFORIA
Advances in Space Research, 72, 12, 5298-5310, 2023, DOI: 10.1016/j.asr.2022.07.003

62. Smeesters, L.; **Schifano, L.**; Rosseel, D.; Verbaenen, J.; Thienpont, H.; **Dewitte, S.**; Berghmans, F.; Vervaeke, M.
Freeform wide-field-of-view imaging telescope improving spaceborne climate monitoring
SPIE Proceedings 12798, International Optical Design Conference 2023, 127980N, 2023, DOI: 10.1117/12.2691627

63. Smeesters, L.; **Schifano, L.**; Rosseel, D.; Verbaenen, J.; Thienpont, H.; Berghmans, F.; **Dewitte, S.**; Vervaeke, M.
Freeform wide-field-of-view near-infrared imaging spectrometer for spaceborne climate monitoring
SPIE Proceedings 12677, Astronomical Optics: Design, Manufacture, and Test of Space and Ground Systems IV; 126770C, 2023, DOI: 10.1117/12.2677406

64. Stankov, S.M.; Verhulst, T.G.W.; Sapundjiev, D.
Automatic Ionospheric Weather Monitoring With DPS-4D Ionosonde and ARTIST-5 Autoscaler: System Performance at a Mid-Latitude Observatory
Radio Science, 58, 2, e2022RS007628, 2023, DOI: 10.1029/2022RS007628

65. Teodorescu, E.; **Echim, M**.; Johnson, J.
Estimating intermittency significance by means of surrogate data: implications for solar wind turbulence
Frontiers in Astronomy and Space Science, 10:1188126, 2023, DOI: 10.3389/fspas.2023.1188126

66. **Verbeke, C.**; Mays, M.L.; Kay, C.; Riley, P.; Palmerio, E.; Dumbović, M.; **Mierla, M.**; Scolini, C.; Hinterreiter, J.
Quantifying errors in 3D CME parameters derived from synthetic data using white-light reconstruction techniques
Advances in Space Research, 72, 12, 5243-5262, 2023, DOI: 10.1016/j.asr.2022.08.056

67. **Verhulst, T.G.W.**; De Franceschi, G.; Cesaroni C.
Ionospheric effects of the Hunga Tonga Volcanic Eruption of 15 January 2022
URSI Radio Science Bulletin, 2021, 378, 95-98, 2023, DOI: 10.23919/URSIRSB.2021.10292826

68. Voitcu, G.; **Echim, M.**; Teodorescu, E.; Munteanu, C.
Kinetic simulations of solar wind plasma irregularities crossing the Hermean magnetopause
Astronomy & Astrophysics, 674, A228, 2023, DOI: 10.1051/0004-6361/202346214

69. West, M.J.; Seaton, D.B.; Wexler, D.B.; … ; **Berghmans, D.**; … ; **Zhukov, A.N.** and 37 co-authors
Defining the Middle Corona
Solar Physics, 298, 78, 2023, DOI: 10.1007/s11207-023-02170-1

70. Whitman, K.; Egeland, R.; Richardson, I.G.; … ; **Dierckxsens, M.**; … ; **Crosby, N.**; … and 121 co-authors
Review of solar energetic particle models
Advances in Space Research, 75, 12, 5161-5242, 2023, DOI: 10.1016/j.asr.2022.08.006

71. Wilgan, K.; **Brenot, H.**; Biondi, R.; Dick, G.; Wickert, J.
Multi-GNSS Tomography: Case Study of the July 2021 Flood in Germany
Gravity, Positioning and Reference Frames, REFAG 2022 (Eds. Freymüller, J.T., Sánchez, L.), International Association of Geodesy Symposia, 156, Springer, Cham, DOI: 10.1007/1345_2023_198

72. Wimmer-Schweingruber, R.F.; Berger, L.; Kollhoff, A.; … ; **Rodriguez, L.; Shukhobodskaia, D.**; … and 26 co-authors
Unusually long path length for a nearly scatter-free solar particle event observed by Solar Orbiter at 0.43 au
Astronomy & Astrophysics, 678, A98, 2023, DOI: 10.1051/0004-6361/202346319

73. **Winant, A.; Pierrard, V.; Botek, E.**
Comparison of radiation belts electron fluxes simultaneously measured with PROBA-V/EPT and RBSP/MagEIS instruments

Annales Geophysicae, 41, 313-325, 2023, DOI: 10.5194/angeo-41-313-2023

74. **Winant, A.; Pierrard, V.; Botek, E.**; Herbst, K.
The atmospheric influence on cosmic ray induced ionization and absorbed dose rates
Universe, 9, 502, 2023, DOI: 10.3390/universe9120502

75. Winslow, R.M.; **Scolini, C.**; Lugaz, N.; Schwadron, N.A.; Galvin, A.B.
On the Contribution of Coronal Mass Ejections to the Heliospheric Magnetic Flux Budget on Different Time Scales
The Astrophysical Journal, 958, 41, 2023, DOI: 10.3847/1538-4357/ad02f2

76. Yardley, S.L.; Owen, C.J.; Long, D.M.; … ; **Berghmans, D.**; … ; **Kraaikamp, E.**; … ; **Rodriguez, L.**; … ; **Verbeeck, C.; Zhukov, A.N.**; … and 71 co-authors
Slow Solar Wind Connection Science during Solar Orbiter's First Close Perihelion Passage
The Astrophysical Journal Supplement Series, 267, 11, 2023, DOI: 10.3847/1538-4365/acd24b

77. Yuan, P.; **Van Malderen, R.**; Yin, X.; Vogelmann, H.; Jiang, W.; Awange, J.; Heck, B.; Kutterer, H.
Characterisations of Europe's integrated water vapour and assessments of atmospheric reanalyses using more than 2 decades of ground-based GPS
Atmospheric Chemistry and Physics, 23, 6, 3517-3541, 2023, DOI: 10.5194/acp-23-3517-2023

78. Yuan, P.; Blewitt, G.; Kreemer, C.; Hammond, W.C.; Argus, D.; Yin, X.; **Van Malderen, R.**; Mayer, M.; Jiang, W.; Awange, J.; Kutterer, H.
An enhanced integrated water vapour dataset from more than 10 000 global ground-based GPS stations in 2020
Earth System Science Data, 15, 2, 723-743, 2023, DOI: 10.5194/essd-15-723-2023

79. Yuan, P.; **Van Malderen, R.**; Yin, X.; Vogelmann, H.; Jiang, W.; Awange, J.; Heck, B.; Kutterer, H.
Characterisations of Europe's integrated water vapour and assessments of atmospheric reanalyses using more than 2 decades of ground-based GPS
Atmospheric Chemistry and Physics, 23, 6, 3517-3541, 2023, DOI: 10.5194/acp-23-3517-2023

80. Zhang, Y.; **Dewitte, S.**; Bi, S.
A Model for Estimating the Earth's Outgoing Radiative Flux from A Moon-Based Radiometer
Remote Sensing, 15, 15, 3773, 2023, DOI: 10.3390/rs15153773

81. Zhang, Y.; **Dewitte, S.**; Bi, S.
The Uncertainty Analysis of the Entrance Pupil Irradiance for a Moon-Based Earth Radiation Observation Instrument
Remote Sensing, 15, 17, 4132, 2023, DOI: 10.3390/rs15174132

82. Žigman, V.; **Dominique, M.**; Grubor, D.; Rodger, C.J.; Clilverd, M.A.
Lower-ionosphere electron density and effective recombination coefficients from multi-instrument space observation and ground VLF measurements during solar flares
Journal of Atmospheric and Solar-Terrestrial Physics, 247, 106074, 2023, DOI: 10.1016/j.jastp.2023.106074

83. Zimbardo, G.; Ying, B.; Nisticò, G.; … ; **Magdalenic, J.**; … and 34 co-authors
A high-latitude coronal mass ejection observed by a constellation of coronagraphs: Solar Orbiter/Metis, STEREO-A/COR2, and SOHO/LASCO
Astronomy & Astrophysics, 676, A48, 2023, DOI : 10.1051/0004-6361/202346011

Presentations and posters at conference

1. Alonso Tagle, M.L.; Maggiolo, R.; Gunell, H.; Cessateur, G.; De Keyser, J.; Lapenta, G.; Pierrard, V.; Vandaele, A.C.
Estimation of the total oxygen loss on Earth with a semi-empirical model of atmospheric escape
IUGG General Assembly, Berlin (Germany), 11-20 July 2023

2. Alonso Tagle, M.L.; Maggiolo, R.; Gunell, H.; De Keyser, J.; Cessateur, G.; Lapenta, G.; Pierrard, V.; Vandaele, A.C.
Evolution of the oxygen escape at Earth over geological time scales
EGU General Assembly 2023, Vienna (Austria), 23-28 April 2023

3. Alonso Tagle, M.L.; Maggiolo, R.; Gunell, H.; De Keyser, J.; Cessateur, G.; Lapenta, G.; Pierrard, V.; Vandaele, A.C.
Modelling Atmospheric Erosion for Terrestrial Planets in the Solar System
Planet ESLAB, ESTEC, Noordwijk (The Netherlands), 20-24 March 2023 (poster)

4. Balis, J.; Lamy, H.; Anciaux, M.; Jehin, E.
Meteoroid speed and trajectory determination from amplitude and phase information of the BRAMS forward scatter radio network
Asteroids, Comets, Meteoroids 2023, Flagstaff (Arizona, USA), 18-23 June 2023

5. Balis, J.; Lamy, H.; Anciaux, M.; Jehin, E.
Phase-enhanced trajectory and speed reconstruction of meteoroids using BRAMS data
International Meteor Conference 2023, Redu (Belgium), 31 August - 1 September 2023

6. Bamahry, F.; Legrand, J.; Bruyninx, C.; Pottiaux, E.; Fabian, A.
Correlation Analysis of GNSS Data Quality Indicators and Position Time Series using Machine-Learning Algorithms
EGU General Assembly 2023, Vienna (Austria), 23-28 April 2023

7. Bamahry, F.; Legrand, J.; Bruyninx, C.; Pottiaux, E.; Fabian, A.
Why considering Machine Learning for quality evaluation of GNSS observations? (challenges we faced and are still facing)
EUREF Symposium 2023, Gothenburg (Sweden), 23-26 May 2023 (invited talk)

8. Bamahry, F.; Legrand, J.; Bruyninx, C.; Pottiaux, E.; Fabian, A.
Using Machine Learning Algorithms for Automated Data Cleaning of GNSS Position Time Series Based on Data Quality Indicators
EUREF Symposium 2023, Gothenburg (Sweden), 23-26 May 2023

9. Bamahry, F.; Legrand, J.; Bruyninx, C.; Pottiaux, E.; Fabian, A.
Using supervised machine learning for flagging GNSS observations based on data quality indicators
IUGG General Assembly, Berlin (Germany), 11-20 July 2023

10. Behlke, R.; Berghmans, D.; Bousquet, D.; Chabanski, S.; Delouille, V.; Dudok de Wit, T.; Grandin, M.; Lilensten, J.; Marchaudon, A.; Pinto, R.; Rodriguez, L.
E-SWAN working group on sustainability
ESWW19, Toulouse (France) and online, 20-24 November 2023 (poster)

11. Belehaki, A.; Verhulst, T.G.W.; Spogli, L.; Cessaroni, C.; Altadill, D.; Galkin, I.; Burešová, D.; Mani, S.; Unger, S.; Barta, V.; Brouard, P.
T-FORS: a project to develop TID forecasting systems
35th URSI General Assembly and Scientific Symposium, Sapporo (Japan), 19–26 August 2023

12. Berghmans, D.
Science Opportunities by the Extreme Ultraviolet Imager (EUI) onboard Solar Orbiter
3rd BINA Workshop, Bhimtal (India), 22-24 March 2023 (invited talk)

13. Berghmans, D.
EUI Report April 19 - Sept 17
Solar Orbiter Science Working Team, Online, 18 September 2023 (invited talk)

14. Berghmans, D.
EUI Report Nov 22-April 16
Solar Orbiter Science Working Team meeting, Paris (France), 19-21 April 2023 (invited talk)

15. Berghmans, D.
The many scales observed by EUI onboard Solar Orbiter
SOLARNET conference: The Many Scales of the Magnetic Sun, Potsdam (Germany), 8-12 May 2023 (invited talk)

16. Berghmans, D.; Auchère, F.
EUV coronagraphic observations of the Extreme Ultraviolet Imager on board Solar Orbiter
PROBA-3 Science Working Team Meeting #9, Brussels (Belgium), 27-29 November 2023

17. Berghmans, D.

Review of technical challenges
30th EUI Consortium meeting, Orsay (France), 13-15 September 2023

18. Berghmans, D.
Recent EUI news
30th EUI Consortium meeting, Orsay (France), 13-15 September 2023

19. Berghmans, D.
Low Latency improvement
Solar Orbiter - Remote Sensing Working Group, Online, 17 January 2023

20. Berghmans, D.
Recent EUI operations
29th EUI Consortium meeting, Online, 25-27 January 2023

21. Berghmans, D.
Planned Campaigns in LTP11
29th EUI Consortium meeting, Online, 25-27 January 2023

22. Bhattacharya, S.
Diagnosing and Calibrating the Multi-Century Sunspot Number Series
Thesis, Public PhD Defense, ULB, Brussels (Belgium) and online, 25 September 2023

23. Björklund, R.; Vigouroux, C.; Langerock, B.; and 13 others
Intercomparison of long-term ground-based tropospheric ozone measurements
EGU General Assembly 2023, Vienna (Austria), 23-28 April 2023 (poster)

24. Botek E.; Pierrard V.; Winant A.
Recent advancements of a deep learning model to forecast the radiation belts electron fluxes at LEO with PROBA-V/EPT data
ESWW19, Toulouse (France) and online, 20-24 November 2023

25. Brenot, H.
GNSS for weather forecasting
8th international training school on Convective and Volcanic Clouds (CVC) detection, monitoring and modeling, Nicolosi (Sicily, Italy), 2-8 October 2023

26. Bučík, L.; Mason, G.M.; Nitta, N.V.; Krupar, V.; Rodriguez, L.; Ho, G.C.; Hart, S.T.; Dayeh, M.A.; Rodríguez-Pacheco, J.; Gómez-Herrero, R.; Wimmer-Schweingruber, R.F.
Recurrent 3He-rich solar energetic particle injections observed by Solar Orbiter
EGU General Assembly 2023, Vienna (Austria), 23-28 April 2023 (poster)

27. Calders, S.; Lamy, H.; Kolenberg, K.
The Radio Meteor Zoo: Engaging Citizen Scientists in Meteor Research
Asteroids, Comets, Meteoroids 2023, Flagstaff (Arizona, USA), 18-23 June 2023 (poster)

28. Carcaboso, F.; Warmuth, A.; Schuller, F.; and 34 others
Diving into Solar Energetic Electron Events: Collaborative Insights from Solar Orbiter's Remote Sensing and In-Situ Instruments
AGU Fall Meeting, San Francisco (California, USA), 11-15 December 2023

29. Cessateur, G.; Lamy, H.; Bosse, L.; Barthelemy, M.; Lilensten, J.; Gullikstad Johnsen, M.; Auriol, F.; Catalfamo, M.; Pujol, O.
PLIP: An imaging Polarimeter for the Auroral line Emissions
EGU General Assembly 2023, Vienna (Austria), 23-28 April 2023

30. Chabanski, S.; Dierckxsens, M.; Poedts, S.; Kochanov, A.; Wijsen, N.; Perri, B.; Baratashvili, T. Jiggens, P.; Deprez, G.; Esteban Niemela, A.
Validation of CME and SEP propagation models in the VSWMC
ESWW19, Toulouse (France) and online, 20-24 November 2023 (poster)

31. Daglis, I.A. and the SafeSpace Team
Predicting Outer Van Allen Belt Dynamics with the Prototype SafeSpace Service
EGU General Assembly 2023, Vienna (Austria), 23-28 April 2023 (poster)

32. De Donder, E.; Messios, N.; Dierckxsens, M.; Echim, M.; Sandberg, I.; Aminalragia-Giamini, S.; Voitcu, G.; Teodorescu, E.; Truscott, P.; Heynderickx, D.
Radiation Environment & Effects NOwcasts for the Moon (REENOM)
ESWW19, Toulouse (France) and online, 20-24 November 2023

33. De Donder, E.; Messios, N.; Dierckxsens, M.; Echim, M.; Sandberg, I.; Aminalragia-Giamini, S.; Voitcu, G.; Teodorescu, E.; Truscott, P.; Heynderickx, D.
Radiation Environment & Effects NOwcasts for the Moon (REENOM)
ESWW19, Toulouse (France) and online, 20-24 November 2023 (poster)

34. De Donder, E.; Messios, N.; Calders, S.; Calegaro, A.; Mezhoud, S.; Heynderickx, D.; Akandouch, M.; Pavano, G.; Clucas, S.; Evans, H.
New SPENVIS system: current status
TEC-EPS Final presentation days, ESTEC, Noordwijk (The Nederlands), 7-8 March 2023

35. De Donder, E.; Messios, N.; Calders, S.; Calegaro, A.; Mezhoud, S.; Heynderickx, D.; Akandouch, M.; Pavano, G.; Clucas, S.; Evans, H.
The SPace ENVironment Information System (SPENVIS) - a new framework
ESWW19, Toulouse (France) and online, 20-24 November 2023 (poster)

36. Deshpande, K.; Magdalenic, J.; Jebaraj, I.C.; Krupar, V.
Coronal Plasma Density Mapping through Radio and In-Situ Observations, and Modeling with EUHFORIA
ESWW19, Toulouse (France) and online, 20-24 November 2023 (poster)

37. D'Huys, E.; Rodriguez, L.; Mierla, M.; Shukhobodskaia, D.; Talpeanu, D.; West, M.; Dorsch, B.; Berghmans, D.; Zhukov, A.N.; Verbeeck, C.
Observations of Erupting Prominences by EUI/FSI Aboard Solar Orbiter
PROBA-3 Science Working Team Meeting #9, Brussels (Belgium), 27-29 November 2023 (invited talk)

38. D'Huys, E.; Rodriguez, L.; Mierla, M.; Talpenau, D.; Shukhobodskaia, D.; Dorsch, B.; West, M.; Berghmans, D.; Zhukov, A.; Verbeek, C.
A statistical Study of Prominence Eruptions Observed by EUI/FSI
30th EUI Consortium meeting, Orsay (France), 13-15 September 2023

39. Dierckxsens, M.
COMESEP SEP Forecast
European SEPVAL 2023 Workshop, Toulouse (France), 18-19 November 2023

40. Dierckxsens, M.
SEP Forecasting within the ESA Space Weather Service Network
European SEPVAL 2023 Workshop, Toulouse (France), 18-19 November 2023

41. Dolla, L.
Planning of ASPIICS Observations
PROBA-3 Science Working Team Meeting #9, Brussels (Belgium), 27-29 November 2023

42. Dolla, L.
ASPIICS data products
PROBA-3 Science Working Team Meeting #9, Brussels (Belgium), 27-29 November 2023

43. Dominique, M.
Quasi-Periodic Pulsations
Solar-C Science Working Group meeting, Tokyo (Japan), 1 October 2023

44. Dominique, M.; Zhukov, A.N.; Nelson, C.; Auchère, F.; Schuehle, U.; Shestov, S.; Verbeeck, C.; Mierla, M.; Berghmans, D.
How can IRIS and Solar-C improve our understanding of the campfires observed by Solar Orbiter/EUI?
The 6th NAOJ symposium Hinode-16/IRIS-13, Niigata (Japan), 25-29 September 2023

45. Dorsch, B.D.; Rodriguez, L.; Magdalenic, J.; Shukhobodskaia, D.; Mierla, M.; Maharana, A.
Analysis of two interacting Coronal Mass Ejections through novel Extreme Ultraviolet Imager observations and modelling
ESWW19, Toulouse (France) and online, 20-24 November 2023 (poster)

46. Echim, M.; Rodriguez, L.; Lapenta, G.; Teodorescu, E.; Bacchini, F.; Shukhobodskaia, D.; Zhukov, A.N.; Aravindakshan, H.; Arr`o, G.; Munteanu, C.; Voitcu, G.
PLAnetary plasma Turbulence and Intermittency coupling with interplanetary transients from data analysis and NUmerical Modelling (PLATINUM) - a new BRAIN-BE collaborative project
ESWW19, Toulouse (France) and online, 20-24 November 2023 (poster)

47. Echim, M.; Voitcu, G.; Munteanu, C.; Teodorescu, E.
Magnetopause properties from global MHD numerical simulations, local Vlasov equilibrium models and in-situ observations
EGU General Assembly 2023, Vienna (Austria), 23-28 April 2023

48. Echim, M.; Voiculescu, M.; Voitcu, G.; Munteanu, C.; Teodorescu, E.; Negrea, C.; Condurache-Bota, S.; Dănilă, E.
Dynamical properties of magnetosheath jets: dawn - dusk asymmetries and kinetic effects from an analysis of Cluster data (2007, 2008)
SMILE SWT#21 - SMILE Consortium Meeting #15, Beijing (China), 9-12 May 2023

49. Echim, M.; Voiculescu, M.; Voitcu, G.; Munteanu, C.; Teodorescu, E.; Negrea, C.; Condurache-Bota, S.; Dănilă, E.
Dynamical properties of magnetosheath jets from an analysis of Cluster data
IUGG General Assembly, Berlin (Germany), 11-20 July 2023

50. Echim, M.; Lamy, H.; Simon Wedlund, C.; De Keyser, J.; Cessateur, G.
Remote sensing the magnetospheric "roots" of stable auroral arcs: an approach based on optical observations from ground and magnetosphere-ionosphere coupling modeling
AGU Fall Meeting, San Francisco (California, USA), 11-15 December 2023 (poster)

51. Gunessee, A.; Marqué, C.; Martínez Picar, A.; Dolla, L.; Delouille, V.

Can a deep learning approach of detecting solar radio bursts perform better than the interquartile range threshold outlier detection method, currently running on the CALLISTO instrument of the Royal Observatory of Belgium?
CESRA Workshop 2023, University of Hertfordshire, Hatfield (UK), 3-7 July 2023

52. Huang, Z.; Teriaca, L.; Aznar Cuadrado, R.; and 16 others
Imaging and spectroscopic observations of EUV brightenings using EUI and SPICE on board Solar Orbiter
SOLARNET conference: The Many Scales of the Magnetic Sun, Potsdam (Germany), 8-12 May 2023 (poster)

53. Katsiyannis, A.C.; Lemaire, J.
Solar wind electron temperature estimation from low corona to 1 au derived by the DYN model
ESWW19, Toulouse (France) and online, 20-24 November 2023 (poster)

54. Kauristie, K.; Maneva, Y.; Verhulst, T.G.W.; De Patoul, J.; Sabbagh, D.; Bagiacchi, P.; Stanislawska, I.; Zalizovski, A.; Tshisaphungo, M.; Haralambous, H.; Tomasik, L.; O'Hara, J.; Perrone, L.
PECASUS Operational Space Weather Products For HF COM
ESWW19, Toulouse (France) and online, 20-24 November 2023

55. Kiss, T.; Chan You Fee, D.; Kagialis, D.; Pierantoni, G.; Belehaki, A.; Galkin, I.; Pierrard, V.; Botek, E.; Winant, A.
The PITHIA e-Science Centre
ESWW19, Toulouse (France) and online, 20-24 November 2023 (poster)

56. Ko, Y.-K.; Pierrard, V.; Shen, C.
Solar Wind Ionic Charge State Distributions Predicted by the Lorentzian Exospheric Model
AGU Fall Meeting, San Francisco (California, USA), 11-15 December 2023 (poster).

57. Lamy, H.; Balis, J.
Mesosphere and Lower Thermosphere Wind Determination using data from the radio forward scatter BRAMS network
EGU General Assembly 2023, Vienna (Austria), 23-28 April 2023 (poster)

58. Lamy, H.; Barthélemy, M.; Bosse, L.; Cessateur, G.; Sequies, T.; Gullikstad Johnsen, M.
Spectroscopic and polarimetric optical observations of aurora at the Skibotn Observatory
47th Annual European Meeting on Atmospheric Studies by Optical Methods ("Optical Meeting"), Stockholm (Sweden), 20-24 August 2023

59. Lamy, H.; Verbeeck, C.; Balis, J.; Anciaux, M.; Calders, S.
Observability Function of the BRAMS Meteor Radio Forward Scatter Network
Asteroids, Comets, Meteoroids 2023, Flagstaff (Arizona, USA), 18-23 June 2023

60. Lamy, H.; Anciaux, M.; Balis, J.; Calegaro, A.; Calders, S.
Status and perspectives of the BRAMS network
61. International Meteor Conference 2023, Redu (Belgium), 31 August - 1 September 2023

62. Lamy, H.; Cessateur, G. ; Bosse, L.
Can Polarisation Measurements of Auroral Emissions Trace the Ionospheric Currents? A case-study
IUGG General Assembly, Berlin (Germany), 11-20 July 2023

63. Lario, D.; Balmaceda, L.A.; Gomez-Herrero, R.; and 17 others
Rapid succession of SEP events associated with a series of EUV jets: Solar Orbiter, STEREO-A and near-Earth spacecraft observations
Solar Wind 16, Pacific Grove (California, USA), 12-16 June 2023

64. Lim, D.; Van Doorsselaere, T.; Berghmans, D.
Rapid oscillations in a solar active region observed by the EUI onboard SolO
Advances in Understanding Alfvén Waves in the Sun and the Heliosphere, Berlin (Germany), 28 May - 2 June 2023

65. Lim, D.; Van Doorsselaere, T.; Berghmans, D.
Energy properties of transverse oscillations of solar coronal loops
WISA 2023, Newcastle upon Tyne (UK), 20-23 June 2023

66. Magdalenic, J.; Senthamizh Pavai, V.
Solar wind observed by the PSP at close to the Sun distances
ESWW19, Toulouse (France) and online, 20-24 November 2023

67. Magdalenic, J.; Senthamizh Pavai, V.; Rodriguez, L.
Solar wind originating from the small coronal holes
EGU General Assembly 2023, Vienna (Austria), 23-28 April 2023

68. Maggiolo, R.; Alonso Tagle, M.L.; Gunell, H.; De Keyser, J.; Cessateur, G.; Lapenta, G; Pierrard, V.; Vandaele, A.C.
Investigating the past atmospheric escape rate at Mars using a semi-empirical model
EGU General Assembly 2023, Vienna (Austria), 23-28 April 2023 (poster)

69. Maharana, A.; Dasso, S.; Rodriguez, L.; Pal, S.; Scolini, C.; Magdalenic, J.; Poedts, S.
CME erosion studies using EUHFORIA

ESWW19, Toulouse (France) and online, 20-24 November 2023 (poster)

70. Malandraki, O.E.; Karavolos, M.; Kokkinis, D.; Latocha, M.; Crosby, N.; Dierckxsens, M.; Núñez, M.; Posner, A.; Heber, B.; Kuehl, P.
State-of-the-art space-based SEP prediction for aviation
ESWW19, Toulouse (France) and online, 20-24 November 2023 (poster)

71. Malandraki, O.E.; Karavolos, M.; Kokkinis, D.; Milas, N.; Crosby, N.; Dierckxsens, M.; Núñez, M.; Kuehl, P.
Forecasting and analysis of solar particle radiation storms: A state-of-the-art solution provided by the HESPERIA SEP Real-Time Forecasting products
EGU General Assembly 2023, Vienna (Austria), 23-28 April 2023

72. Malandraki, O.E.; Karavolos, M.; Kokkinis, D.; Milas, N.; Crosby, N.; Dierckxsens, M.; Núñez, M.; Posner, A.; Heber, B.; Kuehl, P.
Forecasting and analysis of solar particle radiation storms: A state-of-the-art solution provided by the HESPERIA SEP Real-Time Forecasting products
The 16th Hellenic Astronomical Conference, Athens (Greece), 26-28 June 2023

73. Maneva, Y.; Delouille, V.; De Patoul, J.; Verstringe, F.; Vinoelst, L.; Valliappan, P.; Shukhobodskaia, D.; Rodriguez, L.; Magdalenic, J.
Towards building a comprehensive data model and infrastructure for collecting and querying event chains
ESWW19, Toulouse (France) and online, 20-24 November 2023

74. Martínez Picar, A.; Marqué, C.; Gunessee, A.; Mouhaou, D.; Magdalenič, J.
HUMAIN RADIO-ASTRONOMY STATION: Current Status & Collaborative Opportunities
ESWW19, Toulouse (France) and online, 20-24 November 2023 (poster)

75. Mouhaou, D.; Martínez Picar, A.; Marqué, C.; Gunessee, A.
Radio meteor echoes observation with SPADE
International Meteor Conference 2023, Redu (Belgium), 31 August - 1 September 2023

76. Nasi, A.; Katsavrias, C.; Aminalragia-Giamini, S.; and 19 others
Investigating the acceleration efficiency of VLF and ULF waves on different electron populations in the outer radiation belt through multi-point observations and modeling
EGU General Assembly 2023, Vienna (Austria), 23-28 April 2023 (poster)

77. Niemela, A.; Wijsen, N.; Aran, A.; Rodriguez, L.; Magdalenic, J.; Poedts, S.
Understanding SEP propagation in CME-CME interaction scenarios
ESWW19, Toulouse (France) and online, 20-24 November 2023 (poster)

78. Pereira, N.; Bolsée, D.; Van Laeken L.; and the INSPIRE-SAT 7 project
Pre-Flight Radiometric validation and calibration of a miniaturized Earth's Radiative Budget satellite
EGU General Assembly 2023, Vienna (Austria), 23-28 April 2023

79. Pezzini, L.; Zhukov, A.N.; Bacchini, F.; Arro, G.; Lopez, R.; Micera, A.; Innocenti, M.E.; Lapenta, G.
Fully Kinetic Simulations of Proton Instabilities Driven by Anisotropic Two-component Velocity Distributions Observed by Parker Solar Probe
AGU Fall Meeting, San Francisco (California, USA), 11-15 December 2023 (poster)

80. Pierrard, V.
Acceleration of energetic solar particles
Biosphere, Mullard Space Science Laboratory, England, 19-20 September 2023 (invited talk)

81. Pierrard, V.
Biosphere public relation and Propagation of cosmic rays and solar energetic particles in the atmosphere
Biosphere 1st Stakeholder Committee Meeting, Online, 4-5 October 2023

82. Pierrard, V.; Botek, E.; Winant, A.
Space radiation variations during Solar Energetic Particle events and geomagnetic storms in the framework of the Biosphere project
Astromeet, Dubai (United Arab Emirates), 16-18 October 2023 (invited talk)

83. Pierrard, V.
Create an impact and Radiation variation using AtRIS simulations
Biosphere M9 Progress Meeting, Prague (Czech Republic), 1-2 June 2023

84. Pierrard, V.
Acceleration of the solar wind: effects of the electric potential in kinetic exospheric models
Solar Wind 16, Pacific Grove (California, USA), 12-16 June 2023 (invited talk)

85. Pierrard, V.; Botek, E.; Winant, A.
Space radiation variations during Solar Energetic Particle events and geomagnetic storms
RAD 11 Conference, Herceg Novi (Montenegro), 19-23 June 2023

86. Pierrard, V.
Regularized Kappa distributions to model the solar wind electrons
Sigma Phi 2023, Chania (Crete, Greece), 10-14 July 2023 (invited talk)

87. Podladchikova, O.; Veronig, A.; Verbeeck, C.; Schuller, F.; Velli, M.; Warmuth, A.
Picoflares in the Quiet Solar Corona
SOLARNET conference: The Many Scales of the Magnetic Sun, Potsdam (Germany), 8-12 May 2023

88. Pottiaux, E.; Bruyninx, C.
ROB's Analysis Centre Activities to Contribute to E-GVAP: Status and updates - 2023
E-GVAP Annual Symposium 2023, Exeter (UK), 21 November 2023

89. Poyraz, D.; Van Malderen, R.; Smit, H.G.J.; and 25 others
Homogenization of the European Ozonesonde Time Series
TOAR-II Workshop, Cologne (Germany), 8-10 March 2023

90. Reeves, G.D.; Ripoll, J.-F.; Botek, E.; and 17 others
Multi-Platform Observations of a Strong Substorm Injection During a CIR
35th URSI General Assembly and Scientific Symposium, Sapporo (Japan), 19–26 August 2023 (poster)

91. Reeves, G.D.; Ripoll, J.-F.; Botek, E.; and 17 others
Multi-Platform Observations of a Strong Substorm Injection During a CIR
AGU Fall Meeting, San Francisco (California, USA), 11-15 December 2023

92. Ripoll, J.-F.; Thaller, S.; Hartley, D.; Cunningham, G.; Pierrard, V.; Kurth, W.S.; Kletzing, C.
Observations and statistics of the plasmasphere boundaries from the Van Allen Probes
35th URSI General Assembly and Scientific Symposium, Sapporo (Japan), 19–26 August 2023 (poster)

93. Rodriguez, L.; Zhukov, A.N.; Shukhobodskaia, D.
Solar Orbiter - Parker Solar Probe Quadrature Observations
PROBA-3 Science Working Team Meeting #9, Brussels (Belgium), 27-29 November 2023

94. Rodriguez, L.; D' Huys, E.; Mierla, M.; Talpeanu, D.C.; Dorsch, B.; Shukhobodskaia, D.; West, M.; Berghmans, D.; Zhukov, A.N.; Verbeeck, C.
Study of Prominence Eruptions Observed by the EUI/FSI Telescope on Solar Orbiter
ESWW19, Toulouse (France) and online, 20-24 November 2023 (poster)

95. Samara, E.; Magdalenic, J.; Rodriguez, L.; Poedts, S.; Georgoulis, M.K.; Pinto, R.F.; Arge, C.N.; Heinemann, S.G.; Hofmeister, S.J.
The fast component of the solar wind: origins, correlations and modeling with EUHFORIA
EGU General Assembly 2023, Vienna (Austria), 23-28 April 2023

96. Sayez, N.; De Vleeschouwer, C.; Delouille, V.; Bechet, S.; Lefèvre, L.
Segmentation, grouping and classification of sunspots from ground-based observations using deep learning methods
International Workshop on Machine Learning and Computer Vision in Heliophysics, Sofia (Bulgaria), 19-21 April 2023 (poster)

97. Senthamizh Pavai, V.; Magdalenic, J.; Jeong, H.-J.
Performance analysis of AI generated solar farside magnetograms in EUHFORIA
International Workshop on Machine Learning and Computer Vision in Heliophysics, Sofia (Bulgaria), 19-21 April 2023

98. Senthamizh Pavai, V.; Magdalenic, J.; Niemela, A.; Linan, L.
Solar wind modelling at near-Sun distances using the COCONUT coronal model and the EUHFORIA heliospheric model
ESWW19, Toulouse (France) and online, 20-24 November 2023 (poster)

99. Shestov, S.
Mutual HRI and AIA observations and DEM analysis
30th EUI Consortium meeting, Orsay (France), 13-15 September 2023

100. Shestov, S.; Zhukov, A.N.; Inhester, B.
Noise in ASPIICS Images As Seen in the On-ground Calibration Data and Its Theoretical Model
PROBA-3 Science Working Team Meeting #9, Brussels (Belgium), 27-29 November 2023

101. Shukhobodskaia, D.; Zhukov, A.N.; Rodriguez, L.
Heliospheric current sheet at multiple locations in heliosphere
PROBA-3 Science Working Team Meeting #9, Brussels (Belgium), 27-29 November 2023

102. Shukhobodskaia, D.; Rodriguez, L.; Zhukov, A.N.; Echim, M.
CMEs and CIRs observed at the Earth, Venus and Mars for the PLATINUM project
ESWW19, Toulouse (France) and online, 20-24 November 2023 (poster)

103. Smit, H.G.J.; Poyraz, D.; Van Malderen, R.; Thompson, A.M.; Tarasick, D.W.; Stauffer, R.M.; Johnson, B.J.; Kollonige, D.E.

New Insights From The Jülich Ozone-Sonde Intercomparison Experiments: Calibration Functions Traceable To One Ozone Reference Instrument
AGU Fall Meeting, San Francisco (California, USA), 11-15 December 2023 (poster)

104. Tarasick, D.W.; Stauffer, R.M.; Smit, H.G.J.; Thompson, A.M.; Davies, J.; Van Malderen, R.; Johnson, B.J.; Vömel, H.; Kollonige, D.E.
Improving Data Quality in Long-term Canadian Ozone Sounding Records
NOAA Global Monitoring Laboratory Annual Conference, Boulder (Colorado, USA), 23-24 May 2023

105. Tarasick, D.W.; Stauffer, R.M.; Smit, H.G.J.; Thompson, A.M.; Davies, J.; Van Malderen, R.; Johnson, B.J.; Vömel, H.
Improving Data Quality in Long-term Canadian Ozone Sounding Records
IUGG General Assembly, Berlin (Germany), 11-20 July 2023

106. Teodorescu, E.; Echim, M.; Munteanu, C.; Teodorescu, M.; Negrea, C.
Effects of the bow shock properties on the scaling of magnetosheath turbulence
IUGG General Assembly, Berlin (Germany), 11-20 July 2023 (poster)

107. Thompson, A.M.; Van Malderen, R.; Smit, H.G.J.; Stauffer, R.M.; Kollonige, D.E.; Leblanc, T.; Vigouroux, C.; Chang, K.-L.; Petropavlovskikh, I.; Poyraz, D.; Clark, H.; Tarasick, D.W.; Hubert, D.
Homogenized Ground-based and Profile Ozone Datasets from TOARII/HEGIFTOM: Methods and Station Trends
AGU Fall Meeting, San Francisco (California, USA), 11-15 December 2023

108. Vanden Broeck, G.; Bechet, S.; Rauw, G.; Clette, F.
Comparison of the magnetic structures in full-disk solar Ca II K images and Sun-as-a-star S-Index
IUGG General Assembly, Berlin (Germany), 11-20 July 2023

109. Van Malderen, R.; Poyraz, D.; Smit, H.G.J.; and 24 others
Homogenization of the European ozonesonde time series
AGU Fall Meeting, San Francisco (California, USA), 11-15 December 2023 (poster)

110. Van Malderen, R.; Smit, H.G.J.; Poyraz, D.; Nakano, T.; Maillard Barras, E.; Romanens, G.
The Cell Temperature of ECC Ozonesondes in Relation to the Measured Pump Temperature: Impact of Freezing and Boiling Effects on Long-Term Ozone Observations with Ozonesondes
AGU Fall Meeting, San Francisco (California, USA), 11-15 December 2023 (poster)

111. Van Malderen, R.; Smit, H.G.J.; Poyraz, D.; Thompson, A.M.; Tarasick, D.W.; Stauffer, R.M.; Johnson, B.J.; Kollonige, D.E.
New insights from the Jülich Ozone-Sonde Intercomparison Experiments (JOSIE): calibration functions traceable to one ozone reference instrument
NDACC Steering Committee meeting, Murnau (Germany), 11-15 September 2023

112. Van Malderen, R.; Smit, H.G.J.; Thompson, A.M.; and 12 others, and the HEGIFTOM members
Homogenized ground based and profile ozone datasets from the TOAR II/HEGIFTOM project: methods and station trends
CEOS AC-VC-19 / ACSG Joint Meeting 2023, Brussels (Belgium), 24-27 October 2023

113. Van Malderen, R.; Smit, H.G.J.; Thompson, A.M.; and 13 others, and the HEGIFTOM members
Trends in tropospheric ozone derived from homogenized ground-based and in situ datasets within TOAR II
IAGOS Users' Meeting, Brussels (Belgium), 14-16 November 2023

114. Van Schaeybroeck, B.; Van Malderen, R.; Pottiaux, E.; Kawo, A.
The use of GPS and reanalysis data for validation of precipitable water vapor in regional climate models over Ethiopia
AGU Fall Meeting, San Francisco (California, USA), 11-15 December 2023 (invited talk)

115. Van Schaeybroeck, B.; Kawo, A.; Van Malderen, R.; Pottiaux, E.
The use of regional climate models for estimating past and future precipitable water vapor and extreme precipitation over Ethiopia
EGU General Assembly 2023, Vienna (Austria), 23-28 April 2023 (poster)

116. Vansintjan, R. ; Mampaey, B. ; Delouille, V.
The SOLARNET Virtual Observatory (SVO) - Making Solar physics data findable and accessible
ESWW19, Toulouse (France) and online, 20-24 November 2023

117. Verbeeck, C.
CLOSE-UP campfire project
29th EUI Consortium meeting, Online, 25-27 January 2023

118. Verbeke, C.; ; Mays, M.L.; Mierla, M.; Kay, C.; Dumbović, M.; Riley, P.; Scolini, C.; Paouris, E.; Temmer, M.; Balmaceda, L.; Cremades, H.; Martinic, K.; Hinterreiter, J.
Understanding our capabilities in observing and modelling Coronal Mass Ejections
EGU General Assembly 2023, Vienna (Austria), 23-28 April 2023 (invited talk)

119. Voitcu, G.; Echim, M.
X-ray emissivity of high-speed plasma jets in the Earth's magnetosheath: Preliminary results
IUGG General Assembly, Berlin (Germany), 11-20 July 2023 (poster)

120. Voitcu, G.; Echim, M.; Teodorescu, E; De Donder, E.
Investigation of the influence of the dynamic magnetosphere on solar energetic particles propagation
ESWW19, Toulouse (France) and online, 20-24 November 2023 (poster)

121. Voitcu, G.; Echim, M.; Teodorescu, E.; Munteanu, C.
Soft X-ray detection of high-speed plasma jets in the Earth's magnetosheath: numerical simulations
41st SMILE MWG Meeting, SMILE SWT#22 - SMILE Consortium Meeting #16, Rome (Italy), 6-10 November 2023

122. Wang, H.; Liu, J.; Tarasick, D.W.; Smit, H.G.J.; Van Malderen, R.; Zhao, T.
Consistency evaluation of tropospheric ozone from ozonesonde and IAGOS aircraft observations: vertical distribution, ozonesonde types and station airport distance
IAGOS Users' Meeting, Brussels (Belgium), 14-16 November 2023

123. Warmuth, A.; Schuller, F.; Gómez-Herrero, R.; and 15 others, and the Joint STIX-EPD-RPW-EUI Working Group
First results on interplanetary electron events obtained by joint observations of remote-sensing and in-situ instruments on Solar Orbiter
EGU General Assembly 2023, Vienna (Austria), 23-28 April 2023

124. Whitman, K.; Quinn, P.R.; Egeland, R.; Dierckxsens, M.; Mays, M.L.; Collado-Vega, Y.; Bain, H.
SPHINX: An SEP Model Validation Infrastructure developed through Community Challenges and the SEP Scoreboards
ESWW19, Toulouse (France) and online, 20-24 November 2023

125. Wimmer-Schweingruber, R.; Berger, L.; Kollhoff, A.; … and 30 others
Unusually Long Path Length for a Nearly Scatter-Free solar particle event observed by Solar Orbiter at 0.43 au
Solar Wind 16, Pacific Grove (California, USA), 12-16 June 2023

126. Wimmer-Schweingruber, R.; Berger, L.; Kollhoff, A.; … and 30 others
Unusually long path length for a nearly scatter-free solar particle event observed by Solar Orbiter at 0.43 au
AGU Fall Meeting, San Francisco (California, USA), 11-15 December 2023 (poster)

127. Yuan, P.; Van Malderen, R.; Yin, X.; Kutterer, H.
Analysis of diurnal IWV cycle and evaluation of artificial mismatches in ERA5 over Europe by using GNSS
IAG-ICCC Workshop Geodesy for Climate Research, Online, 28-29 March 2023

128. Zhukov, A.N.
PROBA-3/ASPIICS coronagraph
ISTP Next Workshop, JHU/APL, Laurel (Maryland, USA), 8-10 May 2023 (invited talk)

129. Zhukov, A.N.
ASPIICS PI Status Update
PROBA-3 virtual Science Working Team Meeting #8, Online, 12 July 2023

130. Zhukov, A.N.
ASPIICS PI Status Update
PROBA-3 Science Working Team Meeting #9, ROB, Brussels (Belgium), 27-29 November 2023

131. Zhukov, A.N.
Science of the PROBA-3/ASPIICS Coronagraph
PROBA-3 Spacecraft Acceptance Event - Redwire Space, Kruibeke (Belgium), 9 September 2023

132. Zhukov, A.N.; Chitta, P.; Berghmans, D.; and 17 others
Polar Coronal Holes: Fine Structure, Dynamics, and the Link to the Solar Wind
AGU Fall Meeting, San Francisco (California, USA), 11-15 December 2023

133. Zhukov, A.N.; Telloni, D.
Solar Orbiter - Parker Solar Probe Quadrature SOOP
LTP11 SOOP coordinators feedback meeting, 5 September 2023

Public Outreach: talks and publications for the general public

1. Berghmans, D.
Observing the solar corona with the Extreme Ultraviolet Imager (EUI) on Solar Orbiter
3rd Workshop of the Belgian-Indian Network on Astrophysics (BINA), Graphic Era Hill University, India 24 March 2023

2. Berghmans, D.
De Extreme Ultraviolet Imager (EUI) aan boord van Solar Orbiter
Volkssterrenwacht Mira, 30 June 2023

3. Clette, F.; Bechet, S.
Interview pour le MOOC Recherche Reproductible 2
Chesany (France), 28 June 2023

4. D'Huys, E.; Vanlommel, P.
De Ruimte
Basisschool De Oogappel, Gent (Belgium), January 2023

5. Dolla, L.
Comment le champ magnétique façonne l'atmosphère du Soleil
Jeunesse et Science ASBL, Louette-Saint-Pierre (Belgium), 22 November 2023

6. Jacques, D.; Bruyninx, C.; Van Noten, K.; Zeckra, M.; Bamahry, F.; Fabian, A.; Legrand, J.; Miglio, A.; Pottiaux, E.; Mesmaker, D.; Moyaert, A.; Rapagnani, G.; Lecocq, T.; Frederick, B.
EPOS - L'infrastructure de recherche paneuropéenne pour les sciences de la Terre
Science Connection, 69, issue sept-oct-nov 2023

7. Jacques, D.; Bruyninx, C.; Van Noten, K.; Zeckra, M.; Bamahry, F.; Fabian, A.; Legrand, J.; Miglio, A.; Pottiaux, E.; Mesmaker, D.; Moyaert, A.; Rapagnani, G.; Lecocq, T.; Frederick, B.
EPOS - De pan-Europese onderzoeksinfrastructuur voor Aardwetenschappen
Science Connection, 69, issue sept-okt-nov 2023

8. Janssens, J.
Zon en Ruimteweer
MIRA Public Observatory, Grimbergen (Belgium), 3 May 2023

9. Janssens, J.
Best of 2022
STCE YouTube channel, 6 July 2023

10. Lamy, H.; Balis, J.; Calegaro, A.; Ranvier. S.; Lamort. L.
Presentation of the BRAMS network to a wide audience
Journées européennes du patrimoine en Wallonie, Radioastronomical site of Humain (Belgium), 9-10 September 2023

11. Lamy H.
Forty-Second International Meteor Conference, Redu, Belgium August 31-September 3
WGN, Journal of the International Meteor Organization, 51, 1, 3-8, February 2023

12. Lim, D.
Luotaimet avaavat näkymiä Auringon koronaan
Tähdet ja avaruus, June 2023

13. Messios, N.
Radiation studies in support of the design of space mission instruments
STCE Annual Meeting, Space Pole (Belgium), 29 June 2023

14. Miglio, A.; Bruyninckx, C.
Things you always wanted to know about FAIR data (but were afraid to ask)
STCE Annual Meeting, Space Pole (Belgium), 29 June 2023

15. Pierrard, V.
The plasmasphere: Formation and dynamics and The 3D Dynamic Kinetic Model of the Plasmasphere
PITHIA training school, Rome (Italy), 29 May-1 June 2023

16. Pierrard, V.
Access to 3D Dynamic Kinetic Plasmasphere model data products
Fifth Training for PITHIA Partners Workshop, University of Westminster, London (UK), 12-13 September 2023

17. SWIC - Space Weather Introductory Course
D'Huys, E.; Janssens, J.; Vanlommel, P.; STCE collaborators (Marqué, C.; Martinez, A.; Clette, F.; Bechet, S.; Van den Broeck, G.; Verhulst, T.G.W.; Zychova, L.; Chevalier, J.-M.; Bergeot, N.; SIDC/RWC) and international partners (Doornbos E. (KNMI); Sievers, K. (KSAW); Brchnelova, M. (KUL))
Lectures, Exercises, Visits, Quiz, Dedicated courses
    - SWIC 2023/1 on 30-31 January and 2-3 February 2023 (online)
    - SWIC 2023/2 on 27-29 March 2023
    - SWIC 2023/3 on 22-24 May 2023
    - SWIC 2023/4 on 18-20 September 2023

18. SWIC - Space weather for BKG
D'Huys, E.; Janssens, J.; Vanlommel, P.; STCE collaborators (Marqué, C.; Martinez, A.; Lefèvre, L.; Verhulst, T.G.W.; Chevalier, J.-M.; Maneva, Y.; de Patoul, J.; SIDC/RWC) and

international partners (Doornbos E. (KNMI); Witvliet, B. (University of Twente))
Lectures, Exercises, Visits, Dedicated courses

- ROB, Brussels (Belgium), 12-14 June 2023

19. SWIC - SWIC4Forecasters
D'Huys, E.; Janssens, J.; Vanlommel, P.; STCE collaborators (Loumou, K.; Magdalenic, J.; Rodriguez, L.; Maneva, Y.; O'Hara, J.; de Patoul, J.; SIDC/RWC)
Lectures, Exercises, Dedicated courses

- ROB, Brussels (Belgium), 9-11 October 2023

20. SWIC - SWx impacts on ionospheric wave propagation- focus on GNSS and HF
D'Huys, E.; Janssens, J.; Vanlommel, P.; STCE collaborators (Martinez, A.; Lemaitre, O.; Verhulst, T.G.W.; Chevalier, J.-M.; SIDC/RWC) and external partners (Brchnelova, M. (KUL))
Lectures, Exercises, Visits, Dedicated courses

- ROB, Brussels (Belgium), 4-6 December 2023

21. Van der Linden, R.; Berghmans, D.
Impact of Space Weather on the Security of Earth & Space Assets
High Level Course on Aerospace, Defence & Security, Brussels (Belgium), 8 September 2023

22. Van der Linden, R.
STCE - alive and working for you
STCE Annual Meeting, Space Pole (Belgium), 29 June 2023

23. Vanlommel, P.
Space Weather Education Center: also for you
STCE Annual Meeting, Space Pole (Belgium), 29 June 2023

24. Vanlommel, P.; Berghmans, D.
L2: De Zon
VVS Summerschool, Leuven (Belgium), 21 August 2023

25. Vanlommel, P.; D'Huys, E.; Lemaitre, O.
1st E-SWAN school: Space Weather Data, Models and Services
Satellite event (course) before the ESWW2023, Toulouse (France), 18 November 2023

26. Vanlommel, P.; Berghmans, D.; ESA press team
Solar Orbiter Discovers Tiny Jets That Could Power the Solar Wind
ESA news item, 24 August 2023

27. Vanlommel, Petra
Live vanuit de ruimteweerkamer
Dag van de Wetenschap, Planetarium de Heizel, Brussels (Belgium), 26 November 2023

28. Vanlommel, P.; D'Huys, E.
From Physics to Forecasting
Space Weather Training Course, ESA Academy, Redu (Belgium), 8 May 2023

29. Vanlommel, P.; D'Huys, E.; Janssens, J.
STCE Newsletter
Weekly newsletter, 48 issues, 2023

30. Van Malderen, R.
Quality Assurance and Quality Control of ozonesondes
STCE Annual Meeting, Space Pole (Belgium), 29 June 2023

31. Verbeeck, C.
Bestaat er buitenaards leven?
Kiwanis Antwerpen ter Schelde Antwerpen, Belgium, 7 June 2023

32. Verbeeck, C.
De zon
2nd year primary school "Arkades", Herentals (Belgium), 21 December 2023

33. Verbeke, C.
Pas op! Een zonnestorm op komst
Nederlands Tijdschrift voor Natuurkunde, 89, May 2023

34. Verbeke, C.
Te gast op wetenschapshow (buiten)aards
Main theater van het Nerdlandfestical, Wachtebeke (Belgium), 27 May 2023

35. Wimmer-Schweingruber, R.; Berger, L.; Kollhoff, A.; et al.
Unusually long path length for a nearly scatter-free solar particle event observed by Solar Orbiter at 0.43 au
ESA science nuggets, 11 October 2023

36. Winant, A.; Botek, E.; Pierrard, V.
Simulations with the Atmospheric Radiation Interaction Simulator (AtRIS) in the frame of the EURAMET Biosphere project
Lecture at the University of Kiel (Germany), 25 April 2023

37. Winkel, B.; Garrington, S.; Colomer, F.; et al.
Preserving your skies since 1988 - Committee on Radio Astronomy Frequencies (CRAF) - Periodic Review 2011-2021
CRAF, DOI: 10.48550/arXiv.2310.13407, 2023

38. Zhukov, A.N.
Science of the PROBA-3/ASPIICS Coronagraph
Visit of the PROBA-3 spacecraft, Redwire Space, Kruibeke Belgium), 27 November 2023

39. Zychova, L.; Crosby, N.
A Touch of Space Weather – workshop for children
Night in Wolvendael, Uccle (Belgium), 26-27 August 2023

The STCE Annual Meeting took place on 29 June. It started with some general talks on the STCE and SWEC, and was then followed by 3 brainstorming sessions on "Communication and branding", "Internal training and courses", and "Internal organisation and structure" of the STCE. The results were presented at the end of the meeting. There were also interesting talks on FAIR, radiation impacts on space mission instruments, and on ozonesondes. The event was concluded with a STCE bingo and -of course- a sandwich lunch.

List of abbreviations

~	About, proportional to
Δ	Delta (difference)
//	Parallel
⊥	Perpendicular
%	Percentage
1D, 2D, 3D,…	One, two, three,… dimensional
^{3}He	Stable isotope of Helium
Å	Ångstrom (0.1 nm)
A	Article
AAS	American Astronomical Society
ACE	Advanced Composition Explorer
ACM	Asteroids, Comets, Meteoroids (conference)
ACSG	Atmospheric Composition Sub Group
AC-VC	Atmospheric Composition Virtual Constellation
AGU	American Geophysical Union
AI	Artificial Intelligence
AIA	Atmospheric Imaging Assembly (SDO)
ALIS	Auroral Large Imaging System
AM	Amplitude Modulation
AMS	American Meteorological Society
ANeMoS	Athens Neutron Monitor Station
AOGS	Asia Oceania Geosciences Society
APEX	Airborne Prism EXperiment
APL	Applied Physics Laboratory (JHU)
APS	(1) American Physical Society ; (2) Active Pixel System (PROBA2)
AR	(1) Active Region ; (2) Annual Report
ARCAS	Augmented Resolution Callisto Spectrometer
ARTIST	Automatic Real-Time Ionogram Scaler with True height (software)
ASGARD	An educational space programme for schools (no acronym)
ASIMUT	Atmospheric Spectra Inversion Modular Utility Tools (code; BIRA-IASB)
ASIS	Auroral Spectrograph In Skibotn (Sweden)
ASL	Above Sea Level
ASPIICS	Association of Spacecraft for Polarimetric and Imaging Investigation of the Corona of the Sun (PROBA-3)
AT-AP-RASC	ATlantic / Asia-Pacific Radio SCience meeting
AtRIS	The Atmospheric Radiation Interaction Simulator
AU, au	Astronomical Unit; about 150 million km
B	Magnetic field (strength)
B_0	Heliographic latitude of the central point of the solar disk (The range of B_0 is $\pm$7.23°)
BE	Belgium
BELSPO	Belgian Science Policy Office
Benelux	Belgium, The Netherlands, and Luxembourg
Bifrost	MHD code (no acronym); the name of the rainbow bridge from Midgard (the realm of man) to Asgard (the realm of the gods)
BINA	Belgo-Indian Network for Astronomy and Astrophysics
BIRA	Koninklijk Belgisch Instituut voor Ruimte-Aëronomie
BIRA-IASB	Royal Belgian Institute for Space Aeronomy
BKG	German Federal Agency for Cartography and Geodesy (Bundesamt für Kartographie und Geodäsie)
BNCGG	Belgian National Committee for Geodesy and Geophysics
BRAIN-be	Belgian Research Action through Interdisciplinary Networks (BELSPO)
BRAMS	Belgian RAdio Meteor Stations
B.RCLab	Belgian Radiometric Characterization Laboratory
BUKS	Belgium, UK, and Spain
B.USOC	Belgian User Support and Operation Centre
Bz	Component of the IMF perpendicular to the ecliptic ("north-south" component)
°C	Degrees Celsius

C1, C2, C3	Coronagraphs of LASCO (SoHO)
C-class flare	Common x-ray flare
C/N_0	Carrier-to-Noise
CA	COST Action (COST)
Ca II H	A blue line in the solar spectrum at 396.85 nm
Ca II K	A blue line in the solar spectrum at 393.37 nm
CACTus	Computer Aided CME Tracking software
CALLISTO	Compound Astronomical Low frequency Low-cost Instrument for Spectroscopy and Transportable Observatory
CAMS	Cameras for Allsky Meteor Surveillance (Benelux)
CCD	charge-coupled device
CCMC	Community Coordinated Modeling Center
CEOS	Committee on Earth Observation Satellites
CESRA	Community of European Solar Radio Astronomers
CH	Coronal Hole
CH_4	Methane
CH_4TIR	CH4 Thermal InfraRed
CIR	Co-rotating Interaction Region
Cluster	ESA/NASA mission to study the Earth's magnetosphere (no acronym)
cm, cm^2, cm^3	centimeter, square centimeter, cubic centimeter
CME	Coronal Mass Ejection
CMOS	Complementary Metal-Oxide-Semiconductor
CmPA	Centre for mathematical Plasma-Astrophysics (KUL)
CNES	Centre national d'études spatiales (France)
CNN	Convolutional Neural Network
CNRS	Centre national de la recherche scientifique (France)
Co.	Cooperation
CO_2	Carbon Dioxide
COCONUT	COolfluid COroNa UnsTructured (model)
co-Is	co-investigators
COMESEP	COronal Mass Ejections and Solar Energetic Particles
COPUOS	COmmittee on the Peaceful Uses of Outer Space (UN)
COR (1/2)	Coronagraph (Inner/Outer) onboard STEREO
CORS	Continuously Operating Reference Stations (GNSS)
COSPAR	COmmittee on SPAce Research
COST	(European) COoperation in Science & Technology
COTS	Commercial off-the-shelf
CPSR	Core Plasma Supply and Refilling (in Geospace)
CPU	Central Processing Unit
CR	Carrington Rotation
CRAF	Committee on Radio Astronomy Frequencies
CROM	A type of pyrheliometer developed by D. Crommelynck (RMI)
CSL	Centre Spatial de Liège
CubeSat	A small satellite measuring 10cm x 10cm x 10cm
CVC	Convective and Volcanic Clouds
dB FS	Decibels relative to Full Scale
dB-Hz	decibel-Hertz (bandwidth relative to 1 Hz)
DEM	Differential Emission Measure
DeMeLab	Detector Measurements Laboratory (aka STCL)
DICTAT	Dielectric Internal Charging Threat Assessment Tool
Digisonde	Digitally Integrating Goniometric IonoSONDE
DIGISUN	A software application for digitization of scanned sunspot drawings
DLR	German Aerospace Center
dm, dm^2, dm^3	decimeter, square decimeter, cubic decimeter
DOI	Digital Object Identifier
DOU	Dourbes (Intermagnet)
DoY	Day of Year
DPS	(1) Division for Planetary Sciences (EPSC) ; (2) Digital Portable Sounder
Dr.	Doctor
DRBS	Dourbes (Belgium, NMDB)
DSCOVR	Deep Space Climate Observatory

Dst	Disturbance Storm Time index (geomagnetic)
E	East
E, E_- , E_+	Energy, Ingoing energy, Outgoing energy
e.g.	exempli gratia (example given)
e-Callisto	extended Compact Astronomical Low-cost Low-frequency Instrument for Spectroscopy and Transportable Observatory
EC	European Commission
ECC	Electrochemical Concentration Cell
ECMWF	European Centre for Medium-range Weather Forecasts
ed.	Edition
Eds.	Editors
EFW	Electric Field and Waves instrument (Van Allen probes)
EGNOS	European Geostationary Navigation Overlay Service (Galileo/Europe)
EGNSS	European GNSS
EGU	European Geosciences Union
E-GVAP	EUMETNET GNSS water Vapour Programme
EIG	Economic Interest Grouping
EIS	EUV imaging spectrometer (Hinode)
EISCAT	European Incoherent SCATter scientific association
EIT	Extreme ultraviolet Imaging Telescope (SOHO)
ELF	Extreme Low frequency (3-30 Hz)
EM	(1) Electromagnetic (2) Engineering Model
EMFISIS	Electric and Magnetic Field Instrument Suite and Integrated Science (Van Allen Probes)
ENVISAT	Environmental Satellite (ESA)
EnVision	ESA’s Venus orbiter (no acronym)
EPD	Energetic Particle Detector (SolO)
EPN	(1) EUREF Permanent Network (2) Europlanet
EPOS	European Plate Observing System
E-PROFILE	EUMETNET Profiling Programme
EPS	European Physical Society
EPSC	European Planetary Science Congress
EPT	Energetic Particle Telescope (PROBA-V)
ERA	ECMWF re-analysis
ERAI , ERA5	ERA-Interim, 5th ERA
ERB	Earth Radiation Budget
erg	10^{-7} Joule
Es	Sporadic E-layer (ionosphere)
ES	Earth System (Science and Environmental Management (COST)
ESA	European Space Agency
ESAC	European Space Astronomy Centre
ESC	Expert Service Centre (SSCC)
ESD	ElectroStatic Discharge
ESCAPE	(1) European SpaceCraft for the study of Atmospheric Particle Escape (2) European Science Cluster of Astronomy & Particle physics ESFRI research infrastructures
ESERO	European Space Education Resource Office
ESFRI	European Strategy Forum on Research Infrastructures
ESLAB	Environmental Simulation Laboratory
ESOC	European Space Operations Centre
ESPD	European Solar Physics Division (EPS)
ESPM	European Solar Physics Meeting
ESTEC	European Space Research and Technology Centre
E-SWAN	European Space Weather and Space Climate Association
ESWW	European Space Weather Week
et al.	et alii (and other)
etc.	et cetera (and so forth)
ETH	Eidgenössische Technische Hochschule Zürich
EU	European Union
EUHFORIA	European Heliospheric Forecasting Information Asset

EUI	Extreme-Ultraviolet Imager (Solar Orbiter)
EUMETNET	Network of European Meteorological Services
EUMETSAT	European Organisation for the Exploitation of Meteorological Satellites
EUREF	EUropean Reference Frame
EUV	Extreme Ultraviolet
EUVST	EUV High-throughput Spectroscopic Telescope (Solar-C ; Jaxa)
EUVI	Extreme Ultraviolet Imager (STEREO/SECCHI; LGRRS)
eV	electron volt (1 eV = 1.602 × 10^{-19} joules)
EVE	Extreme ultraviolet Variability Experiment (SDO)
ExoMars	Exobiology on Mars (ESA, Roscosmos)
f	frequency
$F_{10.7}$, $F_{10.7\ cm}$	Solar radio flux at 10.7 cm wavelength
F_2	Main ionospheric layer
FAIR	Findable, Accessible, Interoperable, and Re-usable
Fe IX-X	8 respectively 9 times ionized iron
FITS	Flexible Image Transport System
FM	(1) Flight Model (2) Frequency Modulation
FMI	Finnish Meteorological Institute
FNRS	Fonds National de la Recherche Scientifique
foE	Critical frequency E-layer
foEs	Sporadic E critical frequency
foF2	Critical frequency F2-layer
FOV	Field-Of-View
FP7	Framework Programme 7 (EU)
Fri3D	Flux Rope in 3D
FRS	Fonds de la Recherche Scientifique
FSI	Full Sun Imager (Solar Orbiter / EUI)
ft	foot or feet (1 ft = 30.48 cm)
FTE	Full-Time Equivalent
ftp	file transfer protocol
FUV	Far Ultraviolet
G	(1) Gauss (10^{-4} Tesla or 10^5 nT); (2) Gigabyte (10^9 bytes)
Gaia	ESA satellite (no acronym)
Galileo	European GNSS
GASS	General Assembly and Scientific Symposium
GAW	Global Atmospheric Watch (WMO)
GB	Gigabyte (10^9 bytes)
GBO	Ground-Based Observatory
GCR	Galactic Cosmic Rays
GEANT-4	GEometry ANd Tracking (simulation platform)
GEO	A geostationary orbit , i.e. a circular geosynchronous orbit 35.786 km in altitude
GERB	Geostationary Earth Radiation Budget
GeV	Giga electronvolt (10^9 . 1.6 . 10^{-19} Joule)
GFZ	Deutsches GeoForschungsZentrum (German Research Centre for Geosciences)
GHz	Gigahertz (10^9 Hz)
GIC	Geomagnetically induced current
GLE	Ground Level Enhancement
GLONASS	GLObal NAvigation Satellite System (Russia)
GMAC	Global Monitoring Annual Conference
GML	Global Monitoring Laboratory
GNSS	Global Navigation Satellite System
GNSS(GRE)	GNSS corrections based on GPS-GLONASS-GALILEO constellations (GPS/Russia/Europe)
GOES	Geostationary Operational Environmental Satellite
GOME	Global Ozone Monitoring experiment (SCIAMACHY)
GOMESCIA	GOME/SCIAMACHY/GOME-2
GONG	Global Oscillation Network Group
GPS	Global Positioning System (USA)
GRAPE	GNSS Research and Application for Polar Environment

GSE	Geocentric Solar Ecliptic system
GSFC	Goddard Space Flight Center
GTO	Geostationary Transfer Orbit
h	(1) hour ; (2) Planck's constant ($6.62607004 \times 10^{-34}$ m^2 kg / s)
H	(1) Hydrogen ; (2) Heat flux
H-alpha (Hα)	A red visible spectral line at 656.28 nm created by Hydrogen
H2020	Horizon 2020 (EU)
H_2O	Water
He, He II	Helium, ionized Helium
HEGIFTOM	Harmonization and Evaluation of Ground-based Instruments for Free Tropospheric Ozone Measurements
HEK	Heliophysics Events Knowledgebase
Helios 1, 2	Two joint German-American space missions in the 1970s (no acronym)
HESPERIA	High Energy Solar Particle Events foRecastIng and Analysis
HF	High Frequency (3-30 MHz)
HF Com	HF Communication
HI	(1) Neutral atomic Hydrogen ; (2) Heliospheric Imager (STEREO)
Hinode	A JAXA/NASA solar mission : Solar-B satellite ("sunrise")
h_mF_2	peak density height of F_2-layer
HMI	Heliospheric and Magnetic Imager (SDO)
hPa	hectopascal (atmospheric pressure)
HRI	High Resolution Imager (Solar Orbiter / EUI)
HRIEUV	High Resolution Imager in the EUV (Solar Orbiter / EUI)
HRILYA	High Resolution Imager in Ly-α (Solar Orbiter / EUI)
HSRS	Humain Solar Radio Spectrograph
HSS	High Speed Stream
HuRAS	Humain Radio Astronomy Station
HWM	Horizontal Wind Model
HXR	Hard x-rays
Hz	Hertz (per second)
i	The index in a counter or series
I	Current
I-V	Current-Voltage
IABG	Industrieanlagen-Betriebsgesellschaft mbH (German company; PROBA-3)
IAC	International Astronautical Congress
IAG	International Association of Geodesy
IAGA	International Association of Geomagnetism and Aeronomy
IAGOS	In-service Aircraft for a Global Observing System
IAS	Institut d'Astrophysique Spatiale (France)
IASB	Institut royal d'Aéronomie Spatiale de Belgique
IASC	International Arctic Science Committee
IASI	Infrared Atmospheric Sounding Interferometer
IAU	International Astronomical Union
iCACGP	international Commission on Atmospheric Chemistry and Global Pollution
ICARUS	a new inner heliospheric model for the simulation of a steady background solar wind and the propagation and evolution of superposed CMEs (KUL; no acronym)
ICAO	International Civil Aviation Organization
ICCC	Inter-Commission Committee on "Geodesy for Climate Research" (IAG)
ICMA	International Commission on the Middle Atmosphere
ICME	Interplanetary CME
ICON	ICOsahedral Nonhydrostatic (meteorological model)
ICSO	International Conference on Space Optics
ICT	Information and Communication Technologies
IDL	Interactive Data Language
i.e.	"id est" (that is)
IEEE	Institute of Electrical and Electronics Engineers

IGAC	International Global Atmospheric Chemistry project
IGS	International GNSS Service
IMC	International Meteor Conference
IMF	Interplanetary Magnetic Field
IMO	International Meteor Organization
INA	Integrated Nonlinear Analysis
INGV	Istituto nazionale di geofisica e vulcanologia (Italy)
INSPIRE	(1) International Satellite Program in Research and Education (2) Infrastructure for Spatial Information in the European Community (EU)
IOP	Institute of Physics
IPAG	Institut de Planétologie et d'Astrophysique de Grenoble (France)
IPC	International Pyrheliometer Comparison
IPEV	Institut Polaire Français Paul-Émile Victor
IQR	InterQuartile Range
IR	Infrared
IRAP	Institut de Recherche en Astrophysique et Planétologie (France)
IRI	International Reference Ionosphere
IRIS	Interface Region Imaging Spectrograph (NASA)
IRM(B)	Institut Royal Météorologique (de Belgique)
IRSA	Institut Royal pour Sourds et Aveugles (Brussels, Belgium)
ISAS	Institute of Space and Astronautical Science
ISC	(1) International Science Council; (2) International Steering Committee
ISN	International Sunspot Number
ISO	International Organization for Standardization
iso-B lines	Lines of equal magnetic field strength
iso-L lines	Lines of equal L (see L*)
ISS	International Space Station
ISSI	International Space Science Institute
ISSS	(1) International School of Space Science; (2) International School/Symposium for Space Simulations
ISTP	International Solar Terrestrial Program
ISWAT	International Space Weather Action Teams (COSPAR)
ISWI	International Space Weather Initiative
IT	Information Technology
IUGG	International Union of Geodesy and Geophysics
IVOA	International Virtual Observatory Alliance
IWV	Integrated Water Vapour
J	Joule
JAXA	Japan Aerospace Exploration Agency
JGR	Journal of Geophysical Research
JHU	Johns Hopkins University
jHV	jHelioViewer
JOSIE	Jülich Ozone Sonde Intercomparison Experiment
JPEG	Joint Photographic Experts Group
JSON	JavaScript Object Notation
JSWSC	Journal of Space Weather and Space Climate
JUICE	JUpiter ICy moons Explorer
k	wave number
K	(1) Local K index: A 3-hour geomagnetic index, ranging from 0 (quiet) to 9 (extremely severe storm); (2) degrees Kelvin
K*	Local 1-minute resolution K index
Ka-band	"Kürz above": Radio frequency band from 27-40 GHz
KAW	Kinetic Alfvén Waves
KBEL	Local K index for Belgium
keV	kilo-electronvolt (10^3 . 1.6 . 10^{-19} Joule)
kHz	kilohertz (10^3 /second)
KI	Potassium iodide
km, km^2	kilometer, square kilometer
km/s	kilometers per second
KMI	Koninklijk Meteorologisch Instituut

KNMI	Koninklijk Nederlands Meteorologisch Instituut
K_p	“planetarische Kennziffer”, a geomagnetic index, ranging from 0 (quiet) to 9 (extremely severe storm)
KSAW	Klaus Sievers Aviation Weather
KSO	Kanzelhöhe Solar Observatory
KSB	Koninklijke Sterrenwacht van België
KUL, KULeuven	Katholieke Universiteit Leuven
kV	kilovolt (10^3 Volt)
λ	wavelength
λ_e	electron inertial length
l/m^2	Liter per square meter
L-class	Large class satellite (ESA)
L	(1) Letter (manuscript); (2) L-shell (see L*)
L*	Set of Earth’s magnetic field lines which cross the Earth’s magnetic equator at * earth radii from the centre of the Earth (e.g. L = 2); also known as McIlwain parameter
L_0	Heliographic longitude of the central point of the solar disk
L1, … , L5	First, … , fifth Lagrangian point
L1, L2	GPS frequencies: L1 = 1575.42 MHz, L2 = 1227.60 MHz
LASCO	Large Angle Spectrometric Coronagraph (SOHO); small (C2) and wide (C3) field of view
LASP	Laboratory for Atmospheric and Space Physics
Lat	Latitude
LATMOS	Laboratoire ATmosphères, Milieux, Observations Spatiales (France)
LBL	line-by-line
LDE	Long Duration Event
LEO	Low Earth Orbit (below 2000 km ASL)
LIDAR	LIght Detection And Radar
LIEDR	Local Ionospheric Electron Density profile Reconstruction
LMSAL	Lockheed Martin Solar and Astrophysics Laboratory
LOC	Local Organising Committee
LOFAR	Low-Frequency Array
Lon	Longitude
LPV-200	Localizer Performance with Vertical guidance until the aircraft is 200 ft above the runway
Ls	Solar longitude
LT	Local Time
LTP	Long-term planning (Solar Orbiter)
LUT	Look-Up Tables
Ly-α	Lyman-alpha, a spectral line in the VUV at 121.6 nm
LYA	Ly-α
LYRA	Large Yield Radiometer, formerly called Lyman Alpha Radiometer (PROBA2)
LWS	Living With a Star
μm	micrometer (10^{-6} meter)
M-class	Medium class satellite (ESA)
M-class flare	Medium x-ray flare
m, m^2, m^3	Meter, square meter, cubic meter
MAB	Manhay (Intermagnet)
MagEIS	MAGnetic Electron Ion Spectrometer (Van Allen probes)
MAJIS	Moons And Jupiter Imaging Spectrometer (JUICE)
MAPLD	Military and Aerospace Programmable Logic Devices
MB	megabyte (10^6 bytes)
mbar	millibar
MEO	Medium Earth Orbit (between 2000 and 35.786 km ASL)
Meteosat	Series of geostationary meteorological satellites operated by EUMETSAT
METIS	Multi Element Telescope for Imaging and Spectroscopy (SolO)
MeV	mega-electronvolt ($10^6 . 1.6 . 10^{-19}$ Joule)
MHD	Magnetohydrodynamics
MHz	megahertz (10^6/s)
MIT	Massachusetts Institute of Technology
MJD	Modified Julian Day
MLH	mixing layer height
MLP	Multi-Layer Perceptron
MLT	Magnetic Local Time
mm, mm^2	millimeter (10^{-3} meter), square mm

Mm	megameter (10^6 meter)
MMM	Monthly Management Meeting (SIDC)
mm/s	millimeter per second
MOC	(1) Mission Operations Center; (2) Maintenance and Observations Center (PECASUS)
MOMA	Multi-wavelength Observations and Modelling of Aurora
MoMo	Model of Mars Ionosphere
MOMSTER	MObile Meteor STation for Education & outreach
MOOC	Massive Open Online Courses
MPPC	Max Planck-Princeton Center
MPS	Max Planck Institute for Solar System Research
ms	millisecond (10^{-3} second)
MUF, MUF3000	Maximum Usable Frequency, the maximum radio frequency which can be reflected by the ionosphere for a given distance of transmission e.g. 3000 km
MUV	Mid Ultraviolet
ν	Frequency
N	North
N-S	North-South
N_2	Nitrogen
N_2^+	Ionized molecular nitrogen
N_2O	Nitrous oxide (“laughing gas”)
nA	nanoampère (10^{-9} meter)
NAOJ	National Astronomical Observatory of Japan
NARMAX	Nonlinear AutoRegresssive Moving Average eXogenous model
NASA	National Aeronautics and Space Administration
NASU	National Academy of Sciences of Ukraine
NATO	North Atlantic Treaty Organization
Nc, Ns, Ng	the number of spots Ns, the number of groups Ng, and the composite Nc = Ns + 10Ng
NDACC	Network for the Detection of Atmospheric Composition Change
NeQuick	Electron density Quick calculation model (ionospheric model)
Net-TIDE	Pilot Network for Identification of Travelling Ionospheric Disturbances in Europe
NIR	Near IR
NL	The Netherlands
NM	Neutron Monitor
nm	nanometer (10^{-9} meter)
NMDB	Neutron Monitor DataBase
N_mF_2	peak density of F_2-layer
No.	Number of
NO_2	Nitrogen dioxide
NOAA	National Oceanic and Atmospheric Administration
NOMAD	Nadir and Occultation for MArs Discovery (ExoMars)
NRT	Near Real Time
ns	nanosecond (10^{-9} second)
NSO	National Solar Observatory
nT	nano-Tesla (10^{-9} Tesla)
NUV	Near Ultraviolet
NV/SA	Naamloze Vennootschap / Société Anonyme
NWC	Northwest Cape of Australia
NWP	Numerical Weather Prediction
O	Oxygen
O_3	Ozone
O3S	Ozone (O_3) Sonde
O3S-DQA	O3S Data Quality Assessment
ODC	On Duty Center (PECASUS)
ORB	Observatoire Royal de Belgique
ORFEES	Observation Radio Fréquences pour l’Etude des Eruptions Solaires
P	The position angle between the geocentric north pole and the solar rotational north pole measured eastward from geocentric north. The range in P is $\pm 26.3°$
P2SC	PROBA2 Science Center
PB	Petabyte (10^{15} bytes)
PBC	Primary Backup-Center (PECASUS)
PC	Personal Computer
PCF	Polar Crown Filament
PDF	Probability Density Functions

PECASUS	Pan-European Consortium for Aviation Space weather User Services (ICAO)
PFSS	Potential Field Source Surface
pfu	particle (proton) flux unit: the number of particles registered per second, per square cm, and per steradian
PhD	Doctor of Philosophy
PHI	Polarimetric and Helioseismic Imager (Solar Orbiter)
PI	Principal Investigator
PIC	Particle -in-Cell
PICASSO	PICo-satellite for Atmospheric and Space Science Observations
PITHIA-NRF	Plasmasphere Ionosphere Thermosphere Integrated Research Environment and Access services: a Network of Research Facilities (EU)
PLATINUM	PLAnetary plasma Turbulence and Intermittency - coupling with interplanetary transients from data analysis and NUmerical Modelling
PRESTO	(1) Fast warning message for important SWx events (2) PREdictability of the Solar-Terrestrial Coupling (SCOSTEP)
PROBA	PRoject for OnBoard Autonomy
PROBA-V	PROBA-Vegetation
PRODEX	PROgramme de Développement d'Expériences scientifiques (ESA ; Program for the development of scientific experiments)
PROSPER	PRObabilistic Solar Particle Event foRecasting model
ps	picosecond (10^{-12} second)
PSP	Parker Solar Probe
PTB	Physikalish-Technische Bundesanstalt (Germany)
px	pixel
Python	Programming language (no acronym)
Q&A	Questions and Answers
QA	Quality Assurance
QC	Quality Control
QE	Quantum Efficiency
QPP	Quasi-periodic pulsation
ρ_T	gyroradius
R	Resistor
$R_\odot$	Solar radius (696.000 km)
r^2	the square of the correlation coefficient
R&D	Research and Development
R-ESC	Space Radiation ESC (SSCC)
RAD	International Conference on Radiation, Natural Sciences, Medicine, Engineering, Technology and Ecology
RAL	Rutherford Appleton Laboratory
RAS	Royal Astronomical Society
RBSP	Radiation Belt Storm Probes (now called the "Van Allen probes")
R_e	Earh radius (radii)
REENOM	Radiation Environment and Effects NOwcasts for the Moon
REFAG	Reference Frames for Applications in Geosciences
ReLU	Rectified Linear Unit
RF	Radio Frequency
RHESSI	Reuven Ramaty High Energy Solar Spectroscopic Imager
RMI(B)	Royal Meteorological Institute (of Belgium)
RMS	Root Mean Square
RMSE	Root Mean Square Error
ROB	Royal Observatory of Belgium
Roscosmos	Russian Space Agency
RPW	Radio and Plasma Waves (Solar Orbiter)
RSSB	Royal Statistical Society of Belgium
R_s	Solar radius (radii)
R_{sun}	Solar radius (~ 696.000 km)
RWC	Regional Warning Center
Rx	Receiver
σ	sigma (confidence level)
s	second
S	South
S-band	Radio frequency band from 2-4 GHz
S/C	Spacecraft
S-class	Small class satellite (ESA)
SAA	South Atlantic Anomaly
SACS	Support to Aviation Control System

SANSA	South African National Space Agency
SAR	(1) Superactive region; (2) Synthetic Aperture Radar
SATCOM	Satellite Communication
SAWS	SEP Advanced Warning System
SBC	Secondary Backup-Center (PECASUS)
SC24, SC25	Solar Cycle 24, Solar Cycle 25
SCAR	Scientific Committee on Antarctic Research
SCIAMACHY	SCanning Imaging Absorption spectroMeter for Atmospheric CHartographY (ENVISAT)
SCK-CEN	Studiecentrum voor Kernenergie - Centre d'Etude de l'Energie Nucléaire
SCOPE	Solar Coronagraph for OPErations
SCOSTEP	Scientific Committee on Solar Terrestrial Physics
SDO	Solar Dynamics Observatory
SECCHI	Sun Earth Connection Coronal and Heliospheric Investigation (STEREO)
SEE	Single Event Effects
SEESAW	Space Environment Engineering and Science Applications Workshop
SEP	Solar Energetic Particle
SEPEM	Solar Energetic Particle Environment Modelling
SEPVAL	SEP model VALidation working meeting
SEU	Single Event Upset
SFU, sfu	Solar Flux Unit (10^{-22} W m^{-2} Hz^{-1})
SGEPSS	Society of Geomagnetism and Earth, Planetary and Space Science
SHINE	Solar Heliospheric & Interplanetary Environment
SIDC	Solar Influences Data analysis Center
SILSO	Sunspot Index and Long-term Solar Observations (ROB)
SIMBA	Sun-earth IMBAlance
SLP	Sweeping / Segmented / Single/ Split / Spherical Langmuir Probe
SLT	Solar Local Time
SM	Spare Model
SMD	Safety and Metrology Division (Federal Services for Metrology)
SMILE	Solar wind-Magnetosphere-Ionosphere Link Explorer (ESA)
SMILE MWG	SMILE - Modeling Working Group
sms	short message service
S_N , SN	(1) Sunspot Number ; (2) Space weather and Near-earth objects ; (3) Standard normal homogenization tests
SO	Solar Orbiter
SOC	Science Operations Centre
SOHO	SOlar & Heliospheric Observatory
Solar-C	Next Generation Solar physics Mission (JAXA)
SOLARNET	European network of solar physics researchers and facilities (H2020)
SOLCON	SOLar CONstant radiometer
SolEx	Solar Explorer (telescope)
SOLIS	Synoptic Optical Long-term Investigations of the Sun (NSO)
SolO	Solar Orbiter
SOLSPEC	SOLar SPECtrum (spectroradiometer)
SOOP	Solar Orbiter Observing Plan (SolO)
SOP	Standard Operating Procedures
SoSpIM	Spectral Solar Irradiance Monitor (Solar-C)
SOVA	SOlar constant and VAriability
SPADE	Small Phased Array Demonstrator (Humain)
SPD	Solar Physics Division (AAS)
SPENVIS (-NG)	SPace ENVironment Information System (- Next Generation)
SPHINX	Solar Particles in the Heliosphere validation INfrastructure for SpWx
SPICE	Spectral Imaging of the Coronal Environment (SolO)
SPIE	Society of Photo-optical Instrumentation Engineers

SPOCA	Spatial Possibilistic Clustering Algorithm
SPRING	Solar Physics Research Integrated Network Group (SOLARNET)
SPS	Science for Peace and Security (NATO)
sr	steradian
SRB	Solar Radio Burst
SREM	Standard Radiation Environment Monitor (Integral, Rosetta)
SSA	(1) Space Situational Awareness ; (2) singular spectrum analysis
SSCC	SSA Space Weather Coordination Centre (ESA)
SSI	Solar Spectral Irradiance
SSN	SunSpot Number
SSWRF II	2nd international workshop on Small Satellites for Space Weather Research and Forecasting
STCE	Solar-Terrestrial Centre of Excellence
STCL	Space Technology & Calibration Laboratories
STEM	Science, Technology, Engineering, Mathematics
STEAM	Science, Technology, Engineering, Arts, Mathematics
STEREO	Solar-TErrestrial RElations Observatory
STIX	Spectrometer Telescope for Imaging X-rays (Solar Orbiter)
STM	Structural Model
SunPy	software library for solar physics based on Python
SunSCC	Automated tool for sunspot segmentation, clustering, and classification (ROB)
SUVI	Solar Ultraviolet Imager (GOES)
SVO	Solar Virtual Observatory
SW	Space Weather (journal)
SWAP	Sun Watcher using APS detector and image Processing (PROBA2)
SWAVES	STEREO WAVES
SWE	Space Weather

SWEC	Space Weather Education Center
SWEK	Space Weather Event Knowledgebase
SWIC	Space Weather Introductory Course
SWOP	Space Weather OPerations
SWPC	Space Weather Prediction Center (USA)
SWT	Science Working Team
SWx	Space weather
SXR	Soft x-rays
SYM-H	Index to describe the symmetric (SYM) disturbances of the horizontal (H) component of the geomagnetic field
SZA	Solar Zenith Angle
τ, t	Time
T	(1) Tesla ; (2) Terabyte (10^{12} bytes)
TB	Terabyte (10^{12} bytes)
TAP	Table Access Protocol
TEC	Total Electron Content
TEC-EPS	Technical and quality management/Electrical Engineering/ Power & Space Environment Division/Space Environment (ESA)
Tech-TIDE	Warning and Mitigation Technologies for TIDs Effects
TECO	Technical Conference on Meteorological and Environmental Instruments and Methods of Observation
TECu	TEC unit ($10^{16} e \cdot m^{-2}$)
T-FORS	Travelling ionospheric disturbances FORecasting System
TID	Travelling Ionospheric Disturbance
TIR	Thermal InfraRed
TOAR	Tropospheric Ozone Assessment Report
TOAR-II	Tropospheric Ozone Assessment Report, Phase II
TREx	Transition Region Explorer (Canada)
TROPOMI	TROPOspheric Monitoring Instrument (Sentinel-5 Precursor)
TSI	Total Solar Irradiance

Tx	Transmitter
UCL, UCLouvain	Université Catholique de Louvain
UFO	University FOrum (Ghent, Belgium)
UHF	Ultra-high frequency (0.3 - 3 GHz)
UK	United Kingdom
ULB	Université libre de Bruxelles
ULF	Ultra Low Frequency (0.3 - 3 kHz)
Ulysses	A joint ESA/NASA/Canada NRL mission to study the Sun (1990-2009; no acronym)
UNCOPUOS	United Nations Committee on the Peaceful Use of Outer Space
URAN	Ukrainian Radio Interferometer of NASU
URL	Uniform Resource Locator
URSI	International Union of Radio Science - Union Radio-Scientifique Internationale
US(A)	United States (of America)
USAF	United States Air Force
usb, USB	Universal Serial Bus
USET	Uccle Solar Equatorial Table
UT(C)	(Coordinated) Universal Time
UV	Ultraviolet
v	Velocity (speed)
V	Volt, voltage
V1, V2, …	Version 1, 2, …
VenSpec-H	Venus Spectrometer with High resolution (EnVision)
VHF	Very High Frequency (30-300 MHz)
VIP	Very Important Person
VIRGO	Variability of solar IRradiance and Gravity Oscillations (SoHO)
VIS	Visible
VKI	Von Karman Institute
VLF	Very Low Frequency (3-30 kHz)
VO	Virtual Observatory
VSC	Volontaire Service Civique (voluntary personnel for civil services)
VSWMC	Virtual Space Weather Modelling Centre
VTEC	Vertical TEC
VUB	Vrije Universiteit Brussel
VUV	Vacuum Ultraviolet
VVS	Vereniging Voor Sterrenkunde (Belgian Astronomical Association)
W	(1) Watt; (2) West
WAAS	Wide Area Augmentation System (GPS/North-America)
W/m^2	Watt per square meter
WAVES	Radio and plasma wave investigation (WIND, STEREO)
WDC	World Data Center
WFOV	Wide Field Of View
WG	Working Group
WGCV	Working Group on Calibration and Validation
WGN	Werkgroepnieuws (Working Group News, bimonthly journal of the IMO)
WISA	Waves and Instabilities in the Solar Atmosphere
WL	White Light
WMO	World Meteorological Organization
WP	Work Package
WPI	Wave-Particle Interactions
WRC	World Radiation Center
WRF-Chem	Weather Research and Forecasting model coupled with Chemistry
WS	Workshop
WSA	Wang-Sheeley-Arge (model for solar wind)
X-band	Radio frequency band from 8-12 GHz
X-class flare	Extreme x-ray flare
XRT	X-Ray Telescope (Hinode)
Zpc	McIntosh sunspot classification, where 'Z' is the modified Zurich class, 'p' describes the penumbra of the principal spot, and 'c' describes the distribution of spots in the group's interior
ZTD	Zenith Total Delay